NPS-OC-91-006

NAVAL POSTGRADUATE SCHOOL
Monterey, California

THESIS

EVALUATION OF ABSOLUTE POSITIONING USING THE DEFENSE MAPPING AGENCY'S GASP PROGRAM

by

Dennis Bredthauer

September 1991

Thesis Advisor J.R. Clynch

Prepared for:
Naval Postgraduate School
Monterey, California 93943-5000

NAVAL POSTGRADUATE SCHOOL
Monterey, California

Rear Admiral R. W. West, Jr.
Superintendent

H. Shull
Provost

This thesis is prepared in conjunction with research sponsored and funded by the Naval Postgraduate School (NPS).

REPORT DOCUMENTATION PAGE

1a Report Security Classification Unclassified		1b Restrictive Markings	
2a Security Classification Authority		3 Distribution/Availability of Report	
2b Declassification/Downgrading Schedule		Approved for public release; distribution is unlimited.	
4 Performing Organization Report Number(s)		5 Monitoring Organization Report Number(s)	
6a Name of Performing Organization Naval Postgraduate School	6b Office Symbol *(if applicable)* 35	7a Name of Monitoring Organization Naval Postgraduate School	
6c Address *(city, state, and ZIP code)* Monterey, CA 93943-5000		7b Address *(city, state, and ZIP code)* Monterey, CA 93943-5000	
8a Name of Funding/Sponsoring Organization	8b Office Symbol *(if applicable)*	9 Procurement Instrument Identification Number OM&N	
8c Address *(city, state, and ZIP code)*		10 Source of Funding Numbers	
		Program Element No / Project No / Task No / Work Unit Accession No	

11 Title *(include security classification)* EVALUATION OF ABSOLUTE POSITIONING USING THE DEFENSE MAPPING AGENCY'S GASP PROGRAM

12 Personal Author(s) Dennis Bredthauer

13a Type of Report	13b Time Covered	14 Date of Report *(year, month, day)*	15 Page Count
Master's Thesis	From To	September 1991	161

16 Supplementary Notation The views expressed in this thesis are those of the author and do not reflect the official policy or position of the Department of Defense or the U.S. Government.

17 Cosati Codes			18 Subject Terms *(continue on reverse if necessary and identify by block number)*
Field	Group	Subgroup	GPS, GASP, Absolute Positioning

19 Abstract *(continue on reverse if necessary and identify by block number)*

The Geodetic Absolute Sequential Positioning (GASP) program, as utilized by the Defense Mapping Agency (DMA), processes static GPS measurements collected with the TI 4100 GPS receiver to estimate geodetic point (absolute) positions. In this thesis, the GASP program is modified to accept data from different receiver types, the estimated point positions are compared to positions produced by the Transit Doppler positioning system, the between-receiver estimates are compared, the difference between estimates using the broadcast and the precise are examined, and the effects of Selective Availability assessed.

During the Monterey Bay Precision Positioning Experiment (MBPPE), conducted in the Winter of 1990-91, a large set of static GPS positioning data was collected with four types of GPS receiver; the TI 4100, the Trimble 4000ST, the Ashtech LD XII, and the Magnavox MX4200. Additional static GPS measurements were obtained with the TI 4100 receiver at a reference site established to support the experiment. A third data set was collected after activation of Selective Availability. Measurements collected with the TI 4100, Trimble, and Ashtech receivers were subsequently processed with GASP using broadcast and precise ephemerides to produce point position estimates. In order for GASP to accept the data from the Ashtech and Trimble receivers, the program had to be modified.

The positioning results obtained are analyzed for accuracy and precision. The accuracy of the GASP GPS estimates is determined by comparison to independent estimates obtained by the Transit Doppler positioning system. Precision or repeatability (i.e., consistency of the estimated positions) is also examined.

Analysis of the accuracy and repeatability reveals little difference between the positions computed for the three receivers using the precise ephemeris and that all three provide good agreement to the Transit Doppler positions. All three receivers are capable of providing geodetic-quality point positions. It is also clearly demonstrated that the precise ephemeris does produce a more accurate, higher precision solution than the broadcast ephemeris. The activation of Selective Availability has substantially degraded position solutions available from the broadcast ephemeris.

20 Distribution/Availability of Abstract	21 Abstract Security Classification	
☒ unclassified/unlimited ☐ same as report ☐ DTIC users	Unclassified	
22a Name of Responsible Individual .R. Clynch	22b Telephone *(include Area code)* (408) 646-3268	22c Office Symbol OC/Cl

D FORM 1473,84 MAR 83 APR edition may be used until exhausted
All other editions are obsolete

security classification of this page

Unclassified

Approved for public release; distribution is unlimited.

EVALUATION OF ABSOLUTE POSITIONING USING THE DEFENSE MAPPING AGENCY'S GASP PROGRAM

by

Dennis Bredthauer
Civilian, Defense Mapping Agency
B.S., Worcester State College, 1982

Submitted in partial fulfillment of the
requirements for the degree of

MASTER OF SCIENCE IN HYDROGRAPHIC SCIENCE

from the

NAVAL POSTGRADUATE SCHOOL
September 1991

ABSTRACT

The Geodetic Absolute Sequential Positioning (GASP) program, as utilized by the Defense Mapping Agency (DMA), processes static GPS measurements collected with the TI 4100 GPS receiver to estimate geodetic point (absolute) positions. In this thesis, the GASP program is modified to accept data from different receiver types, the estimated point positions are compared to positions produced by the Transit Doppler positioning system, the between-receiver estimates are compared, the difference between estimates using the broadcast and the precise are examined, and the effects of Selective Availability assessed.

During the Monterey Bay Precision Positioning Experiment (MBPPE), conducted in the Winter of 1990-91, a large set of static GPS positioning data was collected with four types of GPS receiver; the TI 4100, the Trimble 4000ST, the Ashtech LD XII, and the Magnavox MX4200. Additional static GPS measurements were obtained with the TI 4100 receiver at a reference site established to support the experiment. A third data set was collected after activation of Selective Availability. Measurements collected with the TI 4100, Trimble, and Ashtech receivers were subsequently processed with GASP using broadcast and precise ephemerides to produce point position estimates. In order for GASP to accept the data from the Ashtech and Trimble receivers, the program had to be modified.

The positioning results obtained are analyzed for accuracy and precision. The accuracy of the GASP GPS estimates is determined by comparison to independent estimates obtained by the Transit Doppler positioning system. Precision or repeatability (i.e., consistency of the estimated positions) is also examined.

Analysis of the accuracy and repeatability reveals little difference between the positions computed for the three receivers using the precise ephemeris and that all three provide good agreement to the Transit Doppler positions. All three receivers are capable of providing geodetic-quality point positions. It is also clearly demonstrated that the precise ephemeris does produce a more accurate, higher precision solution than the broadcast ephemeris. The activation of Selective Availability has substantially degraded position solutions available from the broadcast ephemeris.

THESIS DISCLAIMER

The reader is cautioned that computer programs developed in this research may not have been exercised for all cases of interest. While every effort has been made, within the time available, to ensure that the programs are free of computational and logic errors, they cannot be considered validated. Any application of these programs without additional verification is at the risk of the user.

TABLE OF CONTENTS

LIST OF TABLES

LIST OF FIGURES

LIST OF ABBREVIATIONS

BEPP.....Basic External Processing Program

C/A Code.....Coarse/Acquisition Code

CT.....Conventional Terrestrial Coordinate System

DMA.....Defense Mapping Agency

DoD.....Department of Defense

DOP.....Dilution of Precision

FIC.....Floating Point, Integer, Character

FICA.....Floating Point, Integer, Character, ASCII

GASP.....Geodetic Absolute Sequential Positioning Program

GDOP.....Geometric Dilution of Precision

GPS.....Global Positioning System

MBPPE.....Monterey Bay Precision Positioning Experiment

NAVSTAR.....Global Positioning System

NGS.....National Geodetic Service

P Code.....Precise Code

PRN.....Pseudo Random Noise or Number

RINEX.....Receiver INdependent EXchange Format

RMS.....Root-Mean-Square

SA.....Selective Availability

STARPREP.....GeoSTAR PREProcessor

TI 4100.....Texas Instruments Model 4100 GPS Receiver

UT/ARL.....University of Texas/Applied Research Laboratory

VAX.....Digital Equipment Corporation VAX Computer

WGS 84.....World Geodetic System 1984

ACKNOWLEDGEMENTS

The following individuals and organizations are gratefully acknowledged for their contributions to this project. Thanks to the Ashtec, Trimble, and Magnavox Corporations for providing GPS receivers used in the experiment and for providing valuable technical assistance and advice. Also deserving recognition, the Texas Department of Highways and Public Transportation for supplying the TI 4100 GPS receivers. Thanks to the Defense Mapping Agency for furnishing the GASP programs and related documentation, and for providing the precise satellite ephemerides and clock states, the MX 1502 Transit Doppler receiver and the Transit positions. Special thanks to Steve Malys of the Defense Mapping Agency for graciously answering any questions related to GASP processing. Thanks to Dr. Hal Titus for taking the time to serve as second reader and for his much appreciated input.

This list of acknowledgements would not be complete without thanking the experiment participants themselves. To Commander Kurt Schnebele, Mr. James Cherry, Dr. Stevens Tucker, LCDR. Barry Grinker, LCDR. Manuel Pardo, Mr. Arnold Steed, and to LCDR. Robert Wilson, thank you for committing extensive time and effort to making the Monterey Bay Precision Positioning Experiment a success and for making the long, cold nights at sea and at the Beach Lab tolerable. Also, thanks to Dr. Clynch for his guidance, direction, and, in the end, patience in proofreading numerous revisions. I would also like to thank my wife Elizabeth, and daughter Jennifer, for their support and understanding in uncomplainingly enduring the many hours I spent staring at a computer terminal.

I. INTRODUCTION

A. THESIS DESCRIPTION AND OBJECTIVES

1. Monterey Bay Precision Positioning Experiment Overview

The Monterey Bay Precision Positioning Experiment (MBPPE) was designed to assess the performance of some commercially available Global Positioning System (GPS) receivers and the processing software developed to support the receivers. In particular, the static and dynamic positioning solutions of the Trimble 4000ST, Ashtech LD XII, Magnavox MX4200, and Texas Instruments TI 4100 receivers were examined. All but the MX4200 are geodetic quality receivers. The Trimble, Ashtech and Magnavox models exhibit some of the latest developments currently available in GPS receiver technology. The TI 4100 is an older model but is still widely used throughout the geodetic community.

The overall objective of the experiment was to acquire a large data set of GPS measurements in both static and kinematic modes with the different receivers, to process the data by utilizing processing techniques and software relevant to a given application, to interpret the results from a position accuracy and error analysis perspective, and to evalute the receivers and processing techniques based on these results.

2. Thesis Overview

The purpose of this investigation is to determine whether meter level point position accuracy is attainable with the TI 4100, Trimble, and Ashtech receivers. The Magnavox receiver is not considered in this study because it is a single frequency receiver, whereas the other receivers operate on dual frequencies. This is a serious limitation in determination of point positions since the dual frequency correction cannot be applied to correct for ionospheric refraction.

This study is concerned with one aspect of geodetic positioning, the absolute determination of a point position in some commonly used reference frame. There are two general categories of positioning, static and kinematic. As may be inferred, static positioning involves determining the positions of stationary objects and kinematic positioning the positions of moving objects. Static positioning may be divided into relative and absolute positioning subclasses. Relative positioning is described as the estimation of the vector (baseline) connecting a known station to an unknown station. Absolute or point positioning may be described as the estimation of the vector connecting the

origin of a global reference frame with an unknown station [Ref. 1: p. 1]. It then follows that relative kinematic positioning may be described as the estimation of a vector connecting a known static station to an unknown moving object. Station positions determined by absolute positioning methods may be used as mapping control points, datum transformation ties or in other mapping related applications. Once the absolute position of a station is determined it may be subsequently used as a known station in a relative positioning survey to establish the positions of additional stations.

The tool used to produce the absolute position solutions was the Geodetic Absolute Sequential Positioning (GASP) System of programs developed by the Defense Mapping Agency (DMA) [Ref. 1: p. 1, Ref. 2: p. 487]. GASP estimates the absolute position of a point in the geocentric, earth-fixed, cartesian, Conventional Terrestrial (CT) coordinate system in the World Geodetic System 1984 (WGS 84) reference frame (See Figure 1). One axis of the CT system passes through the intersection of the Greenwich meridian and the equatorial plane. The third axis passes through the Conventional International Origin (CIO) which is the average position of the earth's rotational pole for the years 1900 to 1905. The second axis is orthogonal to the first and third axes in a right-hand sense. [Ref. 3: Sec.5.6]

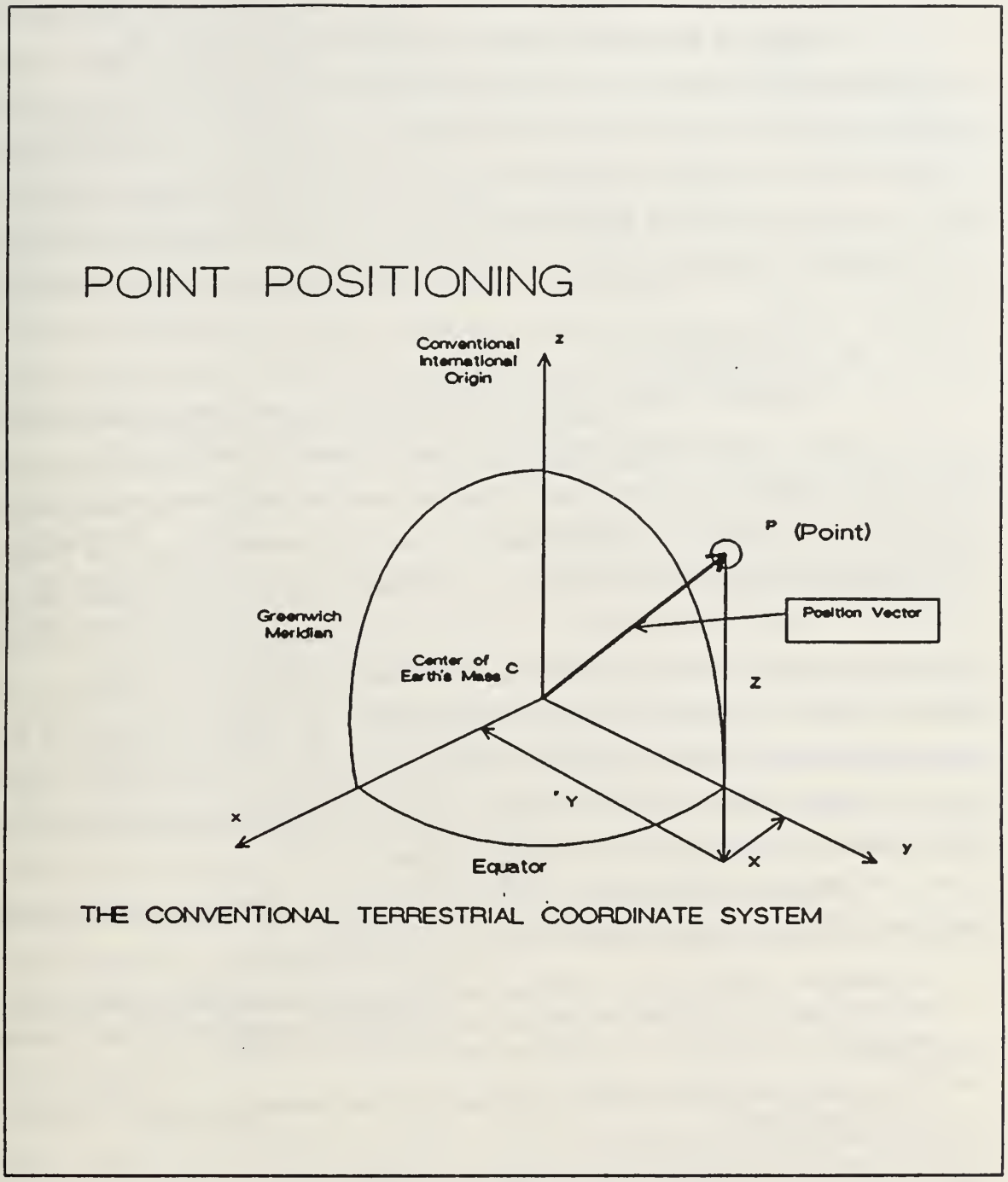

Figure 1. The Conventional Terrestrial Coordinate System

DMA has been processing GPS data collected with the TI 4100 with GASP for the last few years and it has demonstrated that geodetic quality point positions are routinely achievable. This means that a position solution with a standard deviation on each component of less than one meter can be expected, usually with data collected over a span of about four hours at a data collection rate of 30 seconds. Because accuracy results using the TI 4100 data with GASP are well documented, a benchmark had already been established that would provide a reference for the results we would obtain. [Ref. 1: p. 5]

a. Thesis Objectives

Before this project, GASP had the ability to process data collected with the TI 4100 receiver, using the Floating point, Integer, Character, ASCII (or FICA) format as the input format. One of the goals of this thesis was to modify GASP such that the programs would accept the measurements of any GPS receiver type. The Receiver INdependent EXchange (RINEX) format was chosen as a second data format through which receiver measurements could be entered into the program [Ref. 4]. The RINEX format was selected because it is one of the more widely recognized and accepted of the exchange formats currently in use and because both the Trimble and Ashtech data processing packages have programs that will convert their data to the RINEX format. It was also desired that the GASP programs retain the capability to process data in the FICA format for which GASP was originally written.

In addition to modifying the GASP program to accept the data from the Trimble and Ashtech receivers other objectives of this thesis are:

- To compare GPS position solutions produced for the TI 4100, Trimble 4000ST, and Ashtech LD XII GPS receivers to the solutions obtained from an independent method.[1]
- To compare the receiver position solutions for the broadcast ephemeris versus the precise ephemeris
- To examine repeatability (i.e., consistency) of results
- To examine the effects of Selective Availability on the position solution when using the broadcast ephemeris

---

1 The Transit Doppler positioning system was the independent method used in this comparison and the positions derived from this method are taken as the "true" positions.

B. BACKGROUND

1. The Global Positioning System (GPS) - Fundamental Concepts

There are a number of satellite based positioning systems being used to establish the position of an observer on or near the surface of the earth. The Global Positioning System (GPS) is one such system [Ref. 3: Sec. 3.0]. The NAVSTAR Global Positioning System is a passive navigation and satellite positioning system operated by the Department of Defense (DoD). It was developed to afford the user instantaneous three-dimensional position information anywhere in the world. GPS exploits simultaneously received radio frequency signals to determine range measurements between satellites and earth based receivers. These measurements along with a knowledge of the satellite positions can be used to solve for the receiver coordinates.

Through recent advances and upgrades in hardware, software and the development of new techniques in data processing, the systems applications have expanded dramatically. Particularly in the areas of high precision surveying and crustal deformation studies, GPS has rapidly become competitive with other positioning systems and techniques [Ref. 5].

The strength of the GPS system in geodetic work lies in its relative affordability, portabilty, ease of operation, and high accuracy in comparison to other high precision positioning systems [Ref. 6]. For example, the Transit Doppler satellite based positioning system requires two to four days of data collection to produce a geodetic quality point position. GPS, on the other hand, is able to produce a geodetic quality point position in only four hours of data collection [Ref. 1: p. 5]. From a mapping and charting perspective, the fact that it provides position determinations in a unified coordinate system may be its most important feature.

a. GPS System Components

GPS consists of three primary segments: the satellites, the ground control, and the users.

(1) The Satellite Segment. The GPS satellite constellation, as of mid 1991, consists of 16 satellites deployed in high earth orbit (about 20000 km altitude) configured such that a minimum of four satellites are visible to the user at a given time with from five to seven satellites typically available. The satellites are arranged in six orbital planes and have an orbital period of about 12 hours. It is proposed that 24 satellites eventually be deployed to ensure that a minimum of six satellites will be visible to the observer.

Each satellite transmits two radio frequency signals in the L-band, one at a frequency of 1575 MHz (termed L1) the other at 1227 MHz (L2). The L1 frequency is modulated by the Coarse/Acquisition (C/A) code, the Precise (P) code and the Navigation Message. The L2 frequency is modulated only by the P-code and the Navigation Message.

The C/A and P-codes are binary, pseudo-random noise (PRN) codes. Pseudo-random noise codes resemble true random noise except that random noise carries no information whereas PRN codes are generated to be predictable and carry information. In this case, the information is used to determine the time of signal transit from satellite to receiver. Identical codes are generated by both the satellites and the receiver and cross-correlations (determination of the scalar product of the code sequence with a time delayed copy of itself) of the incoming satellite codes with the receiver generated replicas are performed to determine the time reading of the transmitter clock.

The C/A and P-code modulations shift the phase of the carrier L-band frequencies by 180 degrees. They are essentially a sequence of positive and negative ones superimposed onto the carriers at frequencies of 1.023 MHz and 10.23 MHz respectively. If the code value is minus one the carrier phase is shifted, if plus one there is no effect on the carrier signal (See Figure 2).

The C/A-code sequence repeats every millisecond yielding a C/A code cycle of 300 kilometers. There are 2^{10} C/A code chips in one code cycle so that the length of one code chip corresponds to about 300 meters. Since it is possible for receivers to measure fractions of chips, the C/A code may be used as a medium accuracy navigation signal. C/A codes are exclusive to a particular satellite making it possible to distinguish between signals received simultaneously from the satellites.

The P-code sequence repeats every 267 days and is subdivided into 38 seven day segments. Each satellite is assigned a one week segment of the code. Thus all satellites can transmit on the same frequency and still be distinguished from each other. This weekly subdivision creates an identification system based on the PRN segment assigned to a particular satellite. If, for example, a satellite is assigned the seventh weekly segment of the code sequence, it is identified as PRN 7. Codes are initialized once per week at Saturday midnight. Since the length of a P-code chip corresponds to about 30 meters, the P-code supplies a more precise measurement than the C/A-code.

Critical satellite hardware components are the on-board atomic oscillators (highly stable and precise cesium and rubidium clocks) which control the generation of the carrier frequencies and code modulations. The signals are coherently

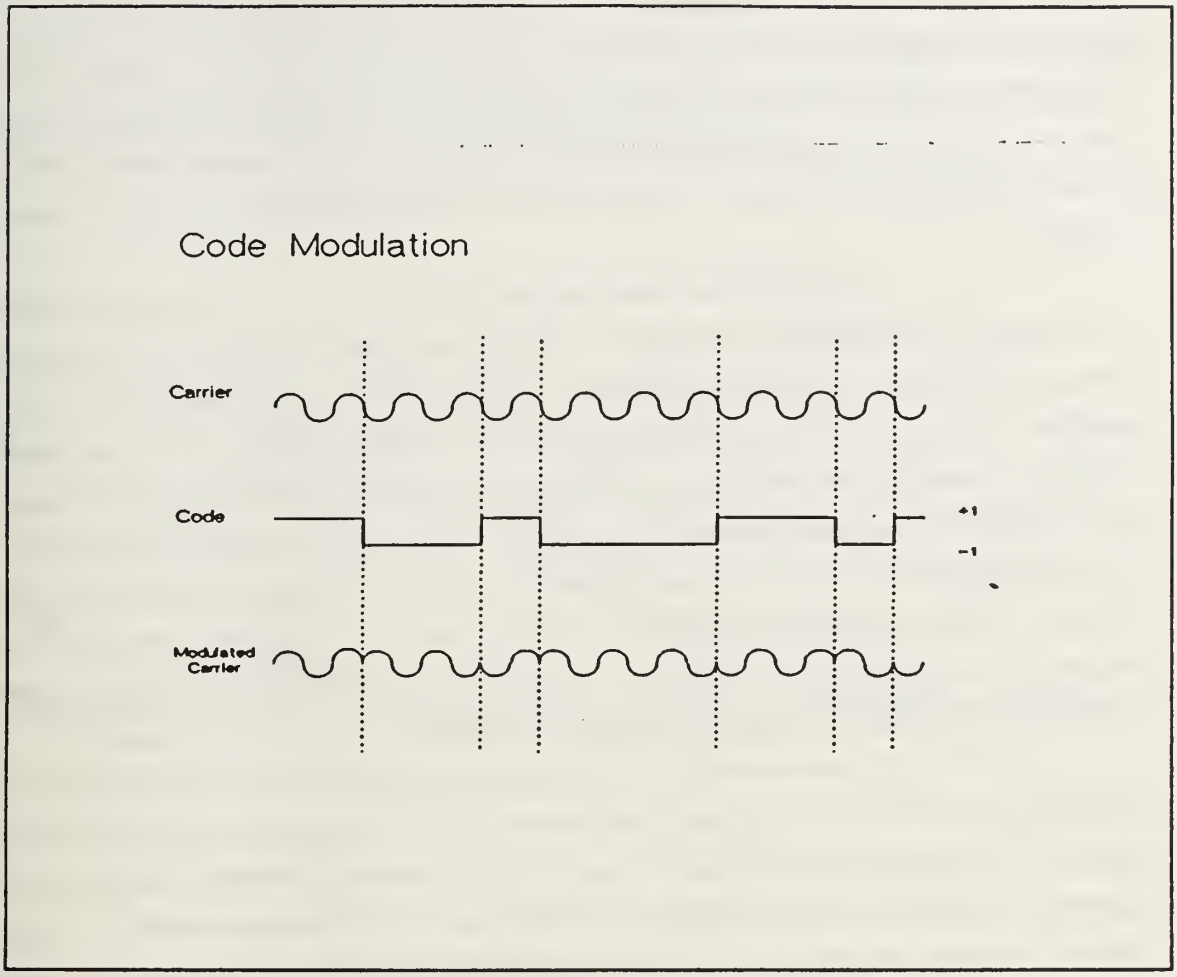

Figure 2. Code Modulation

generated from the same fundamental frequency, designated $f_0 = 10.23\ MHz$. The two carrier frequencies are multiples of the fundamental with $f_{L1} = 154 f_0$ and $f_{L2} = 120 f_0$ The C/A-code modulation has a chip rate one-tenth the fundamental frequency (f_0/ 10) and the P-code a chip rate equal to the fundamental frequency (f_0).

The Navigation Message is a low data rate message (broadcast at 50 bits per second) that contains information on satellite health, satellite clocks and the Broadcast Ephemerides. The contents of the navigation message are updated hourly.

Before the receiver position can be determined, the positions of the orbiting satellites must be known. The broadcast ephemerides are a set of predicted or extrapolated orbital parameters which define the satellites position with time and are used principally in real-time positioning. Satellite tracking information, received by five

ground tracking stations (identified in the next section), is used in a least squares adjustment to estimate the satellite positions. The positions of the ground tracking stations are held fixed in the estimation process. The broadcast ephemeris information is valid only over a specified time interval (about six hours), not over the entire orbit. The main reason the navigation message is updated hourly is so the broadcast ephemeris remains current.

The Keplerian orbit description contained in the broadcast ephemeris is the means by which the conventional terrestrial coordinates of the satellites are computed. Six Keplerian elements and a reference time are needed to completely describe the satellites orbit in the CT coordinate system. Five of these elements define the satellite orbit and the other describes the position of the satellite in the orbit as a function of time. The other broadcast ephemeris parameters transmitted in the Navigation Message describe the deviations or perturbations of the satellite motion from the smooth ellipse defined by the six Keplerian elements refered to above. For the complete list of the broadcast parameters and the computations required to convert the Keplerian orbital parameters to coordinates in the conventional terrestrial system, see Appendix A.

If more accurately determined satellite orbits are required than are provided in the broadcast ephemeris, a post-computed or precise ephemeris may be obtained. The Defense Mapping Agency and the U.S. National Geodetic Service are the agencies responsible for generating and distributing this information to the user upon request. Because the precise ephemeris is computed after satellite observations are made and is an interpolation of satellite position based on a least squares adjustment using ten ground stations rather than five, much better accuracies for the satellite position are attainable. The precise ephemerides, as supplied by either DMA or NGS, differ from the broadcast ephemerides in both data presentation and in the frequency with which satellite positions are estimated. The precise ephemeris furnishes satellite positions already computed in the CT coordinate system and gives the satellite velocities in the directions of the coordinate axes. The CT satellite positions and velocities are determined every 15 minutes in contrast to the hourly updates of the broadcast ephemerides.

(2) The Ground Control Segment. This segment consists of five globally distributed monitoring stations that track the satellites and transmit tracking information to the master control station in Colorado Springs, Colorado. It is here that computations are performed to provide the broadcast ephemeris contained in the updated navigation message. The updated navigation message is then uploaded to the satellites for broadcast to the user. The navigation message, as previously stated, contains infor-

mation on the health status of the satellites, and information on the satellites orbits and atomic clocks. The five monitoring stations are located at Diego Garcia, Ascension Island, Kwajalein, Hawaii, and Colorado Springs (See Figure 3).

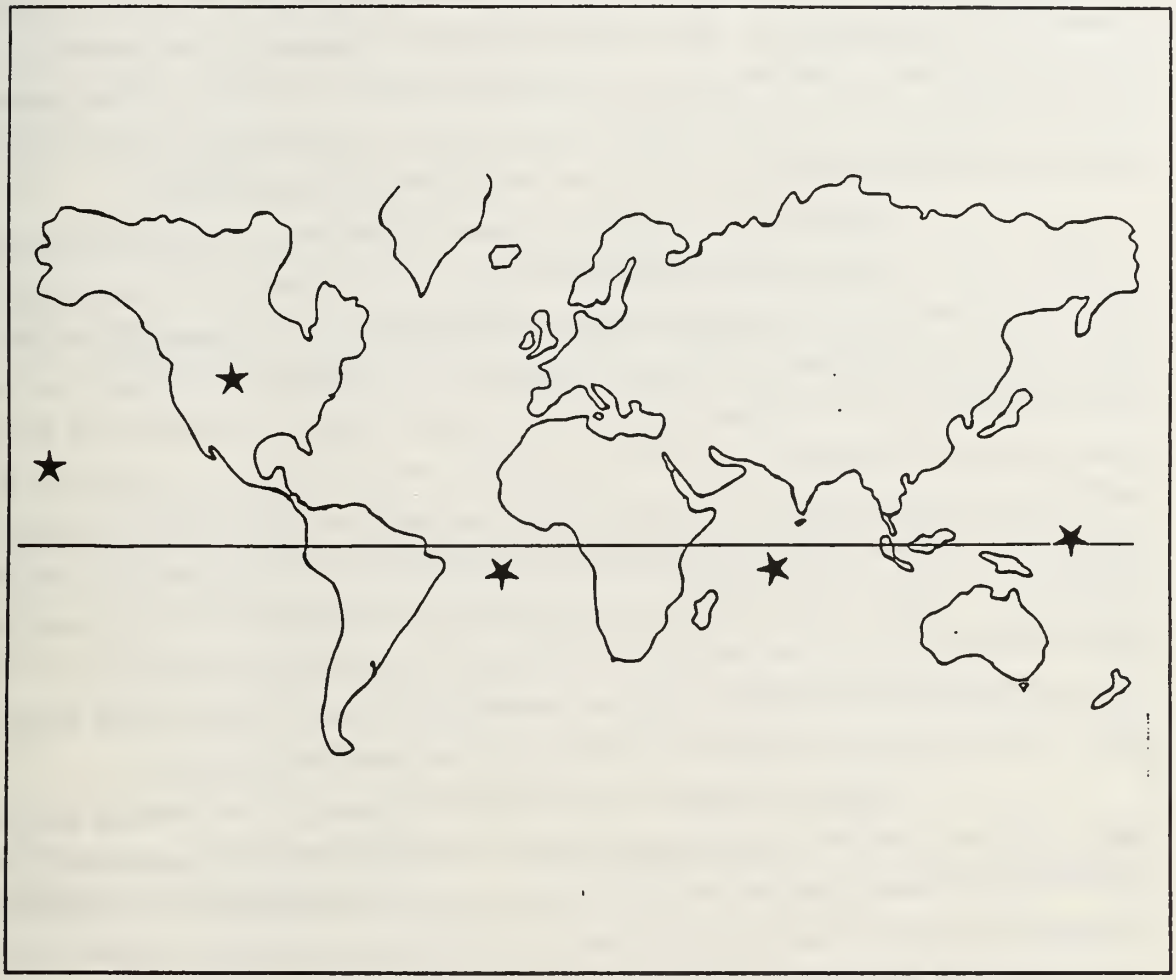

Figure 3. GPS Control Stations

(3) The User Segment. The user segment is composed of civilian and military users exploiting some type of GPS receiver and receiving antenna system. GPS receivers have the ability to receive the L1 and L2 signals from a number of satellites simultaneously by devoting specific channels to each satellite signal. Once the signals are channeled they can be individually processed. The three most commonly used types of GPS receiver are the code-correlating receivers, squaring channel receivers, and receivers that incorporate elements of both of these techniques. The code-correlating technique is normally employed to decode the broadcast message and also to provide pseudorange

measurements from either the C/A or P-codes. The TI 4100 provides pseudorange measurements from the P-code while the Trimble and Ashtech pseudoranges are derived from the C/A-code. Once the carrier signal has been demodulated (i.e. the navigation message and PRN codes removed), the carrier frequencies may be processed to provide carrier phase measurements. The squaring channel technique provides carrier phase measurements but cannot be used to extract the broadcast message (satellite position and clock information must be supplied externally) nor provide pseudoranges (for details on the pseudorange and carrier phase measurements see the next section).

Essentially, code-correlating receivers operate by internally generating a replica of the incoming code modulated satellite signal. The start of the code replica will be offset due to the propagation delay between satellite and receiver. The replica is then incrementally shifted or cross-correlated with the incoming coded signal and the clock controlling the generation of the replica signal is corrected to reflect the shifts. Once the replica is aligned to the incoming signal, it stays locked to it. At this point, the replica code generator clock reads identically to the satellite clock and the signal transmission time is determined by differencing this time from the time recorded on a receiver clock on GPS time. This time difference multiplied by the speed of signal propagation gives the pseudorange. Once code lock is attained, the code may be removed from the incoming signal and the satellite navigation message extracted. The signal, now demodulated, may at this point be used for processing carrier phase measurements.

Squaring channel receivers operate by squaring the incoming satellite signal effectively removing any phase reversals resulting from code modulations impressed on the signal at the satellite. This produces a signal that is double the frequency of the incoming signal (See Figure 4). The phase difference between this squared signal and an internally generated replica is still easily determined however. The accumulated phase difference (whole and fractional cycles) is continuously counted and from this the carrier based change in range is determined by multiplying by the wavelength of the squared signal.

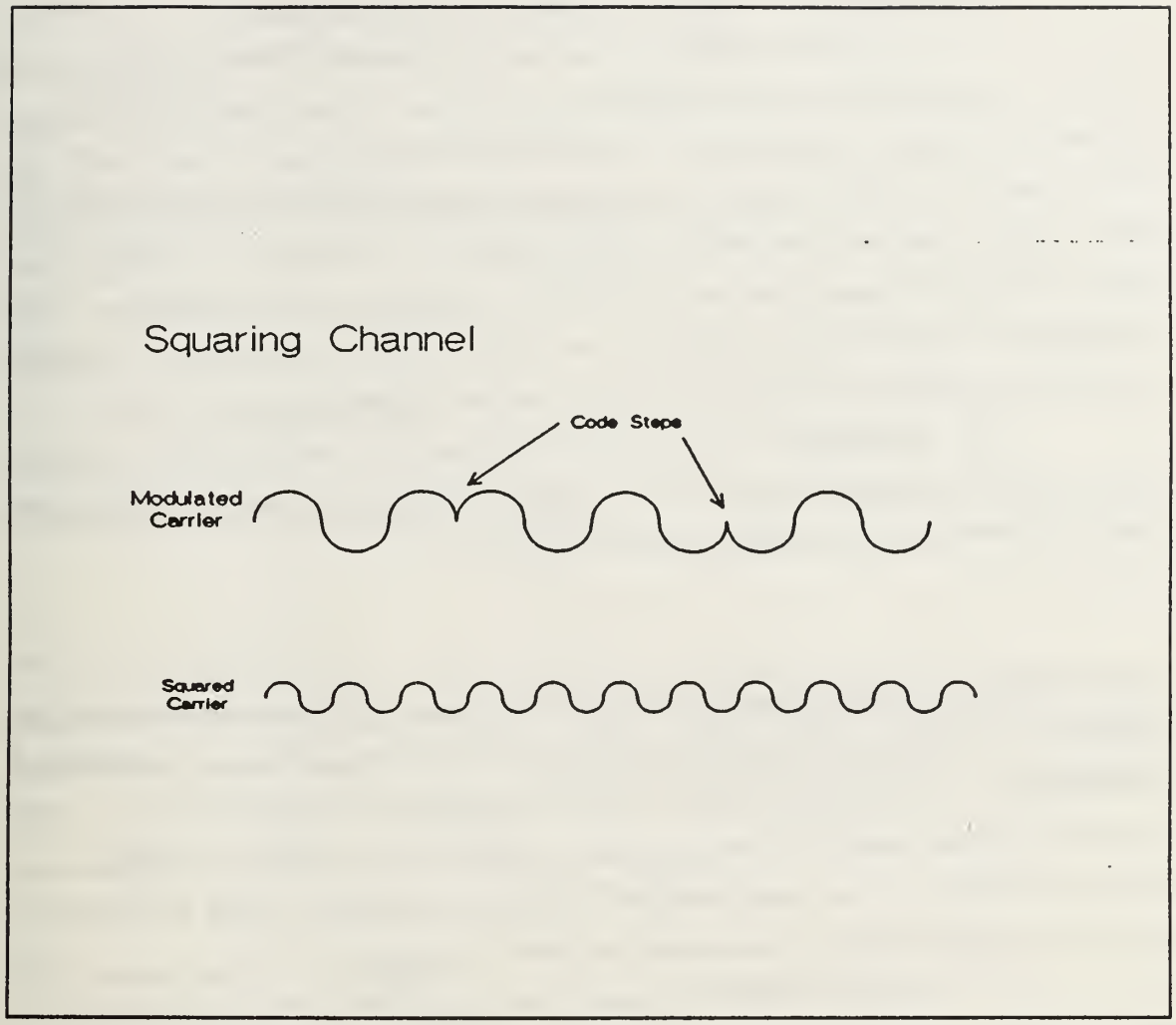

Figure 4. Squaring Channel

GPS receivers are equipped with quartz crystal oscillators rather than the more precise, stable, and expensive atomic oscillators used aboard the satellites. These oscillators do however provide more than sufficient precision and short term stability for the typical length of a surveying session. Like the satellite clocks, the receiver clocks control signal generation.

Internal receiver software estimates the receiver position by employing least squares or Kalman filtering algorithms using the broadcast ephemeris satellite positions and pseudorange or carrier phase measurements. All receivers estimate the receiver clock bias in addition to the postion parameters and then use this value to reset the receiver clock to GPS time.

b. GPS Operating Principles - Emphasis on Point Positioning

(1) GPS Observables and Observation Equations. There are two types of observation that may be exploited to determine positions, the pseudorange measurement and the carrier phase measurement. For point positioning particularly with GASP, the carrier phase is of primary interest and so is emphasized here. Pseudorange measurements to the extent they are used by GASP, serve only to monitor the validity of the carrier phase measurements and are not used in the actual position estimation. The fundamentals of pseudorange positioning are briefly touched on, however, in an effort to convey some general concepts and introduce some common terms.

(2) Pseudorange. Under ideal conditions (i.e., precisely known satellite location, signal propagation speed, and perfectly synchronized satellite and receiver clocks) the travel time of the signal would be given by

$$\tau = t_r - t_x$$

where t_r is the time of signal reception at the receiver and t_x is the time of satellite signal transmission. This time difference would then be converted to distance units (ρ) by multiplying by the appropriate speed of signal propagation (c), where $\rho = c\,\tau$. This range measurement, along with the range measurements of two additional satellites and the known locations of the three satellites, could then produce a system of equations that can be solved to uniquely determine the receiver positions.

In the real world, we must be concerned with error sources and their effects. A major source of error in any GPS measurement is the inability of the receiver and satellite clocks to maintain alignment with the reference time standard (GPS time). Of these two types of clock error, that associated with the receiver dominates due to the lower precision and stability of these clocks. The Allan variance is often cited as an indication of oscillator stability. The Allan variance values for receiver crystal quartz oscillators are typically several orders of magnitude larger than the satellite atomic oscillators. Satellite clocks take longer to warm-up and to stabilize initially but they maintain stability much longer than do receiver clocks.

To address the problem of clock errors, we introduce a combined satellite and receiver, first order clock correction term as a fourth parameter in our system of equations. Expressing the receiver clock offset from GPS time as

$$\tau_r = t_r - t$$

where,

t_r is the receiver clock time

t is GPS time

and the satellite clock offset from GPS time as

$$\tau_x = t_x - t$$

where,

t_x is the satellite clock time

the combined clock correction term becomes

$$d\tau = \tau_r - \tau_x$$

Because of clock and other types of errors, the measured range between satellite and receiver is not the true range but is rather a biased range referred to as the pseudorange. Designating the pseudorange as ρ_r the system of observation equations is represented by:

$$\rho_{r_i} = \rho_i + c\, d\tau_i$$

with i greater than or equal to 4,

where ρ_i, the true range from the ith satellite, is given by

$$\rho_i = [(x_{s_i} - x_r)^2 + (y_{s_i} - y_r)^2 + (z_{s_i} - z_r)^2]^{1/2} = |\vec{X}_{s_i} - \vec{X}_r|$$

In this equation,

x_{s_i} is the x coordinate of the ith satellite

y_{s_i} is the y coordinate of the ith satellite

z_{s_i} is the z coordinate of the ith satellite and

x_r, y_r, z_r are the unknown receiver coordinates.

The addition of this fourth parameter requires a minimum of four observation equations to solve for the receiver coordinates and the clock correction. If τ_ρ is now introduced to

express the time delay associated with other error sources the pseudorange equation becomes:

$$\rho_{r_i} = \rho_i + c\,(d\tau_i + \tau_{p_i})$$

The pseudorange is the observable most often used to obtain a navigation solution where submeter level accuracy is not required. Three dimensional navigation solutions currently offer best case positional accuracy at 16 meters. While certainly suitable for navigating a vessel, a position in error by 16 meters could not be used as a reference for establishing or extending mapping control. For high precision relative or point positioning, phase observables are needed. Because the carrier phase wavelength is shorter than the code modulations to the carrier signal (20 centimeters for L1 as opposed to 30 meters for the P-code), the carrier signal may be used to provide a more precise distance measurement.

(3) Carrier Phase. It is possible to obtain distance (or more exactly change of distance) information by measuring the phase of the carrier signal. The difference between the phase of a receiver generated carrier signal and the incoming, Doppler shifted, satellite carrier signal gives the carrier beat phase observable

$$\phi_{meas} = -\frac{f}{c}\,\rho + f\,d\tau - f\,\tau_p$$

where, ϕ is in cycles and f is the signal frequency.

The total continuous carrier beat phase measurement consists of an accumulating count of the whole and fractional difference in cycles since the time of signal acquisition. What is not recorded is an unknown number of integer cycles at initial signal reception (the whole number of cycles between the receiver and satellite). The unknown number of cycles is referred to as the cycle or integer ambiguity. The total continuous carrier phase can be expressed

$$\phi_{total} = \phi_{meas} + N(t_0)$$

where $N(t_0)$ is the integer ambiguity. A carrier phase equation comparable to the pseudorange equation can be written,

$$\begin{aligned}\rho_{\phi_i} &= \lambda\,\phi_{meas_i} \\ &= \rho_i - c\,(d\tau_i + \tau_{p_i}) + \lambda\,N(t_0)_i\end{aligned}$$

where, ρ_ϕ is the phase biased pseudorange,

τ_p is the signal time delay associated with other error sources and

$\lambda = c/f$ is the signal wavelength.

See Figure 5 for a graphic representation of the carrier phase concept.

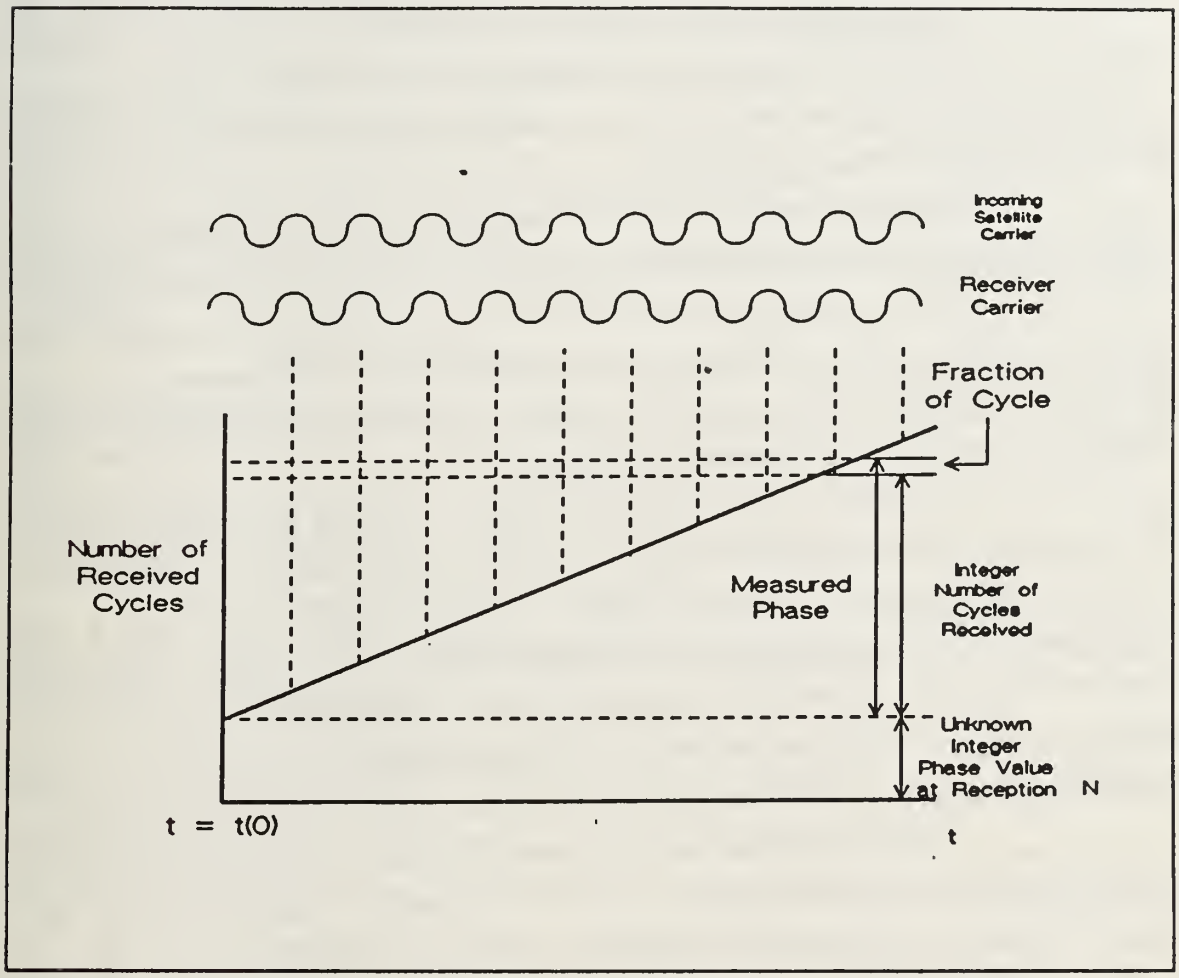

Figure 5. Components of Carrier Phase Measurements

c. Measurement Errors and Error Models

There are two types of errors that effect GPS measurements and degrade the accuracy of the estimated position, systematic errors and random errors. Systematic errors are errors resulting from a predictable source. These errors are typically of constant magnitude under a set of given conditions. When the cause is understood, these errors can be removed by a correction model or a change in observation procedure.

Measurement biases resulting from systematic errors produce offsets between the values that are observed and the "true" value. After systematic errors are eliminated from measurements, random errors remain. These errors are defined by repeated measurements. A repeated measurement will not yield identical values each time due to the occurrence of random errors. They indicate how well a measurement may be repeated and characterize the precision of a measurement. If they are the only error source, they are a measure of accuracy. Random errors are usually small and the probability of a positive or negative error of a given magnitude are the same. Random errors are dealt with in a least squares adjustment. [Ref. 7, 8]

GPS systematic errors can be divided into three general categories: satellite errors, station errors, and observation dependent errors. Satellite errors include errors in the computed satellite ephemeris or in the model for the satellite clock provided in the navigation message. Station errors occur as a result of errors in the receiver clock. Observation dependent errors are related to factors that influence the speed of signal propagation, ambiguities in phase observables, etc.

(1) Satellite and Receiver Clock Errors. Inability to perfectly synchronize the receiver clock and the more tightly controlled satellite clock to a standard reference (or GPS) time produces time offsets. If, for instance, there exists a one microsecond timing misalignment between satellite time and receiver time, a 300 meter range bias will result. Additionally, the clocks may be misaligned in frequency (a frequency bias) or the frequencies may change over time (frequency drift). Any of these will produce clock errors. Random error (or noise) also effects the time measurements.

The timing behavior of the satellite clocks is carefully monitored by the ground stations and the drift of the clocks from standard GPS time determined. The amount of the satellite time offset, frequency offset, and frequency drift are then expressed as coefficients of a second-order polynomial that are transmitted in the navigation message. The polynomial coefficients are determined via a least squares adjustment performed at the master control station in Colorado Springs. The polynomial has the form,

$$\tau_x = a_0 + a_1 (t - t_0) + a_2 (t - t_0)^2$$

where, t_0 is some reference epoch,

a_0 is the satellite clock time offset,

a_1 is the frequency offset, and

a_2 is the frequency drift. In this manner, satellite clock synchronization to GPS time is typically maintained to within 20 nanoseconds.

GPS receiver clock errors must be modeled if the user desires a high accuracy solution. Receiver clock errors may be treated in a fashion similiar to that for the satellite clocks. The polynomial coefficients may be estimated as additional parameters in a least squares adjustment along with the receiver coordinates.

(2) Orbit Errors. The positions of the satellites with time are well known but, due to forces acting on the satellites that may not be adequately modeled, are not perfectly determined. The error in satellite position propagates to contribute to error in the receiver position. The magnitude of this error depends on whether the broadcast (predicted) ephemeris or the precise (post-fit) ephemeris is used to determine the satellite positions.

Improving the models used to describe the forces acting on the satellite is one approach to obtaining more accurate satellite positions. Another is to include parametric models for the forces as part of the orbit estimation process performed by the control segment. Depending on the application, the effects of orbit errors may be ignored altogether or the data may be differenced to reduce or eliminate these effects.

(3) Observation Dependent Errors. The speed of signal propagation is influenced by many factors including; signal interaction with the ionosphere and troposphere, relativistic effects on the signal, etc.

(a) Signal Interaction with the Ionosphere— Signal interaction with the free electrons found in the ionosphere produces a change in path length that may be on the order of tens of meters. The free electrons are released from gas molecules ionized by incoming solar ultra-violet radiation. Any condition that acts to release more electrons, such as increasing the amount of incoming solar radiation (midday or during increased sunspot activity), will correspondingly lengthen the signal path. Satellite-receiver geometry also plays a role as the total number of free electrons along the path is a function of the distance that the signal travels through the ionosphere. Thus when a satellite is near the horizon the signal encounters more electrons than when near the zenith. This ionospheric effect is frequency dependent and is inversely proportional to the square of the signal frequency. A comparison of measurements on L1 and L2 may be used to derive a dual frequency correction given by

$$d\rho_{L1} = \frac{[\rho_{L1} - \rho_{L2}]}{\Gamma}$$

where Γ is defined by

$$\Gamma \equiv \left[\left(\frac{f_{L1}}{f_{L2}} \right)^2 - 1 \right]$$

For single frequency receivers, an ionospheric model must be used in place of the dual frequency correction or ignored altogether. [Ref. 2: p. 489]

(b) Tropospheric Interaction— Tropospheric effects are a result of refraction in the neutral atmosphere and are not frequency dependent. This effect may be separated into two components: the dry component, and the wet component. The dry component comprises about 90% of the total effect and is a function of the surface atmospheric pressure. It is approximated in the vertical by

$$DTC = 2.27 \times 10^{-3} (m/mb)\, P_0$$

where P_0 (the atmospheric pressure) is in millibars and DTC (the dry term range contribution) is in meters. In the zenith direction, this corresponds to a maximum range bias of about 2.5 meters. The DTC increases with decreasing satellite elevation angle and at five degrees above the horizon it ranges from 20-30 meters.

Estimating the effects of the wet component is a more complicated proposition. It depends on the total water vapor content along the signal path and hence on the temperature, pressure, and humidity. Surface temperature, pressure and humidity values are used to estimate the magnitude of the integrated effect by employing an atmospheric model such as the Hopfield or Chao models [Ref. 2: p. 490]. If observations from water vapor radiometers are available, they will most accurately profile atmospheric conditions along the path.

(c) Integer Ambiguity— In differential positioning applications, missing whole cycles (refered to as integer ambiguities) in the carrier phase measurements must be resolved if we are to fully exploit the more precise nature of phase measurements. Efforts must be made to account for any whole cycles not recorded in the observations. This may be the result of a loss of phase lock between receiver and satellite due to some obstruction to the signal. Also the initial number of whole cycles between satellite and receiver (the integer ambiguity) must be determined. Many techniques have been developed to resolve the absense of any cycles from the measurements. In point positioning with GASP, resolution of the integer ambiguity is not a problem as we shall see.

Other effects that must be accounted for include: relativistic effects, earth rotation (i.e., receiver position in motion) during time of signal transmission, and offset of the satellite transmitting antenna position from the position of the satellite center of mass (the position given by the ephemeris). Corrections to account for the effects of these error sources are applied to the phase biased pseudorange and the pseudorange observables before the GASP model is formed and the estimation algorithm is executed. Details on the models employed to compute these corrections are given in the chapter on GASP processing.

(4) Comments on Selective Availability. Selective Availability (SA) is the intentional degradation of the position solution available to a select segment of the user community (i.e., most civilians and unfriendly military) operating in a real-time navigation mode. It may be implemented by the DoD at their discretion. The solution degradation is accomplished by broadcasting inaccurate positions for the orbiting satellites or by dithering the satellite clock so that an inaccurate signal transmission time is obtained. This will not greatly effect relative positioning applications since receiver differencing schemes remove these errors. For point positioning applications that rely on the post-computed precise ephemeris, only the clock dither will effect the solutions.

d. Geometric Effects

In addition to the errors just presented, the configuration of the satellites relative to the receiver also has an effect on the determination of the receiver position. This geometric influence is referred to as the Dilution of Precision or DOP factor. It is roughly represented by the ratio of the positioning accuracy (σ_p) to the measurement accuracy (σ_0) or

$$DOP \approx \frac{\sigma_p}{\sigma_0}$$

Actually there are a number of DOP factors. The most commonly referred to of these, the Geometric Dilution of Precision (GDOP), is more precisely defined as the square root of the trace of the covariance matrix (the trace being the sum of the four diagonal elements; the three position variances and the time variance). The DOP is a measure of the geometric strength of the satellite configuration that changes with time. The time of most favorable observation for obtaining a user position is when the DOP is small (with a DOP of less than five preferred) and falling. Since the number and the positions of the satellites visible to the observer changes over time, many possible geometric scenarios are available over a tracking session. A GPS survey should be planned to take

best advantage of changing geometric scenarios. For point positioning, a geodetic quality position solution can usually be obtained with approximately four hours of data collection. During times of very favorable geometry, a geodetic quality point position may be obtained in a shorter time.

e. Differencing Techniques

By forming linear combinations of the basic pseudorange or carrier phase equations, a number of error sources common to the measurements being differenced will cancel or be greatly reduced. The accuracy of the computed position can be significantly improved by employing differencing because many sources of measurement error are removed or reduced. The three types of differencing combinations often used are: differencing between two satellites, differencing between two receivers, and differencing between two epochs (time periods). These are referred to as single differences. The differencing schemes involving the carrier phase equations are the only ones presented here since they are used to form the GASP model. Differencing schemes that involve the pseudorange equation are ignored since pseudorange observations do not contribute to the position estimation except as a means of screening the carrier phase observations. Also, differencing techniques involving multiple receivers are neglected in this treatment except to state what types exist and the what errors they effect.

Between-epoch single differencing involves differencing two equations of the instantaneous carrier phase for one satellite and one receiver. The carrier phase equation at epoch 1 is described by

$$\rho_{\phi_1} = \rho_1 - c\,(d\tau_1 + \tau_{p_1}) + \lambda\, N(t_0)$$

The carrier phase equation at epoch 2 is given by

$$\rho_{\phi_2} = \rho_2 - c\,(d\tau_2 + \tau_{p_2}) + \lambda\, N(t_0)$$

Differencing then yields

$$\rho_{\phi_1} - \rho_{\phi_2} = (\rho_1 - \rho_2) - c\,(d\tau_1 - d\tau_2 + \tau_{p_1} - \tau_{p_2})$$

Introducing δ as the difference notation the equation may be written

$$\delta\rho_{\phi} = \delta\rho - c\,(\delta d\tau - \delta\tau_p)$$

See Figure 6 for a graphic depiction of between-epoch single differencing.

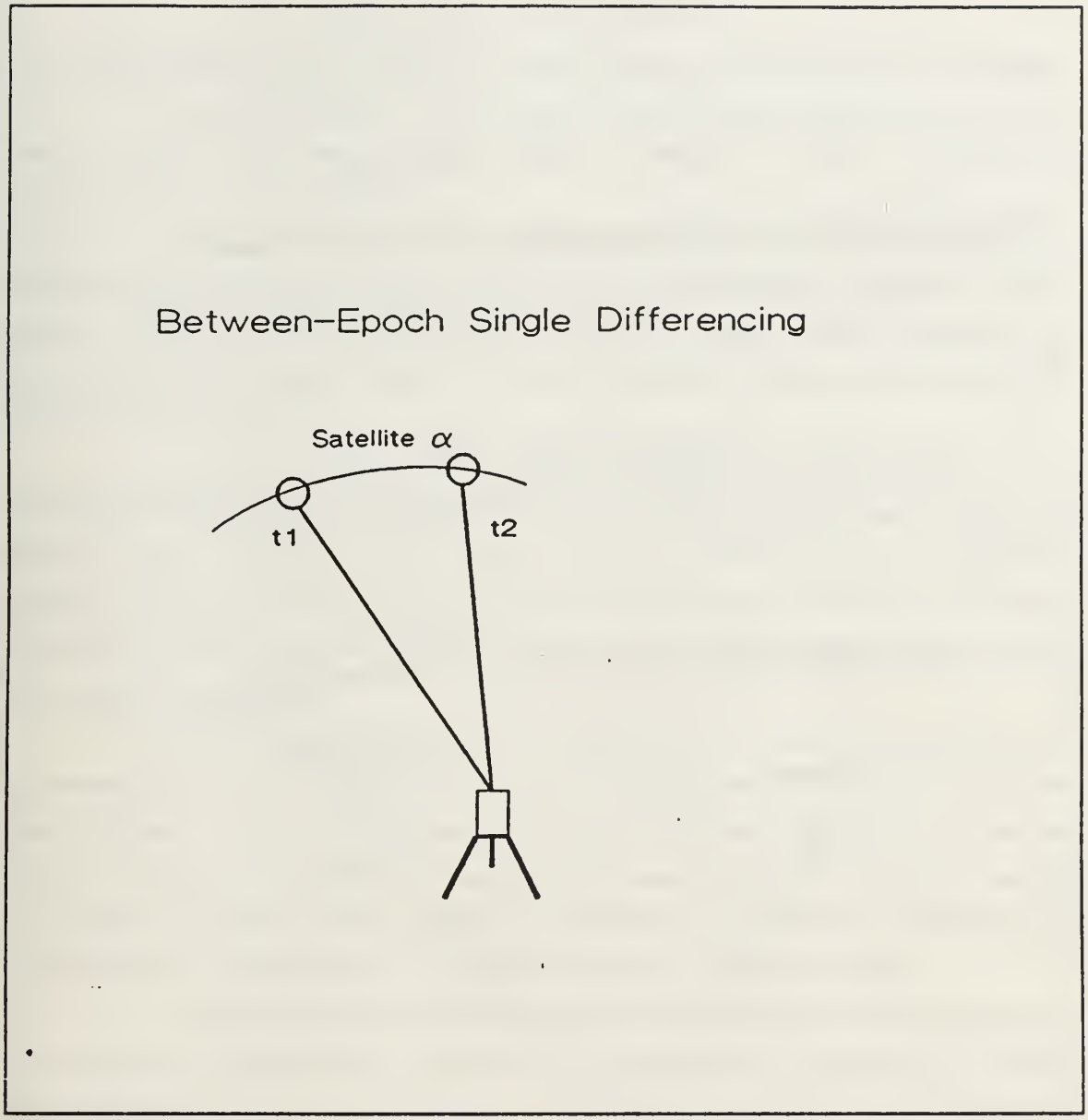

Figure 6. Between-Epoch Single Differences: Differencing Range Equations of One Satellite Over Two Consecutive Measurement Epochs

The advantage of this scheme is that the initial integer ambiguity is removed.

Similiar manipulations can be performed to yield between-satellite single differences (See Figure 7). For two satellites represented by the superscripts α and β, phase equations are given by,

$$\rho_{\phi}^{\alpha} = \rho^{\alpha} - c\,(d\tau^{\alpha} + \tau_{p}^{\alpha}) + \lambda\, N(t_0)^{\alpha}$$

and,

$$\rho_{\phi}^{\beta} = \rho^{\beta} - c\,(d\tau^{\beta} + \tau_{p}^{\beta}) + \lambda\, N(t_0)^{\beta}$$

The between-satellite single difference equation for the carrier phase is

$$\rho_{\phi}^{\alpha} - \rho_{\phi}^{\beta} = \rho^{\alpha} - \rho^{\beta} - c\,(d\tau^{\alpha} - d\tau^{\beta} + \tau_{p}^{\alpha} - \tau_{p}^{\beta}) + \lambda\,(N(t_0)^{\alpha} - N(t_0)^{\beta})$$

or,

$$d\rho_{\phi} = d\rho + c\,(d\tau_{x} - d\tau_{p}) + \lambda\, dN$$

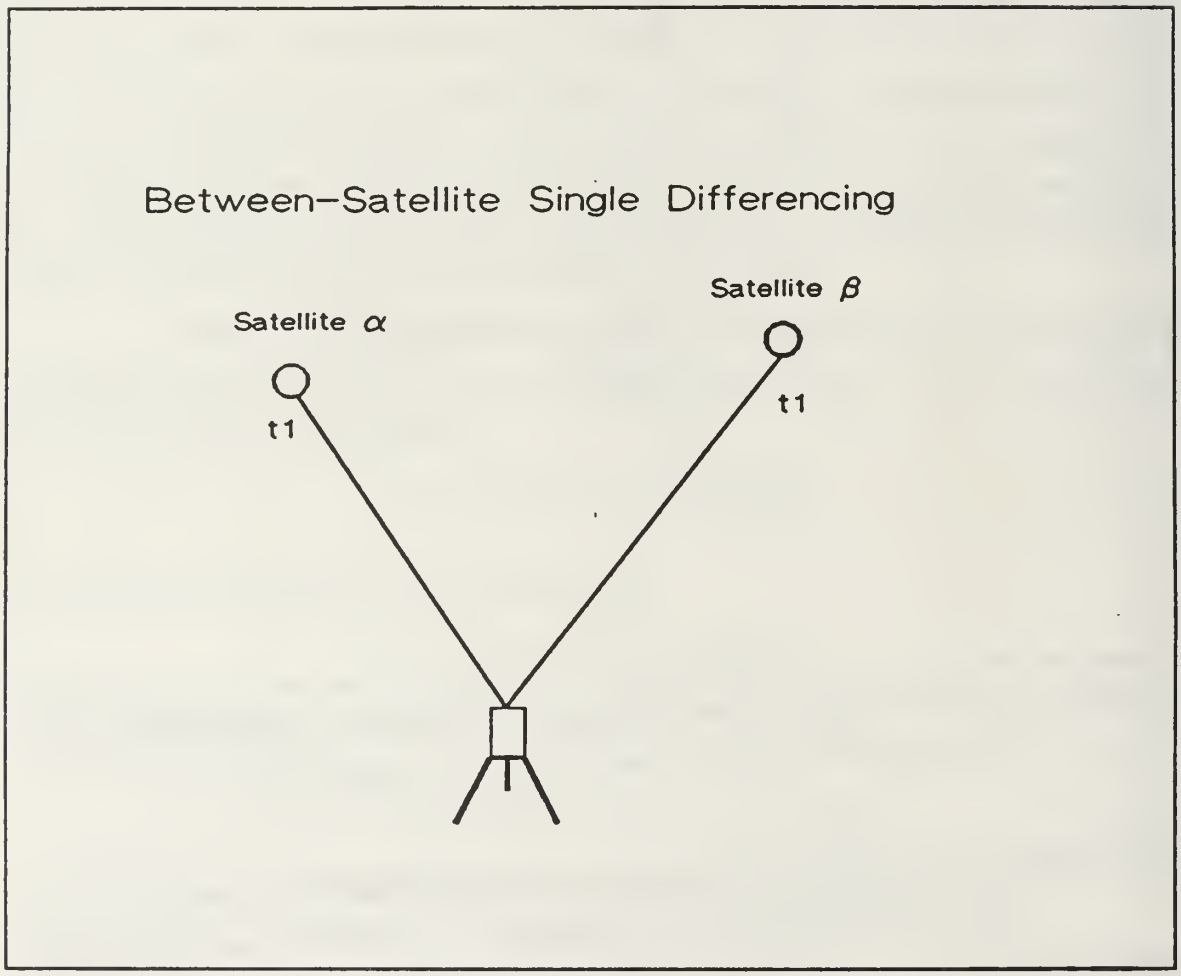

Figure 7. Between-Satellite Single Differences: Differencing Range Equations of Two Satellites Over One Measurement Epoch

For between-satellite single differencing, receiver clock errors are removed or reduced.

It is also possible to form between-receiver single difference equations to remove satellite clock and orbit errors. This is important in relative positioning but cannot be used in point positioning.

We can now form double difference equations from the single difference equations. For example, a satellite-receiver double difference may be formed by differencing two between-satellite single differences (involving the same pair of satellites) over two receivers. This scheme removes or reduces the effects of errors associated with satellite and receiver clocks.

Receiver-time double differences and satellite-time double differences may be formed in a similiar manner. Receiver-time double differencing removes or reduces the effects of errors associated with satellite clocks and eliminates integer ambiguities. Satellite-time double differencing (essentially the GASP model, see Chap. III for more details) removes or reduces the effects of errors associated the receiver clock and eliminates integer ambiguities.

It is also possible to construct an equation for a receiver-satellite-time triple difference observable. This gives the change in the receiver-satellite double difference from one epoch to the following epoch. With triple differencing, in addition to the cancellation of integer ambiguities for carrier phase measurements, all clock and satellite orbit errors are removed. Triple differencing is widely used in relative positioning applications [Ref. 9]. This technique cannot be employed in point positioning.

The disadvantages to differencing are that the number of observations has been reduced and mathematical correlations are introduced as a product of the differencing process. This produces a weaker solution than that provided by not differencing. Correlation matrices should be computed to equate the differenced data to the undifferenced data but generally differenced observables are treated as uncorrelated.

Now that systematic errors have been reduced or removed by error modeling (i.e., applying measurement corrections) or by differencing and the mathematical model has been defined by forming the undifferenced or differenced observation equation, the receiver coordinates and other parameters may be estimated by invoking the method of least squares. For a more complete explanation of the use of the least squares method in GPS, see Appendix B.

2. Positioning with Transit Doppler

The method of Transit Doppler positioning is briefly reviewed here. Since this method was used to provide the independent reference positions to which the GPS derived point positions were compared, some insight into Transit Doppler positioning is necessary.

The U.S. Navy Navigation Satellite System or Transit has been in continuous operation since the mid 1960's. Transit can be regarded as the forerunner of GPS in many respects. Many of the ideas and techniques developed during the era of Transit positioning have been refined and employed in GPS. It is anticipated that Transit will be replaced by GPS in the near future. Like GPS, Transit consists of three segments: the satellites, the ground control, and the users.

Six active Transit satellites are deployed in circular polar orbit at an altitude of approximately 1100 kilometers. This height was selected because excessive orbital height would provide too low a rate of change of Doppler frequency. If the orbit were too low, the Doppler frequency rate of change, ionospheric refraction, and especially the effects of atmospheric drag become too great. The orbital period of the satellites is about 107 minutes. See Figure 8 for a general representation of the Transit Positioning System.

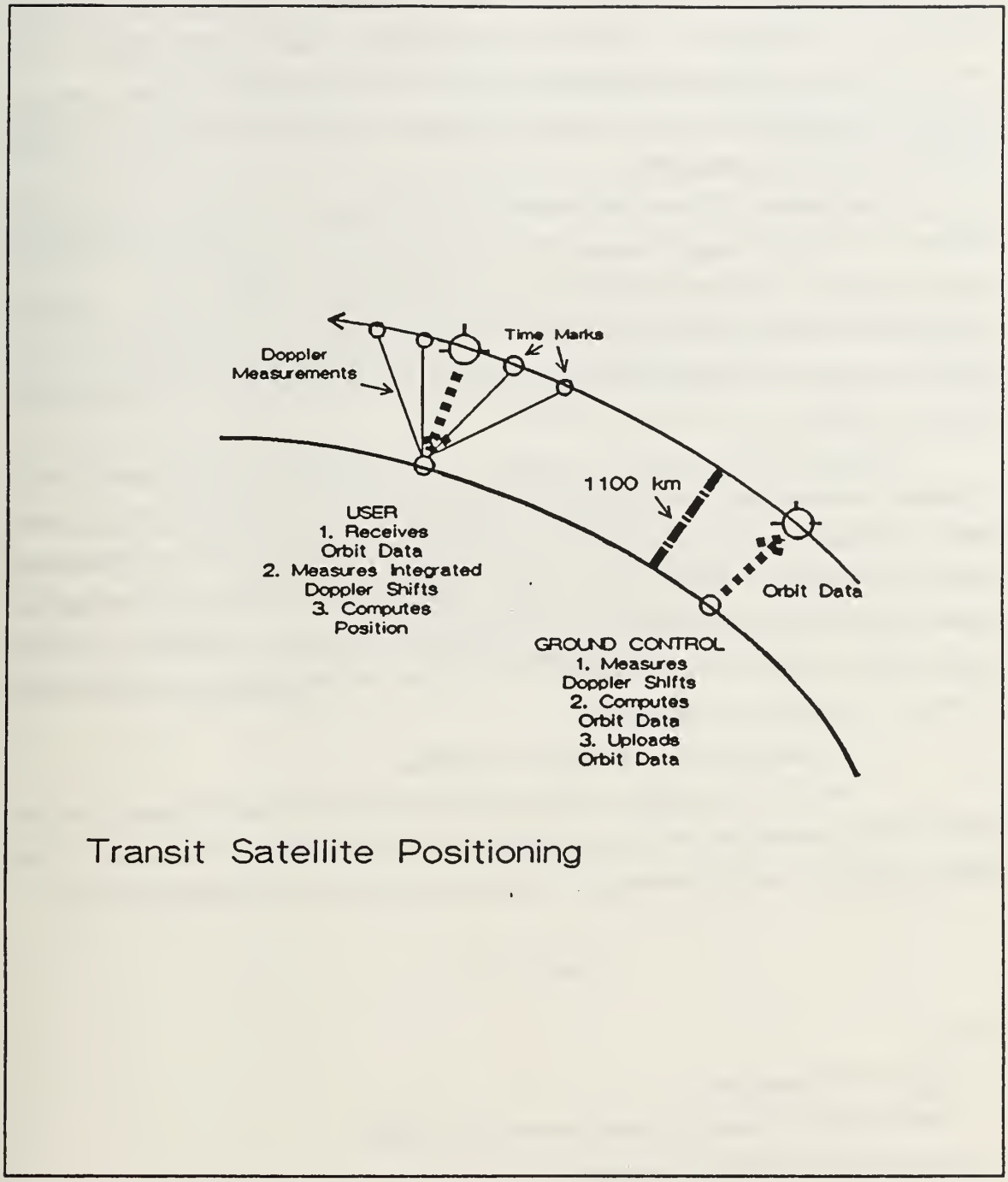

Figure 8. The Transit System: Overview of the Transit Doppler System Segments and Functions

Each satellite transmits two separate frequencies at 400 MHz and 150 MHz. The frequency generation is controlled by a single highly stable crystal oscillator. The use of two frequencies permits the determination of an ionospheric refraction correction. A broadcast message containing orbital information is superimposed on the two carrier frequencies by phase modulation.

Three major differences between GPS and Transit may already be noted; the differences in satellite height, the use of only six satellites as opposed to 24 GPS satellites, and the use of crystal oscillators rather than the more precise atomic oscillators on-board the satellites. By having only six satellites available with fewer than this actually visible, it takes much more time to acquire an equivalent number of Transit observations.

Tracking stations record the Doppler measurements (i.e., the Doppler shift in the frequency transmitted by the satellite) on each satellite pass. This information is relayed to the central processing or control station where the satellite orbits are determined and extrapolated, then this ephemeris data is updated and uploaded to the satellites (about every 12 hours) for subsequent rebroadcast to the user. In addition, a timing station is responsible for monitoring the time signals received from the satellites and adjusting the satellite clocks as needed.

a. The Basic Principle of Doppler Positioning

The received frequency will differ from the transmitted frequency due the Doppler effect because the receiver and satellite are moving relative to each other. If the satellite transmits a stable frequency f_s, then the frequency at the receiver is given by

$$f_r = f_s\left(1 - \frac{\dot{r}}{c}\right)$$

where,

$\dot{r} = \frac{dr}{dt}$ is the range rate

r is the distance or range between receiver and satellite

c is the speed of signal propagation.

The Doppler frequencies (or Doppler shifts) are measured by subtracting the received shifted frequencies f_r from a constant receiver reference frequency f_s (the 400 and 150 MHz frequencies alluded to earlier). The time of closest approach of the satellite is the time when f_r equals f_s. Integrated Doppler measurement techniques that count the number of accumulated cycles of Doppler shift are utilized in most Transit Doppler

receivers. The reason for this is that counting cycles can be performed more precisely than instantaneously measuring the frequency.

The receiver position may be determined by continuously counting the number of cycles of the Doppler frequency. Referred to as the Continuously Integrated Doppler (CID) measurement mode, these observations along with accurate positions for the satellite can be used to establish the receiver position in two dimensions. For three-dimensional positioning, multiple satellite passes must be observed.

The Doppler counts must be corrected for the effects of atmospheric refraction in both the ionosphere and the troposphere. In this respect, all other errors (relativity, earth rotation, etc.) that effected the GPS measurements will be present in the Transit Doppler measurements as well. Attempts, such as error modeling, should be made to minimize their impact.

For the point positioning mode, the one of interest in this study, the observations from multiple satellite passes were collected with a single Doppler receiver over about a four day period. Precise ephemerides were used to compute the satellite positions from which the CT coordinates of the site were determined. The estimated accuracies for a position solution achievable under this type of scenario is believed to be on the order of one meter.

II. EXPERIMENTAL PROCEDURE

A. GENERAL

The Monterey Bay Precision Positioning Experiment was conducted in early December 1990. Aspects of the experiment relevant to point positioning will be emphasized in this and following sections. A large data set of static and kinematic GPS measurements was collected over four consecutive nights, from December 4 through December 7, with four commercially available GPS receivers. Each night's collection session lasted about six hours, from 11:00 p.m to 5:00 a.m. local time. This time window was selected because it was the period of maximum satellite visibility for the week of the experiment. This would permit the tracking of at least four satellites simultaneously, a crucial consideration from the standpoint of kinematic operations (at least four satellites are needed to solve for a three- dimensional position and clock bias). Fortunately, this was also the time when ionospheric effects on the measurements were minimal. All GPS measurements were recorded at a rate of one per second.

The MBPPE static GPS positioning data was collected at the Naval Postgraduate School's Beach Lab in Monterey, California. An array of five marks, refered to as the Doppler Array, was established to serve as the receiver reference points. In order to initialize the kinematic operations, a reference array (the Lobos Array) was established at the Monterey Bay Aquarium Research Institute's pier in Moss Landing, California. One of the points in this array would provide additional static GPS measurements that would be utilized in this thesis. Another site, established on the roof of the NPS Mapping, Charting, and Geodesy building (in Monterey), would supply static GPS measurements for the Selective Availability test. See Figure 9 for a map of the experiment area.

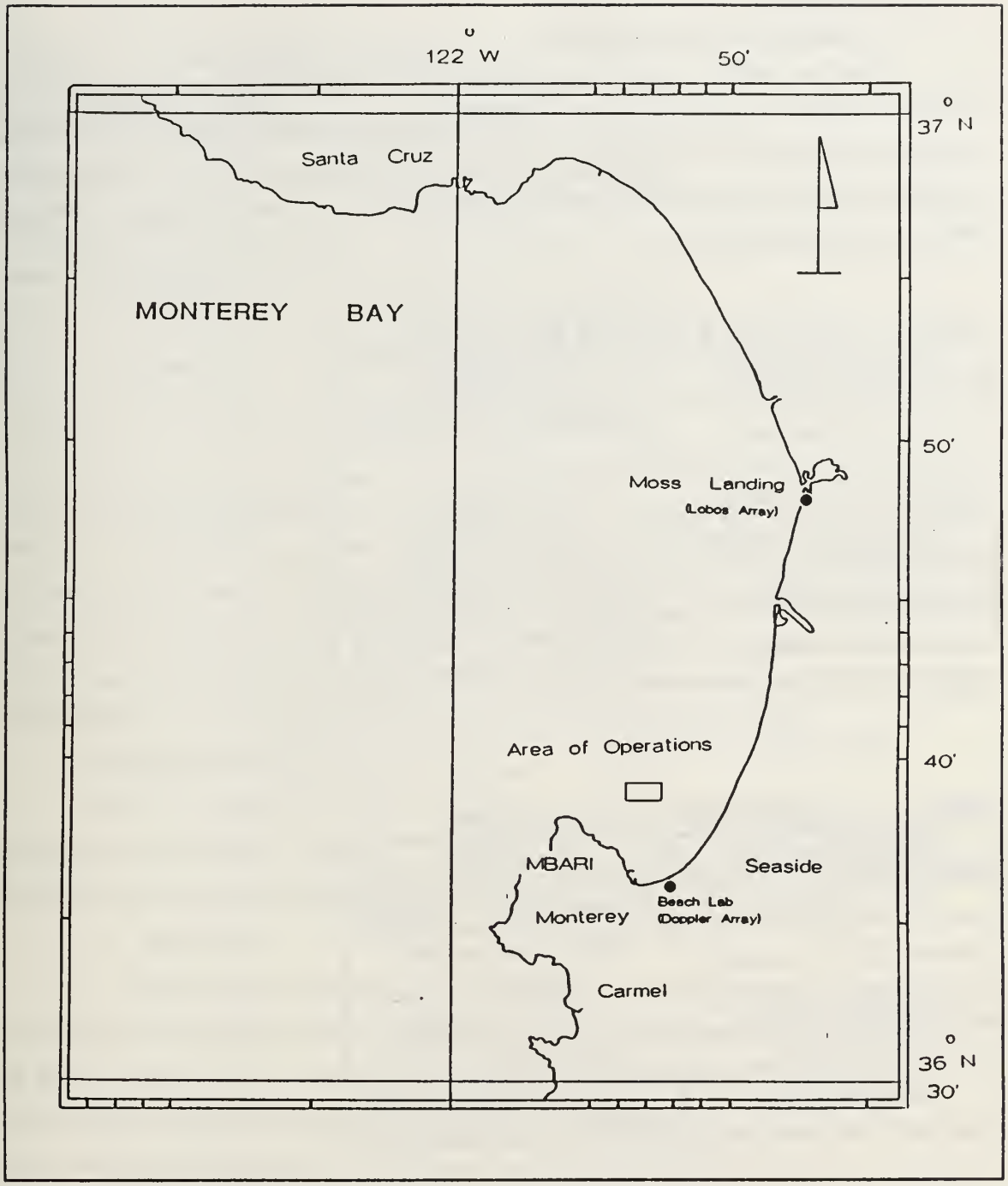

Figure 9. Map of Experiment Area

B. EQUIPMENT

1. Acquisition and Familiarization

The four models of GPS receiver used in the experiment were the TI 4100, the Trimble 4000ST, the Ashtech LD XII, and the Magnavox MX 4200. Two rubidium oscillators accompanied the TI 4100 receivers. For a summary of some of the features available on each, see the following tables (the Magnavox is excluded since it was not used in point positioning).

Table 1. ASHTECH RECEIVER FEATURES

Standard Features	Comments
No. of Channels	12 dual frequency channels
Internal RAM Capacity	6 MB - internal datalogging
Recording Interval	1 second or more
Frequencies	Dual Frequency L1/L2
Measurements	L1/L2 Carrier Phase, C/A Code Pseudorange on L1

Table 2. TRIMBLE RECEIVER FEATURES

Standard Features	Comments
No. of Channels	8 dual frequency channels
Internal RAM Capacity	1 MB - used external datalogger (PC)
Recording Interval	1 second or more
Frequencies	Dual Frequency L1/L2
Measurements	L1/L2 Carrier Phase, C/A code Pseudorange on L1

Two of each type of receiver was acquired either from the vendors themselves or from some other source. The Ashtech, Trimble, and Magnavox models were borrowed from the respective vendors, while the TI 4100s were on loan from the Texas Department of Highways and Public Transportation. The receivers were obtained a few weeks prior to the data collection target dates so that the experiment participants could

Table 3. TI 4100 RECEIVER FEATURES

Standard Features	Comments
No. of Channels	4 dual frequency channels
Internal RAM Capacity	external datalogging via PC only
Recording Interval	1 second or more
Frequencies	Dual Frequency L1/L2
Measurements	L1/L2 Carrier Phase, P code Pseudoranges on L1/L2

become properly familiarized with the equipment. One person was assigned the responsibility of learning the operational aspects of a particular receiver (as applicable to experiment requirements). Once acquainted with the equipment, a document describing the essential details of the receiver operation was drafted by each individual. Then all other participants were cross-trained on the different receivers. This would ensure that everyone would be able to start-up operations and trouble shoot if the situation arose.

2. Equipment Set-Up and Data Collection

One of each type of receiver was located at a static shore site, the Naval Postgraduate School's Beach Lab. The others were located aboard the Research Vessel POINT SUR where the kinematic segment of the experiment was conducted.

a. Beach Lab

Before the commencement of data collection, the locations of the stations over which the individual receiver antennas would be set-up had to be established. At the Beach Lab shore site, the absolute position of a pre-existing mark (identified as DOP) had previously been established by the Transit Doppler method. This was used as the reference mark from which the positions of five new marks would be established (designated DOP1 - DOP5). This configuration of closely spaced shore marks (about five meters separation between marks) was refered to as the Doppler Array. The monuments were set and the positions of the marks were determined by employing conventional terrestrial survey techniques using a steel measuring tape to to obtain distances and a Wild T2000 theodolite to observe horizontal and vertical angles.

After the conclusion of the experiment data collection stage, the Transit Doppler station position for the mark DOP3 was resurveyed using a MX 1502 Transit Doppler receiver furnished by the DMA. Because the position for the mark had been established prior to the October 1989 Loma Prieta earthquake, a post-earthquake position for the mark was required. The Transit Doppler data was collected over four days and was submitted to DMA for the determination of the DOP3 position solution. The positions of DOP3 and the other stations comprising the shore site array were then updated based on the new information produced by this Transit Doppler survey. These were the independent position solutions to which the GPS solutions were compared.

Each receiver-antenna was assigned to an individual monument. The Ashtech antenna was set up over DOP1, the Trimble over DOP2, the Magnavox over DOP4, and the TI4100 over DOP5. Except for the second night of data collection, when two antenna cables were inadvertantly attached to the wrong receivers (affecting the Ashtech and TI receivers), this configuration remained intact throughout the experiment. See Figure 10 for the Doppler Array layout.

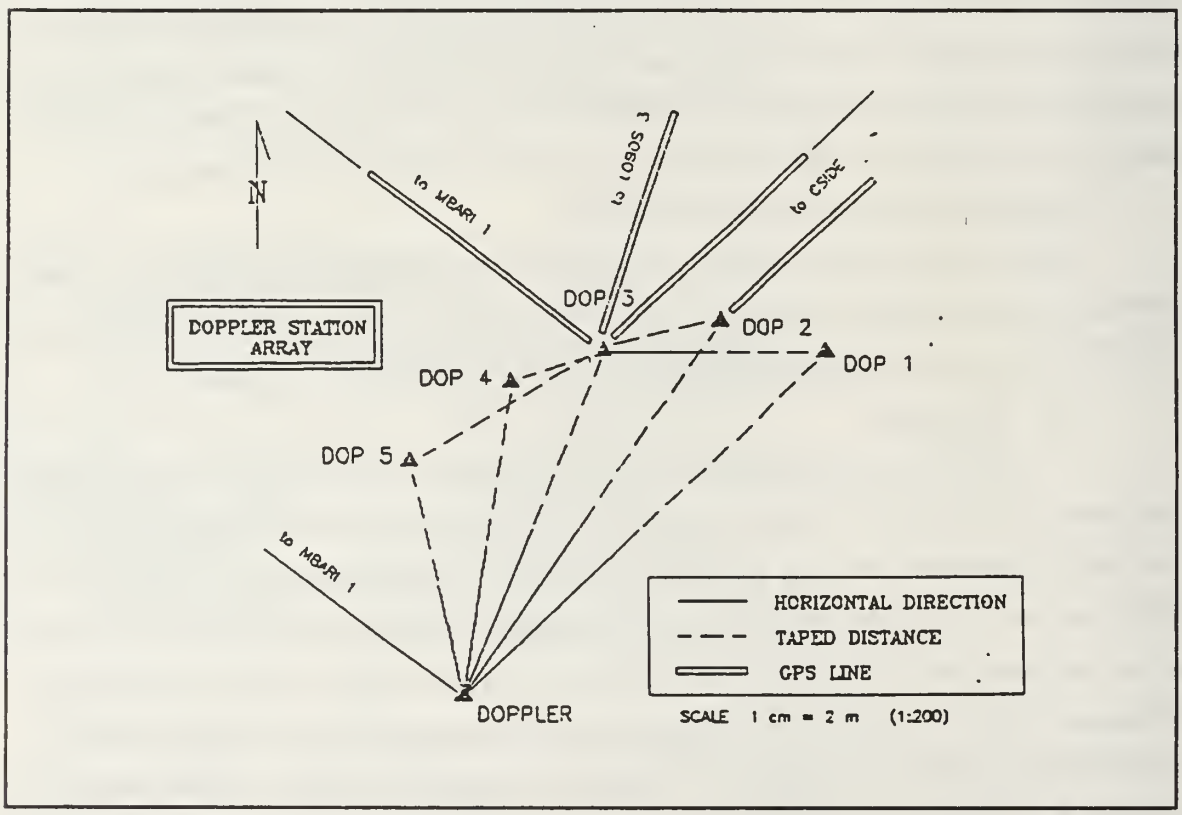

Figure 10. The Doppler Array: The NPS Beach Lab Receiver Monument Sites, Ashtech Set-up Over DOP1, Trimble Over DOP2, TI 4100 Over DOP5

The Krupp Atlas Polartrack range and azimuth laser positioning system was set up over mark DOP3. This was used to determine the reference trajectory of the ship in the kinematic operations.

The heights of the receiver antennas from their marks were measured both at the start and end of nightly operations. These measurements are necessary to adjust the solution from the antenna electrical center to the mark.

Meteorological data (i.e., temperature, pressure, and relative humidity) was not recorded on site but was obtained from the NPS Meteorology Department for the nights of the experiment. Because the location of the School's meteorology recording station is in close proximity to the Beach Lab site (less than 1000 meters), the weather data should closely reflect conditions at the Beach Lab.

b. The Lobos Site

In order to initialize the kinematic operations, the pre-departure and post-arrival positions of the POINT SUR, GPS antenna array (located atop the mast in the crows nest) had to be established. The positions of four reference points located in the vicinity of the POINT SUR's dock were determined for this purpose. This station group is refered to as the Lobos array (See Figure 11).

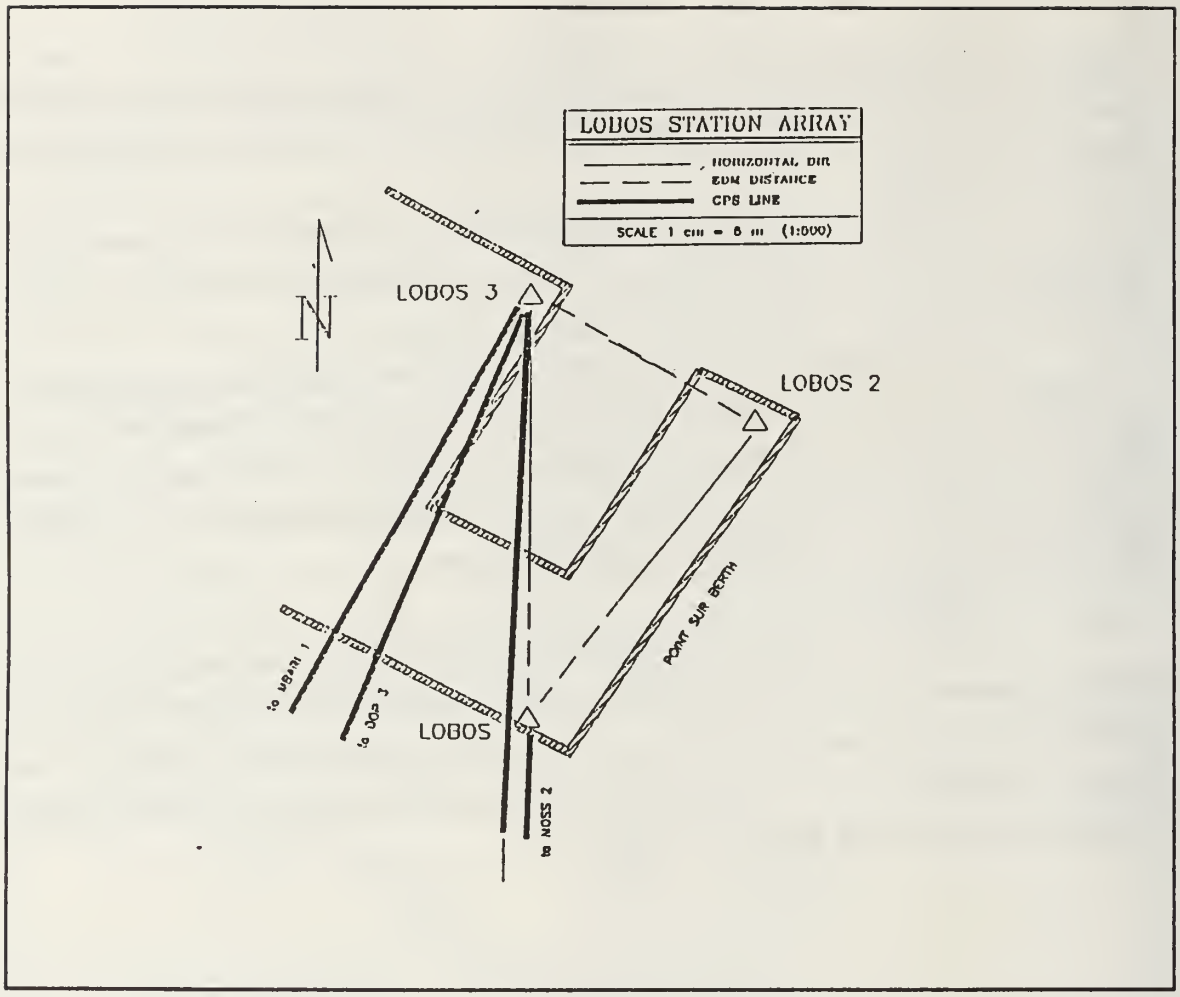

Figure 11. The Lobos Array: The Moss Landing Monument Sites, TI 4100 Receiver Set-up Over LOBOS3

Following the experiment, the position of one of the points, LOBOS3, was resurveyed with both GPS and Transit Doppler. The TI 4100 receiver was used for the GPS survey. The GPS data was collected continously over a three day period (February 5-7, 1991) at a measurement collection rate of 30 seconds. This supplied three independent data sets, one for each day of the survey. The Transit Doppler survey, conducted from January 31 - February 4, 1991, established the Transit Doppler position for the mark. The independent GPS solutions are compared to the Transit Doppler solution in later sections.

The height of the TI 4100 antenna above the mark was measured at at the beginning and at the completion of the three day collection session. Weather data was again obtained from the NPS Meterology Station. Although the degree to which this data accurately represents conditions at Moss Landing is not known, it was felt it should adequately reflect LOBOS3 weather conditions.

In determining the point positions for the Beach Lab and Moss Landing sites, the precise satellite ephemerides and clock models were obtained from DMA for the time of applicability. This provided a comparison of the solutions estimated with this information versus the solutions estimated with the broadcast ephemeris and clock data collected during the surveys.

c. Building 224

As of early July 1991, Selective Availability (SA) had been activated by the DoD. GPS data was collected for two days (July 16 and 17) at a site that had been previouly established on the roof of the NPS Mapping, Charting, and Geodesy center (site: BLDG 224.3). The data was collected with two different TI 4100 receivers at a measurement rate of 30 seconds. The antenna height above the mark was recorded. No weather data was obtained for this test. The data was then processed with GASP using the broadcast ephemeris only and the site position solution was compared to the known site position in order to evalute the effect of SA on the computed position.

III. DATA PROCESSING WITH GASP

A. PROCESSING FLOW OVERVIEW

Before the raw receiver data could be processed, some preliminary operations had to be performed to convert the data into a format suitable to the GASP program. The raw data was translated on a PC into a GASP compatible ASCII format (i.e., FICA or RINEX). The actual procedures and programs involved depend upon the particular receiver and are covered in more detail in the next section. Once the data had been converted and all other required data assembled in the proper formats, the processing was initiated.

GASP consists of two major program units. The first, called the GeoSTAR PREProcessor or STARPREP, accepts input from a FICA or RINEX data file and from files containing satellite ephemeris and clock information, meteorological data, and station information (such as antenna height above mark and a priori station coordinates). STARPREP then computes and applies a series of measurement corrections to the L1 phase biased pseudorange and pseudorange measurements. Once corrected, these measurements are referred to as two-frequency corrected measurements. Also, measurement time tags are adjusted to reflect the correct GPS time of signal transmission and the satellite positions are interpolated to correspond to the corrected time tags. This information, along with the corrected observations and the values computed for the measurement corrections, is output to a "point" file. A station information file is also generated containing the *a priori* station position, antenna height, and other relevant data. These files are subsequently used as the input to the second major program unit, GASP.

The GASP unit accepts input from the point and station files, forms the GASP observable, and performs the estimation for the point position in CT coordinates. See Figure 12 for a general depiction of the processing flow.

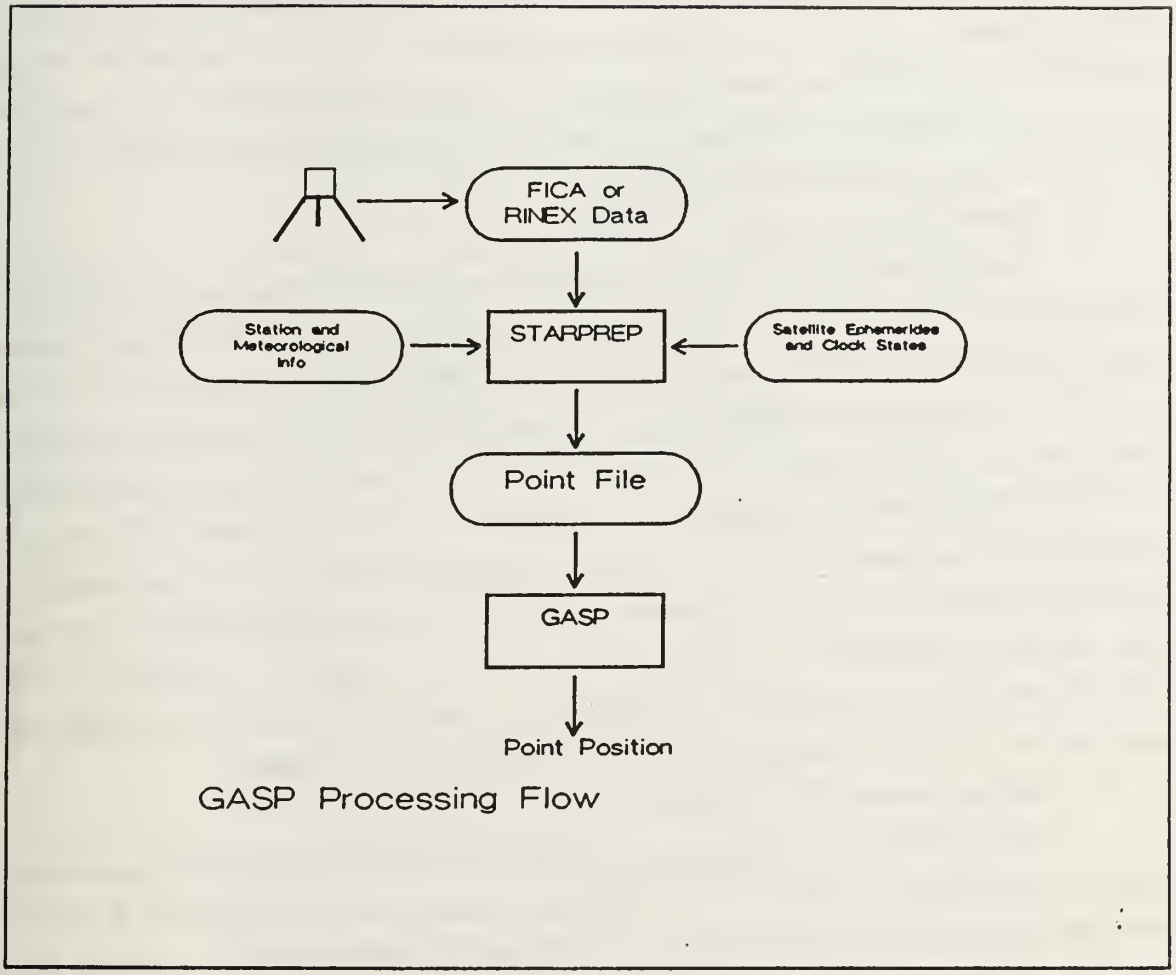

Figure 12. GASP Processing Flow

B. PERSONAL COMPUTER (PC) OPERATIONS

The operations required to convert the receiver data into a GASP acceptable format varied for each receiver. An outline of the general procedure for each receiver is presented.

1. TI 4100 Receiver Data Conversion

The raw tracking data collected with the TI4100 Basic External Processor Program (or BEPP) operating system had to be converted to the Floating point, Integer, Character, ASCII (FICA) format. This involved the use of utility programs developed by the University of Texas, Applied Research Laboratory (UT/ARL). The raw tracking data was converted to the Floating point, Integer, Character (FIC) binary format by the program GS2FIC. This format was then converted to the FICA format by the FICFICA

program. Because the Beach Lab data was collected at a one second measurement rate, it was necessary to decimate the data to 30 seconds in order to alleviate file storage problems. Also, GASP documentation suggests a 30 second measurement rate and over our collection periods it would provide more than a sufficient number of observations to produce meter level position solutions.

2. Trimble Receiver Data Conversion

The first step in the conversion of the Trimble raw tracking data to the RINEX format was to download the data collected by the receiver into a restructured binary format. TRIMVEC (Trimble supplied processing software) accomplished this task. Then the TRRINEX programs, developed by the creators of the RINEX format (a team from the University of Bern, Switzerland), were utilized to convert the Trimble binary format to the RINEX format. The Beach Lab, Trimble data was also decimated to 30 seconds. One difference between the FICA and RINEX formats should be noted at this point, the broadcast ephemeris and clock information obtained by the receivers from the Navigation Message is presented as separate data blocks in a single FICA data file. In the RINEX format, this information is presented as a separate file altogether. This fact became important when considering the RINEX modifications to GASP.

3. Ashtech Receiver Data Conversion

The Ashtech raw data also had to be downloaded before RINEX conversion could be implemented. The Ashtech GPPS processing software performed both the downloading and the RINEX conversion. ASHTORIN was the program used to perform the conversion. It too permitted the Ashtech Beach Lab measurements to be decimated to 30 seconds.

4. PC to VAX Data Transfer

The observation and broadcast ephemeris data, now in either the FICA or RINEX format, had to be transferred to the NPS Digital VAX computer. This is where the GASP programs and program code resided and where processing would be done. The data was transferred to the VAX via 9-track tape using the Overland Data Tape Software, DEPOT program. The precise ephemerides and clock information, furnished by the DMA for the weeks of applicability, were also transfered to the VAX. Meteorological and station data files were created in the GASP specified formats for the different days and receiver stations. See Figures 13 and 14 for examples of the meteorological and station files.

```
91 578 352800.0 1017.012.3 93.0
91 578 356400.0 1018.011.1 93.0
91 578 360000.0 1018.010.0 92.0
91 578 363600.0 1018.010.0 92.0
91 578 367200.0 1018.5 8.6 92.0
91 578 370800.0 1018.5 8.6 91.0
91 578 374400.0 1018.0 8.2 91.0
91 578 378000.0 1018.0 8.2 91.0
91 578 381600.0 1018.0 7.8 90.0
91 578 385200.0 1017.5 7.2 90.0
91 578 388800.0 1017.5 6.6 90.0
91 578 392400.0 1017.5 6.6 90.0
```

Field 1 - 2-digit year identification

Field 2 - GPS week number

Field 3 - GPS time of week

Field 4 - Barometric pressure in millibars

Field 5 - Temperature in Celsius

Field 6 - Relative humidity in percent

Figure 13. Sample STARPREP Meteorological File Contents and Record Description

Record 1

Field 1 - Site I.D. (format I8)
Field 2 - Record type (format A1)
Field 3 - Station I.D. (format F10.0)
Field 4 - Station type (format A1)
Field 5 - Station name (format A30)
Field 6 - Station Latitude in rads (format D16.10)
Field 7 - Station Longitude in rads (format D16.10)
Field 8 - Station Latitude in degrees (format D15.9)
Field 9 - Station Longitude in degrees (format D15.9)
Field 10 - Station height in meters (format F10.6)

Record 2

Field 1 - Site I.D. 2 (format I8)
Field 2 - Record type (format A1)
Field 3 - Site type (format A1)
Field 4 - Antenna offset north of mark (format F8.6)
Field 5 - Antenna offset east of mark (format F8.6)
Field 6 - Antenna height offset (format F8.6)
Field 7 - Year, day of antenna set up (format I5)
Field 8 - Elevation angle cutoff for 16 sv's (format 16F4.1)

Figure 14. Sample STARPREP Station File Contents and Record Description: Sv's, referred to in record 2, field 8, is another term for satellites.

C. DATA FILE EDITS AND RUNSTREAM GENERATION

Prior to STARPREP processing, the following information contained in the FICA or RINEX observation files was validated:

- the *a priori* station coordinates
- the antenna height
- the year, month, and day of session
- week-crossovers

- the PRN numbers of the satellites tracked
- the measurement record interval (or rate)

Special attention had to be paid to the last item since the decimation process did not automatically update the measurement rate in the header block for the TI 4100 data.

Much of the data collected at the LOBOS3 site, corresponding to periods when fewer than three satellites were available, was discarded. This still provided three independent data sets (one for each day of site occupation) of between eight and 11 hours duration at a 30 second recording rate. The BLDG 224.3 data set, collected continuously over two days at 30 seconds, was divided into five independent subsets ranging from about four to nine hours. The data sets and subsets, time spans, and the number of satellites used from the individual data sets are identified in the following tables.

Table 4. BEACH LAB DATA SET IDENTIFICATION AND TIME SPANS

Day	Receiver	Time Span (hours)	No. of Satellites Used
338	TI 4100	6.2	8
	Ashtech	5.6	9
	Trimble	6	9
339	TI 4100	6.2	8
	Ashtech	6	9
	Trimble	6	9
340	TI 4100	7.1	8
	Ashtech	6.8	9
	Trimble	7.5	9
341	TI 4100	6.5	8
	Ashtech	6.9	9
	Trimble	6.7	9

Table 5. LOBOS3 DATA SET IDENTIFICATION AND TIME SPANS

Day	Time Span (hours)	No. of Satellites Used
36	8.6	8
37	10.8	8
38	10.8	8

Table 6. BLDG 224.3 DATA SET IDENTIFICATION AND TIME SPANS

Day	Subset	Time Span (hours)	No. of Satellites Used
197	A	4.8	6
	B	8.4	6
198	C	3.8	5
	D	7.0	6
	E	9.2	6

A runstream on the VAX was generated that signified what data files were to be used as input, output or temporarily created, the unit numbers assigned to each file, which of the available satellites were to be used as the source of observations, whether broadcast or precise ephemeris and clock states were to be used, the corrections to be applied, etc. The runstream is a VAX batch file that begins execution of the STARPREP routine, deletes temporary files at the completion of processing and, in general, controls the processing operations. See Figure 15 for a sample precise ephemeris runstream.

```
$! command procedure to run STARPREP (PRECISE EPHEMERIS AND CLOCKS)
$!-------------------------------------------------------------------
$! The GPS data file (FICA format) must be loaded in
$! the directory: [MALYS.STARFILES].  The Precise Ephemerides
$! and Precise Clock Files must also be located in [MALYS.STARFILES]
$!-------------------------------------------------------------------
$ WRITE SYS$OUTPUT " I AM RUNNING STARPREP. STANDBY, IT WON'T TAKE LONG."
$ set default [bredtheuer.starfiles]
$ define sys$output star341tP.out
$ dir
$ type [bredtheuer.starprep.OBJECT]runstar341RP.com
$ run [bredtheuer.starprep.OBJECT]starprep3
ASGFILES 04 STATIONLOG.DAT
ASGFILES 07 RINDOF2341t.DAT
ASGFILES 10 PTDF2tO341P.PNT
ASGFILES 11 DOF1341A.90N
ASGFILES 12 02BLBAO341T.TEM
ASGFILES 13 06BLBAO341T.TEM
ASGFILES 14 09BLBAO341T.TEM
ASGFILES 15 11BLBAO341T.TEM
ASGFILES 16 12BLBAO341T.TEM
ASGFILES 17 13BLBAO341T.TEM
ASGFILES 18 16BLBAO341T.TEM
ASGFILES 19 18BLBAO341T.TEM
ASGFILES 20 19BLBAO341T.TEM
ASGFILES 24 EF290336.EPH
ASGFILES 25 EF690336.EPH
ASGFILES 26 EF990336.EPH
ASGFILES 27 EF1190336.EPH
ASGFILES 28 EF1290336.EPH
ASGFILES 29 EF1590336.EPH
ASGFILES 30 EF1690336.EPH
ASGFILES 31 EF1890336.EPH
ASGFILES 32 EF1990336.EPH
ASGFILES 36 MIdop20341P.DAT
ASGFILES 37 RCdop20341P.DAT
ASGFILES 38 @Vdop20341P.DAT
ASGFILES 39 STOP2tO341P.DAT
ASGFILES 40 FC90336.EPH
ASGFILES 41 MMET341.DAT
ASGFILES 42 MRCV.DAT
ASGFILES 43 MSAT.DAT
ASGFILES 44 MSTA341.DAT
ASGFILES 51 TEMPO2.TEM
ASGFILES 52 TEMPO6.TEM
ASGFILES 53 TEMPO9.TEM
ASGFILES 54 TEMP11.TEM
ASGFILES 55 TEMP12.TEM
ASGFILES 56 TEMP15.TEM
ASGFILES 57 TEMP16.TEM
ASGFILES 58 TEMP18.TEM
ASGFILES 59 TEMP19.TEM
PROCSEQ  EDIT  TTAGCOR  OATACOR
CMPUTCOR  ID  IR  ER  TH  SC  GR  SA
APPLYCOR  ID  IR  ER  TH  SC  GR  SA
PLOTCORR  ID  IR  ER  TH  SC  GR  SA
EPHEMRIS  P
EDCNTROL  RCVOPT  TOLOPT  METOPT
DEBUGSON  OBUG
LOGICALS  SETERM
SELECTSV  2  6  9 11 12 15 16 18 19
ENDINPUT
$!-----------------------------------------THAT'S ALL THERE IS TO IT
$ DELETE *.TEM;*
$!-----------------------------------------SEND OUTPUT FILES TO GASP
$ rename/log ptOF2tO341P.pnt [bredtheuer.gaspfiles]*
$ rename/log stOF2tO341P.det [bredtheuer.gaspfiles]*
$ deass sys$output
$!
$ write sys$output "STARPREP HAS COMPLETED. See STAR020.OUT for results."
$!
```

Figure 15. Sample STARPREP Runstream for Precise Ephemeris

D. STARPREP

1. Input

Much of the information presented in the following sections on STARPREP and GASP processing is found in Malys, et al [Ref. 1].

STARPREP accepts input data from an observation file (pseudorange and carrier phase measurements in either FICA or RINEX format), broadcast or precise ephemeris and clock data from file input (or in the case of the FICA broadcast ephemeris data as part of the FICA observation file), a meteorological file, and a station file. The carrier beat phase measurements are converted to kilometers by multiplying by the nominal L1 or L2 wavelength. In the TI 4100 FICA observation file, the time of signal transit between satellite and receiver is given rather than the actual pseudorange. This is converted to the pseudorange by multiplying by the speed of light in a vacuum. RINEX presents this as the pseudorange originally so that no conversion to distance units is necessary.

2. Error Models

The time and data corrections applied during the course of STARPREP processing will be briefly discussed and the error models used to compute the corrections presented. This material is originally presented by Malys, et al [Ref. 2: pages 489-491].

a. Time of Transmission

Measurement time tags are adjusted from time of reception (t_r) to time of transmission (t_x) by,

$$t_x = t_r - \frac{\rho_r}{c}$$

where, ρ_r is the pseudorange observation at t_r and

c, the speed of light in a vacuum, equals 299792.458 kilometers per second. See Appendix C for a list of the constants used in the GASP programs.

b. Satellite Clock

For the broadcast ephemeris, the predicted satellite clock parameters available in the navigation message are used to compute the satellite clock offset from GPS time by,

$$\tau_x = a_0 + a_1 (t_x - t_0) + a_2 (t_x - t_0)^2$$

where, t_0 is the time of applicability of a_0, a_1, a_2

a_0 is the predicted satellite clock time offset

a_1 is the predicted frequency offset

a_2 is the predicted frequency drift.

For the precise ephemeris, the precise clock states are used to compute the satellite clock correction at the observation epochs.

c. Receiver Frequency Offset

The TI 4100 receiver L1 and L2 reference signals are offset from the L1 and L2 carrier frequencies by -6000 Hz and +7600 Hz respectively. A correction is computed which removes the number of cycles in the data due to these biases. The epoch of the initial recorded carrier beat phase measurement for a satellite is used as the reference for subsequent carrier phase measurements. For example, the correction for L1 phase data in cycles is given by,

$$N_{rec} = -6000\,(t - t_1)$$

where, N_{rec} is the number of cycle counts

t is some affected epoch, in seconds, and

t_1 is the initial epoch recorded for the satellite, in seconds.

The Trimble and Ashtech receivers do not have offsets in their reference signals so the values assigned to the offsets were set equal to zero for RINEX processing runs with these receivers.

d. Ionosphere

Signal interaction with the free electrons found in the ionosphere produces a change in signal path length. This ionospheric refraction index is frequency dependent so a comparison of measurements on L1 and L2 may be used to derive a dual frequency correction. Defining the quantity Γ as

$$\Gamma \equiv \left[\left(\frac{f_{L1}}{f_{L2}} \right)^2 - 1 \right]$$

a dual frequency ionospheric correction for the pseudorange is given by,

$$d\rho_{r_{L1}} = \frac{(\rho_{r_{L1}} - \rho_{r_{L2}})}{\Gamma}$$

This can only be applied to data collected with the TI 4100 receiver since it is the only model that supplies pseudoranges from the L2 signal.

The dual frequency ionospheric correction for the carrier phase for the TI 4100 receiver is given by,

$$d\rho_{\phi_{L1}} = \frac{(\rho_{\phi_{L1}} - \rho_{\phi_{L2}})}{\Gamma} + \frac{1}{\Gamma}\left[\lambda_{L1}(-6000) - \lambda_{L2}(7600)\right](\Delta t)$$

where, λ_1 and λ_2 are the transmitted wavelengths and Δt is the interval between the initial epoch of observation and the epoch being corrected [Ref. 2 : p. 489]. For the Trimble and Ashtech receivers with no receiver frequency offset, this reduces to,

$$d\rho_{\phi_{L1}} = \frac{(\rho_{\phi_{L1}} - \rho_{\phi_{L2}})}{\Gamma}$$

e. Troposphere

Tropospheric effects are a result of refraction in the neutral atmosphere and are not frequency dependent. This effect may be separated into two components: the dry component, and the wet component. The dry component comprises about 90% of the total effect and is a function of the surface atmospheric pressure and satellite elevation angle. Estimation of the wet component is more difficult than estimating the dry component. It depends on the total water vapor content along the signal path and hence on the temperature, pressure, and humidity.

In GASP, one of two tropospheric models may be selected to compute the integrated tropospheric correction, the Chao or Hopfield models. Both models use surface weather data and the satellite's elevation angles to compute the correction. The temperature, pressure, and relative humidity are used to compute the wet and dry components of the zenith tropospheric delay values (Z_{wet}, Z_{dry}). The satellite elevation angles are then used to compute the wet and dry multipliers (F_{dry}, F_{wet}). The total correction, for either model, may be generally given by,

$$d\rho_{trop} = (Z_{dry} F_{dry} + Z_{wet} F_{wet})$$

See Chao and Hopfield [Refs. 10, 11] for more detailed explanations of these two models.

The Hopfield model was selected as the tropospheric model for all the results produced in this study. A few of the similiarities and differences between the two models should be noted. Both models produce similiar zenith values for the wet and dry

components. The major difference is the dependency of the correction on the satellite elevation angles. The Chao model, originally developed for use in arid locations, is not as accurate as the Hopfield model in estimating the wet tropospheric component off the zenith [Ref. 12].

f. General Relativity

If using the broadcast ephemeris, the general relativity correction is computed as a function of the broadcast orbital elements and is given by,

$$d\rho_{rel} = -2.0 \left[\frac{GM^{1/2}}{c} \right] (e)\,(a^{1/2})\,[\,\sin(E_a)]$$

where, GM, the product of the universal gravitational constant and the Earth's mass, equals $3.986005 \times 10^5 km^3/\sec^2$, and

e is the eccentricity of the satellite orbit

a is the semi-major axis of the satellite orbit

E_a is the eccentric anomaly at the observation epoch.

For a more thorough description of the broadcast orbital elements see Appendix A.

If the precise ephemeris is used, the correction is given by,

$$d\rho_{rel} = \frac{-2.0\,\vec{X} \bullet \vec{V}}{c}$$

where, $\vec{X}$ is the satellite position vector and

$\vec{V}$ is the satellite velocity vector at the observation epoch. See [Ref. 13] for a full explanation of this effect.

g. Earth Rotation

To account for the fact that the Earth is rotating while the signal is traveling from satellite to receiver, the Earth rotation correction is given by,

$$d\rho_{er} = \frac{\omega}{c}\,[(X_2 - X_{r2})\,X_1 - (X_1 - X_{r1})\,X_2]$$

where, ω, the WGS 84 value for the Earth's rotation rate, equals $7.2921151467 \times 10^{-5}$ radians per second,

$\vec{X}$ is the interpolated satellite position vector

$\vec{X}_r$ is the receiver's *a priori* position vector

1, 2 are the vector components along the X and Y axes of the WGS 84 reference frame.

h. Satellite Antenna Offset

The precise ephemeris contains the positions of a satellites center of mass. To adjust this position to the electrical center of the satellites transmitting antenna, this satellite antenna offset is approximated as,

$$d\rho_{sa} = \vec{R} \cdot \vec{S}$$

where, $\vec{R}$ is the range vector from the *a priori* receiver position to the satellite and

$\vec{S}$ is the scaled vector from the satellite's center of mass to the satellite sub-point. $\vec{S}$ is given by,

$$\vec{S} = SA_0 (\hat{e}_x)$$

where, SA_0 is the L-band satellite antenna offset in the nadir direction (0.88m) and

$\hat{e}_x$ is the unit vector from the center of mass of the Earth to the satellite.

The broadcast ephemeris gives the position for the phase center of the satellite transmitting antenna [Ref. 14: p. 83]. This would make application of this adjustment unnecessary when using the broadcast ephemeris. The GASP program does not distinguish between the precise and broadcast ephemeris in this regard. This results in a range error that is common to all satellites when the broadcast ephemeris is used. Because this error is common to all satellites, the GASP algorithm will effectively remove this error.

The data sets were originally processed with this correction applied for both ephemerides. Two of the previously processed data sets were reprocessed using the broadcast ephemeris, this time without the satellite antenna correction applied. The maximum difference for any component over the two data sets was on the order of two centimeters. It can be reasonably concluded that the GASP differencing scheme has eliminated this source of error.

3. Output

The STARPREP preprocessor generates three main files; the point file, the station file, and the output file. GASP accepts the point and station files as input. The output file contains plots of all the applied data corrections for each satellite over time, plots of the uncorrected range and carrier phase measurements over time, and a summary of file information. This file is helpful in identifying problems that may have arisen

during the course of processing. The point file contains the two-frequency corrected observations, the values computed for the individual corrections, the corrected measurement time tags, and the interpolated satellite positions (in CT coordinates) corresponding to the corrected time tag. The station file contains the *a priori* station coordinates and the height of the antenna above the mark. See Figure 16 for a general summary of STARPREP processing.

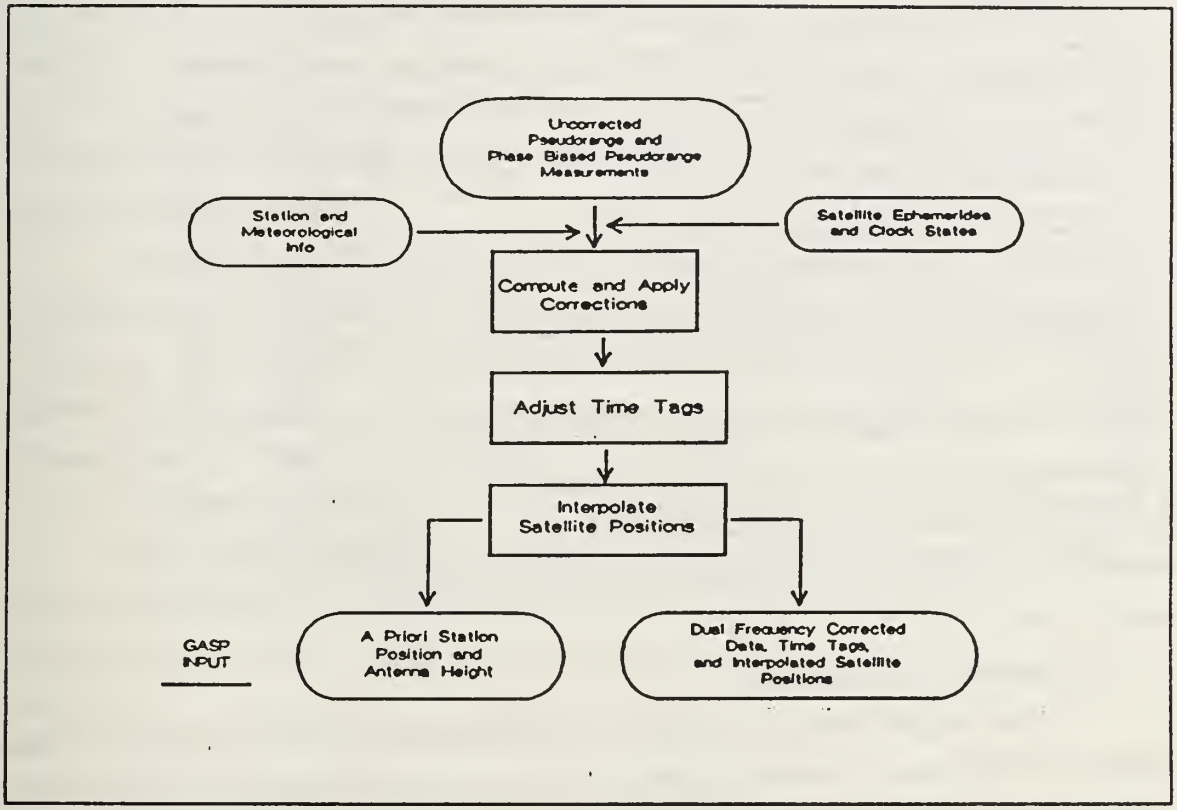

Figure 16. STARPREP Processing

E. GASP

1. GASP Runstream Generation

Prior to GASP processing, a GASP runstream was created. This runstream specifies the station and point files to be used as input, assigns a filename to the GASP output file, and if desired, permits the selection of non-standard GASP processing options. Standard options preset certain processing values or features but these may be overridden by the operator. See Table 7 for a list of the available processing options and standard values and features.

Table 7. GASP RUNSTREAM PROCESSING OPTIONS AND STANDARD VALUES OR FEATURES

Processing Options	Standard Values or Features
Plot to Printer	P
Elevation Angle Cutoff (Degrees)	15
RMS Screening Multiplier	3.00
Pseudorange Editing Tolerance (meters)	5.00
Estimate Fourth Parameter	N
Minimum of 'N' Satellites Per Epoch Pair	2
Use Offset to *A Priori* Station Position	N
Standard Deviation on GASP Observables (cm)	20.0
Standard Deviation on A Priori Position Components (km)	0.05
PRN Number as 'Base' Sat, Default is 00 for Sequencing	00
Number of Batch Least Squares Iteration	3
Number of Sequential Estimation Iterations	1

2. Automatic Data Editing

After the point and station files have been entered into GASP, two kinds of data editing are performed to ensure consistency between the pseudoranges and phase biased pseudoranges observed from each satellite. First, the corrected pseudoranges over two successive epochs are subtracted and the corrected phase biased pseudoranges corresponding to the same epochs are also subtracted. If these "delta" ranges differ by more than some user specified tolerance, the GASP observables (i.e., the two carrier based phase biased pseudoranges) are rejected from the data set. This is referred to as pseudorange editing. Note that this is the only use of the corrected pseudoranges. They serve only to monitor the phase biased pseudoranges for outliers and are not used in the estimation process.

For the processing runs performed for this study, the standard pseudorange editing tolerance of five meters was initially selected. After a few runs with the Trimble and Ashtech receiver data, it became apparent that a significant percentage of the data was being rejected from the data set (on the order of 35% or more). In order to avoid

this, the pseudorange editing tolerance was relaxed to ten meters. This held down the amount of data rejected to under 20 percent in most cases. There are two possible explanations for why such a large amount of data was rejected. The first, and most probable, an ionospheric correction could not be computed for the Trimble and Ashtech pseudorange data since no pseudorange measurements were supplied on the L2 signal for these receivers. This would produce some discrepancy between the corrected pseudorange and the phase biased pseudorange where an ionospheric correction was applied. A second possible explanation is that the pseudoranges are observed from the C/A-code modulations rather than the more precise P-code modulations. The increased measurement noise on the C/A-code observations may also have contributed to the higher rejection figures.

The second edit test performed on the data uses the Root-Mean-Square (RMS) of the residuals of the previous iteration as the rejection criterion. The RMS is initialized before the first iteration. Any phase biased pseudorange observables with a residual greater than three times the RMS of the previous iteration are rejected from the data set. These editing schemes are executed prior to the formation of the GASP observable.

3. The GASP Observable

The between-epoch single difference equation is used to form what is known as the GASP observable. Two consecutive carrier based phase biased ranges from the same satellite are differenced. Recall that this between-epoch single difference equation was given by,

$$\delta\rho_\phi = \delta\rho - c\,(\delta d\tau - \delta\tau_p)$$

This between-epoch difference is then differenced with the corresponding between-epoch difference from another satellite. The resulting equation is given by

$$\begin{aligned}\Delta\delta\rho_\phi &\equiv \delta\rho_\phi^\alpha - \delta\rho_\phi^\beta \\ &= (\delta\rho^\alpha - \delta\rho^\beta) - c\,(\delta\tau_x^\beta - \delta\tau_x^\alpha + \delta\tau_p^\alpha - \delta\tau_p^\beta)\end{aligned}$$

where α and β signifies the two satellites. It may be expressed more conveniently as,

$$\Delta\delta\rho_\phi = \Delta\delta\rho - c\,(\Delta\delta\tau_x - \Delta\delta\tau_p)$$

Since the satellite clock errors and the errors associated with various other sources have been modeled, the equation becomes,

$$\Delta\delta\rho = \Delta\delta\rho_{\phi} + c\,(\Delta\delta\tau_x - \Delta\delta\tau_p)$$

The value $\Delta\delta\rho$ is the GASP observable. See Figure 17 for a conceptual representation of the GASP observable.

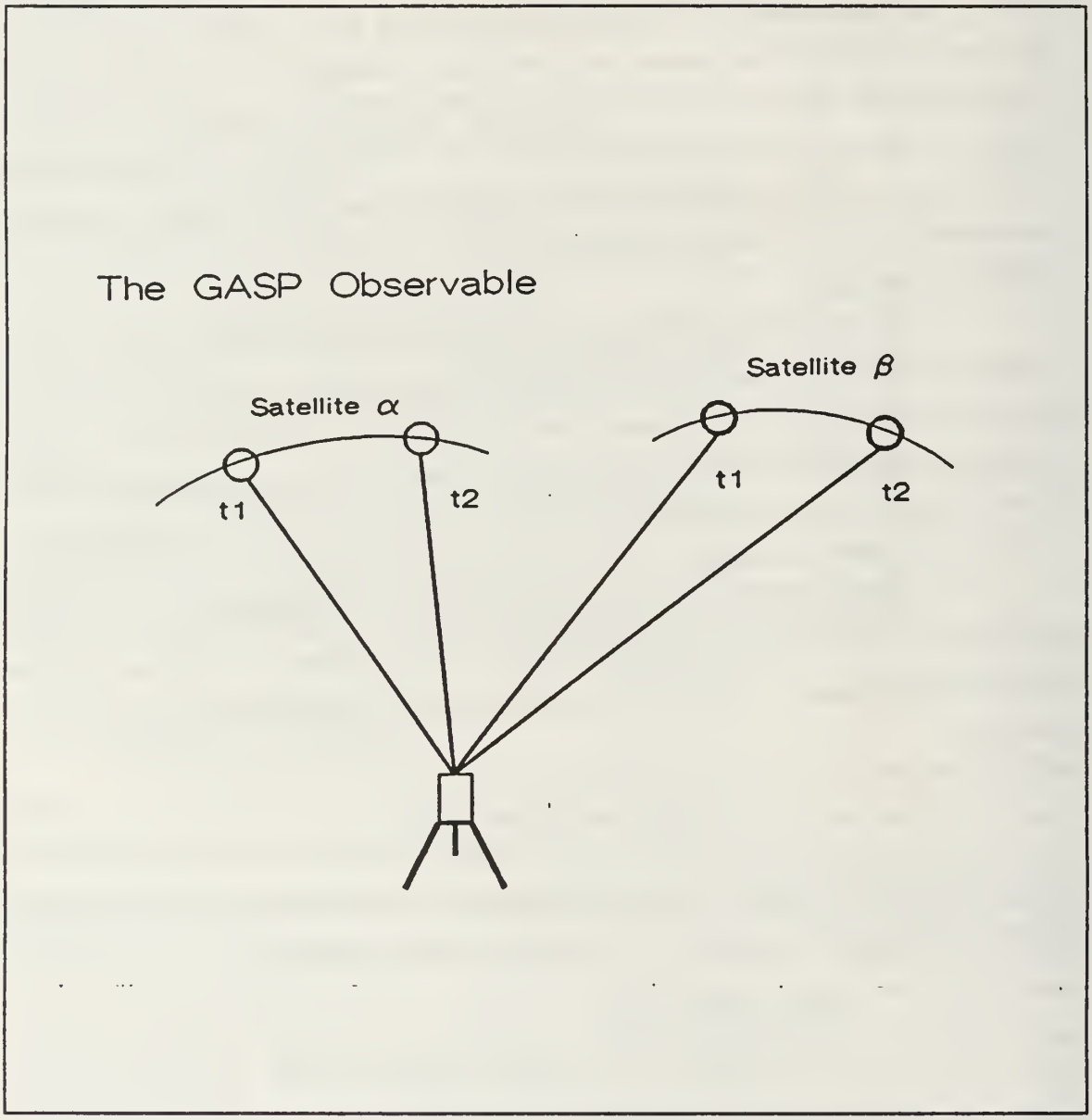

Figure 17. The GASP Observable: Differencing Over Satellites Over Two Consecutive Measurement Epochs

This type of differencing scheme reduces the effects of errors in satellite clocks and orbits, and removes receiver clock errors and integer ambiguities. For a four channel receiver with all channels simultaneously tracking satellites, three GASP observables can be formed for a given epoch pair. At least two satellites per epoch pair are required to form an observable for that epoch pair. For each epoch pair, one satellite is used as the reference from which the others are differenced. The reference satellite is selected sequentially, so that for every new epoch pair processed, the next higher satellite PRN number is used as the reference. The selection sequence cycles back to the lowest PRN number once the list of tracked satellites is exhausted. Individual epochs are used only once to form an observable.

Reference satellite sequencing reduces correlation among the observables. Precision, the RMS of the residuals, and the variance-covariance matrices of the estimated parameters are all improved using this type of satellite selection rather than selecting the satellite with the most stable clock as the reference. [Ref. 1: p. 24]

For example, if the L1 phase biased pseudoranges are represented by ρ_ϕ , four satellites simultaneously tracked signified by superscripts α, β, γ, and η (in order of ascending PRN number), and four consecutive epochs represented by subscripts 1, 2, 3, and 4, a between-epoch difference can be formed for each satellite given by

$$\rho^{\alpha}_{\phi_1} - \rho^{\alpha}_{\phi_2} = \delta\rho^{\alpha}_{\phi_{12}}$$

$$\rho^{\beta}_{\phi_1} - \rho^{\beta}_{\phi_2} = \delta\rho^{\beta}_{\phi_{12}}$$

$$\rho^{\gamma}_{\phi_1} - \rho^{\gamma}_{\phi_2} = \delta\rho^{\gamma}_{\phi_{12}}$$

$$\rho^{\eta}_{\phi_1} - \rho^{\eta}_{\phi_2} = \delta\rho^{\eta}_{\phi_{12}}$$

The three GASP observables formed by satellite sequencing for this first epoch pair are given by,

$$\delta\rho^{\alpha}_{\phi_{12}} - \delta\rho^{\beta}_{\phi_{12}} = \Delta\delta\rho^{\alpha\beta}_{\phi_{12}}$$

$$\delta\rho^{\alpha}_{\phi_{12}} - \delta\rho^{\gamma}_{\phi_{12}} = \Delta\delta\rho^{\alpha\gamma}_{\phi_{12}}$$

$$\delta\rho^{\alpha}_{\phi_{12}} - \delta\rho^{\eta}_{\phi_{12}} = \Delta\delta\rho^{\alpha\eta}_{\phi_{12}}$$

Then using β as the reference satellite for the next epoch pair at 3 and 4, the GASP observables are given by,

$$\delta\rho^{\beta}_{\phi_{12}} - \delta\rho^{\alpha}_{\phi_{12}} = \Delta\delta\rho^{\beta\alpha}_{\phi_{12}}$$

$$\delta\rho^{\beta}_{\phi_{12}} - \delta\rho^{\gamma}_{\phi_{12}} = \Delta\delta\rho^{\beta\gamma}_{\phi_{12}}$$

$$\delta\rho^{\beta}_{\phi_{12}} - \delta\rho^{\eta}_{\phi_{12}} = \Delta\delta\rho^{\beta\eta}_{\phi_{12}}$$

The next epoch pair at 5 and 6 would use satellite γ as the reference and epoch pair 7 and 8 would use satellite η. Reference selection would then return to satellite α for epoch pair 9 and 10.

4. Batch Least Squares and Sequential Estimation

After the GASP observables have been formed, a least squares technique is used to estimate the station position components in the CT coordinate system. These are the only parameters estimated. A clock correction parameter is not estimated. It is assumed that the modeled satellite clock states have sufficiently aligned the satellite clocks to GPS time and that the receiver clock error has been removed by differencing. The interpolated satellite positions are held fixed in the estimation providing the reference frame in which estimation takes place. After three iterations of a batch least squares, the estimated parameters, the variance-covariance matrix for the parameters, and the RMS of the residuals provide the input to the second estimation step (for more on the least squares method see Appendix B).

This is a sequential estimation algorithm based on a Kalman filtering routine. The Kalman state is the receiver position vector. It does not include any clock states. Fundamentally, a Kalman filter updates measurements from one observation epoch to the next. This allows the parameter estimates and covariances to be updated at each measurement epoch. The batch method provides a measure of data noise to the sequential processor. The final RMS of the residuals from the batch processor is taken as the variance of one GASP observable processed through the sequential processor. Since the sequential processor updates the station coordinates for each new observable processed, the estimated station coordinates can be plotted as a function of time. Plots of the covariances and convergence in CT coordinates as a function of time may also supplied.

For the processing runs performed in this study, a comparison was made between the final batch least squares component estimates and the final component esti-

mates that had passed through the sequential processor. The magnitude of the mean component differences, averaged for all processing runs using the precise ephemeris, was about 15 centimeters.

5. Output

The most important information contained in the output file generated by GASP is the estimated station position. This is presented as the X, Y, and Z coordinates of the CT coordinate system and in geodetic coordinates; latitude, longitude, and height (ϕ, λ, h) relative to the WGS-84 ellipsoid. Estimates for the uncertainty in the coordinates is obtained from the variance-covariance matrix for the estimated parameters. A correlation matrix is computed that expresses the linear independence among the estimated parameters from the parameter variance-covariance matrix. *A posteriori* standard deviations for the estimated station coordinates are obtained by taking the square root of the diagonal elements (i.e., the variances) of the variance-covariance matrix. These provide estimates for the precision of the estimated point position components. The GASP processing sequence is graphically depicted in Figure 18.

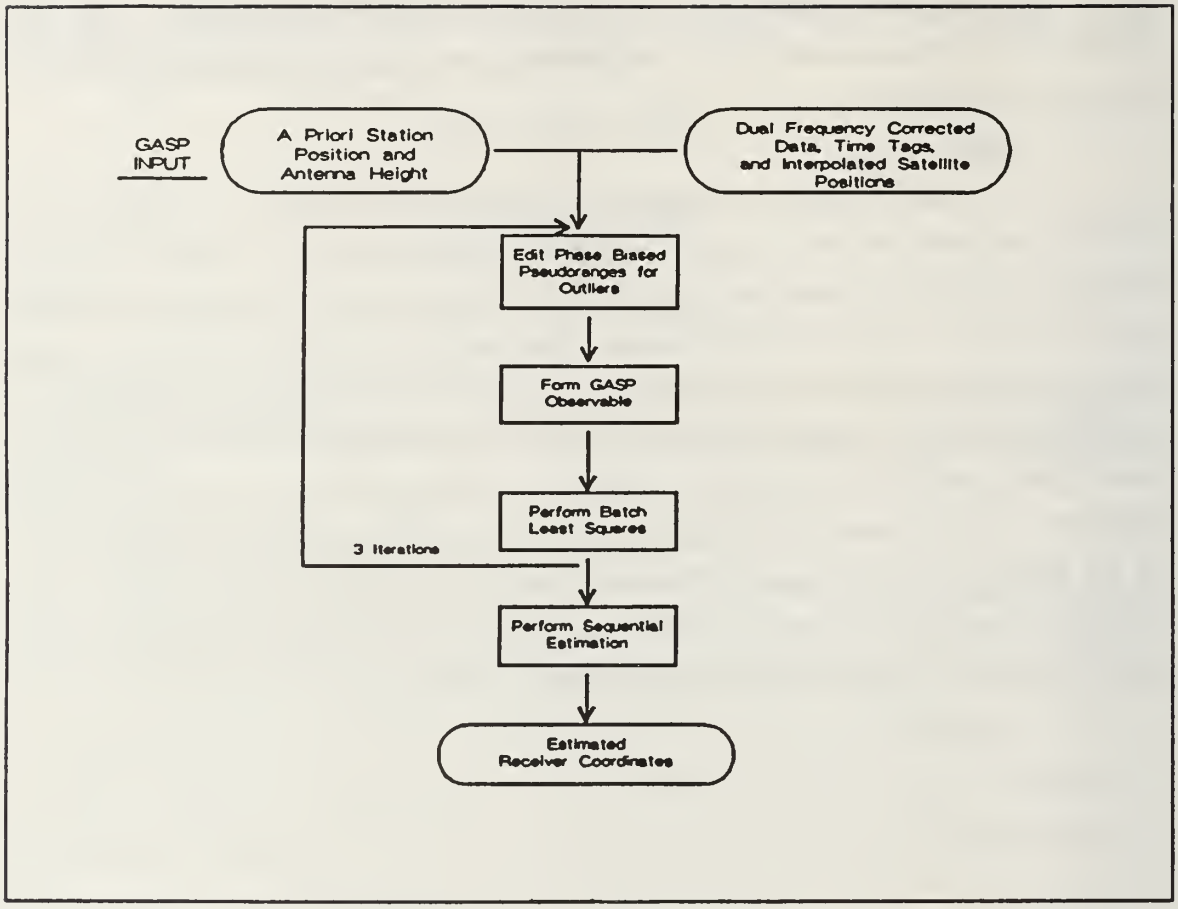

Figure 18. GASP Processing

F. PROGRAM MODIFICATIONS

In order for GASP to accept the data collected with the Trimble and Ashtech receivers, it was necessary to modify the program to allow the introduction of data presented in the RINEX format.[2] This meant altering some existing program units and creating two new program modules for STARPREP. The first reads the RINEX observation file. The STARPREP subroutines BLK006 and BLK124 that read the FICA measurement and station data blocks were used as models in building the RINEX subroutine. The second module, called RINNAV, reads the RINEX navigation file that contains the broadcast ephemeris information. It was modeled after the STARPREP

---

2 RINEX data may be presented in one of two possible forms; the original RINEX format and the RINEX 2 (version 2) format. GASP processing runs utilized data presented in the original RINEX format. Program code designed to process data in the RINEX 2 format, although present, is untested. [Ref. 15]

subroutine BLK009 that reads the FICA data blocks containing the broadcast ephemeris data.

To differentiate between FICA format and RINEX format input, a file naming convention was implemented. The program path to read either format is keyed to the first four characters of the input observation filename. For the RINEX data collected with the Ashtech receiver, the first four characters of the filename **must** be RINA. For the RINEX Trimble data, the first three characters **must** be RIN and the fourth character anything other than A. For FICA data collected with the TI 4100, the first three characters may be anything except RIN. The reason for distinguishing between the RINEX Ashtech and Trimble data is due to a problem that occurred during processing. A wavelength factor of one was specified for the L1 signal and a wavelength factor of two specified for the L2 signal in the RINEX observation file for both the Ashtech and Trimble receivers. Using these wavelength factors with the Ashtech receiver caused all the observables to be rejected by the pseudorange edit. This was because of an incompatibility between the internal receiver software and the receiver hardware. Apparently, the receiver software had not been updated to reflect changes in the hardware. To circumvent this problem, the L2 wavelength factor for the Ashtech receiver is reset to one based on the RINEX filename. Once the receiver software is updated, the program statement that resets the wavelength factor will need to be deleted.

Also keyed to the filenames are values assigned to the receiver frequency biases. The TI 4100 receiver incorporates receiver frequency biases of -6000 Hz on the L1 signal and 7600 Hz on the L2 signal. The Ashtech and Trimble receivers do not incorporate these biases.

Because the Trimble and Ashtech receivers possess more tracking channels than the TI 4100 and could thus supply simultaneous observations from more satellites, we felt we should take advantage of this feature by modifying GASP to accomodate data collected on these additional channels. The Trimble receiver records observations on eight dual frequency channels and the Ashtech receiver on twelve. Because increasing the dimensions of the program arrays might cause space problems and adversely affect processing, a cautious approach was taken and storage expanded to accomodate eight channels per epoch. Basically, this was accomplished by simply redimensioning the arrays that stored the input measurements, two-frequency corrected observations, time tags, and interpolated satellite positions.

The program revisions to include more channels led to modifications to expand the maximum number of satellites that could supply observations over the course of a col-

lection session. The previous limit of eight was changed to twelve. Thus, the number of satellites allowed per collection session should not be a limiting factor to the potential benefits of using more receiver channels. If twelve satellites per session were to be utilized, allowances for additional files associated with the extra satellites (and the RINEX broadcast ephemeris file) would be necessary. The maximum number of permissible program files was reset from 60 to 62 and program statements assigning unit numbers to particular files or setting limits on the unit numbers for certain file groups (such as the precise ephemeris and temporary files) were respecified. Specifically, the unit number assigned to the RINEX broadcast ephemeris file is 11, the upper and lower limits on the unit numbers for the first set of temporary satellite files changed to 12 and 23, limits on the precise ephmeris files changed to 24 and 35, limits on the output data files changed to 36 and 39, and the limits on the last group of temporary files changed to 51 and 62.

IV. RESULTS AND ANALYSIS

In order to provide some measure for the accuracy of the computed positions, the known station position components are differenced from the GPS CT estimated position components for the various receivers and collection sessions. The known station positions are the Transit Doppler positions. This supplies the ΔX, ΔY, and ΔZ offsets from the "true" positions. Component differences ΔX, ΔY,and ΔZ are converted to ΔE, ΔN, and ΔU (in local, cartesian east, north, and up coordinates) because this is a more familiar and easily comprehended reference frame. The following discussion and analysis will concentrate on the tables and plots that present the results in the local east, north, and up coordinate system. For the reader interested in the results presented in CT coordinates (X, Y, and Z), see the tables in Appendix D.

The difference results are displayed in the form of tables and associated target plots. In the target plots, the Transit positions are represented by the origin and the symbols depict the values computed for the component differences. The GASP estimated formal error (one sigma) standard deviations are presented as the $\pm$ terms in the difference tables or as error bars in the difference plots.

The known station positions are the Transit Doppler derived positions. Mark BLDG 224.3 was established by a GPS relative positioning survey using the Transit Doppler mark DOP3 as the reference. See Appendix E for a summary of the estimated positions and estimated standard deviations on the positions for both the Transit Doppler and GPS point determinations.

Repeatability, also defined as precision, yields a measure for the consistency of a given set of position results. The repeatability is determined by calculating the mean and the standard deviations (i.e., the observed errors) on a set of position component differences. Two types of repeatability were determined. One averages over days by receiver accentuating the differences between the receivers. The other averages over receiver by day accentuating the difference between days. In the repeatability target plots, the mean differences are represented by the target symbols and the standard deviations are represented by the error bars.

A. BEACH LAB RESULTS

Table 8 presents the accuracy results of the Ashtech, Trimble, and TI 4100 receivers for the Beach Lab collection sessions using the broadcast ephemeris for the satellite po-

sitions. It can be seen from this table and the corresponding target plots (figures 19 and 20) that the GASP estimated components give fairly good agreement with the Transit Doppler estimates. The average Root-Sum-Square (RSS) of the component differences (i.e., the magnitude of the difference vector) is at about the two meter level. The origin is within the ensemble of the position differences and formal errors. The estimates produced with the TI 4100 receiver were slightly better overall than the Trimble and Ashtech estimates but all were comparable. The Trimble results are the most widely dispersed and the Ashtech results slightly less scattered. The TI 4100 results exhibited the least dispersion of the three receivers.

It also appears that, between the differences computed in the north and east directions, the greatest dispersion is produced in the east, i.e., the estimated east components are less precise than the north. For all three components, the north component shows the least dispersion i.e., the best agreement is between the GASP estimated north component and the Transit Doppler north component. Comparison of the ΔH and ΔU component differences shows more dispersion in the vertical than in the horizontal.

A lack of overlap between the GASP estimated formal errors, due to the scatter of the component differences, is also conspicuous. This suggests that the GASP formal errors underestimate the actual observed errors. The GASP formal errors appear to underestimate error in the east component to a greater degree than the north component. The dispersion of the vertical versus the horizontal differences suggests, overall, the GASP estimated errors were better at representing the horizontal errors than the vertical. This visual interpretation is supported by the values computed for the bottom line of the table which shows the mean component differences and standard deviations on the means over all receivers and days. The numbers indicate that the east and up components were underestimated by a factor of about three and the north by a factor of approximately two.

Also, as compared to the differences computed for the other three days, the day 339 results seem "off". This may be due to poorer broadcast ephemeris satellite positions for this day.

Table 8. BEACH LAB COMPONENT DIFFERENCES (ΔE, ΔN, ΔU) USING BROADCAST EPHEMERIS: Solution Differences Between GPS and Transit Doppler Methods, Second Term is GASP Estimated Formal Error, RSS is Magnitude of the Difference Vector

Day of Year 1990	Receiver	ΔE (m)	ΔN (m)	ΔU (m)	ΔH (m)	RSS (m)
338	TI 4100	$-0.6 \pm .6$	$-1.4 \pm .6$	$0.3 \pm .5$	$1.5 \pm .8$	1.6
	Ashtech	$0.3 \pm .6$	$0.1 \pm .4$	$-1.8 \pm .5$	$0.4 \pm .7$	1.9
	Trimble	$-0.6 \pm .6$	$1.1 \pm .4$	$-2.5 \pm .5$	$1.3 \pm .7$	2.8
339	TI 4100	$-0.4 \pm .6$	$-1.5 \pm .6$	$1.7 \pm .5$	$1.6 \pm .8$	2.3
	Ashtech	$3.3 \pm .7$	$1.0 \pm .5$	$-3.5 \pm .5$	$3.4 \pm .8$	4.9
	Trimble	$2.9 \pm .6$	$1.2 \pm .5$	$-3.9 \pm .5$	$3.1 \pm .7$	5.0
340	TI 4100	$-0.6 \pm .5$	$-0.6 \pm .5$	$0.5 \pm .5$	$0.9 \pm .7$	1.0
	Ashtech	$0.8 \pm .6$	$-0.1 \pm .5$	$-1.9 \pm .5$	$0.8 \pm .6$	2.1
	Trimble	$0.4 \pm .5$	$0.8 \pm .4$	$-1.5 \pm .4$	$0.8 \pm .6$	1.7
341	TI 4100	$1.4 \pm .5$	$-0.8 \pm .5$	$-0.5 \pm .4$	$1.6 \pm .7$	1.7
	Ashtech	$-1.8 \pm .5$	$0.3 \pm .4$	$-0.5 \pm .5$	$1.8 \pm .6$	1.9
	Trimble	$0.3 \pm .5$	$-0.0 \pm .4$	$0.2 \pm .5$	$0.3 \pm .6$	0.4
Mean Component Difference and Standard Deviation about Mean		0.5 ± 1.5	$0.0 \pm .9$	-1.1 ± 1.7	1.5 ± 1.0	2.2 ± 1.3

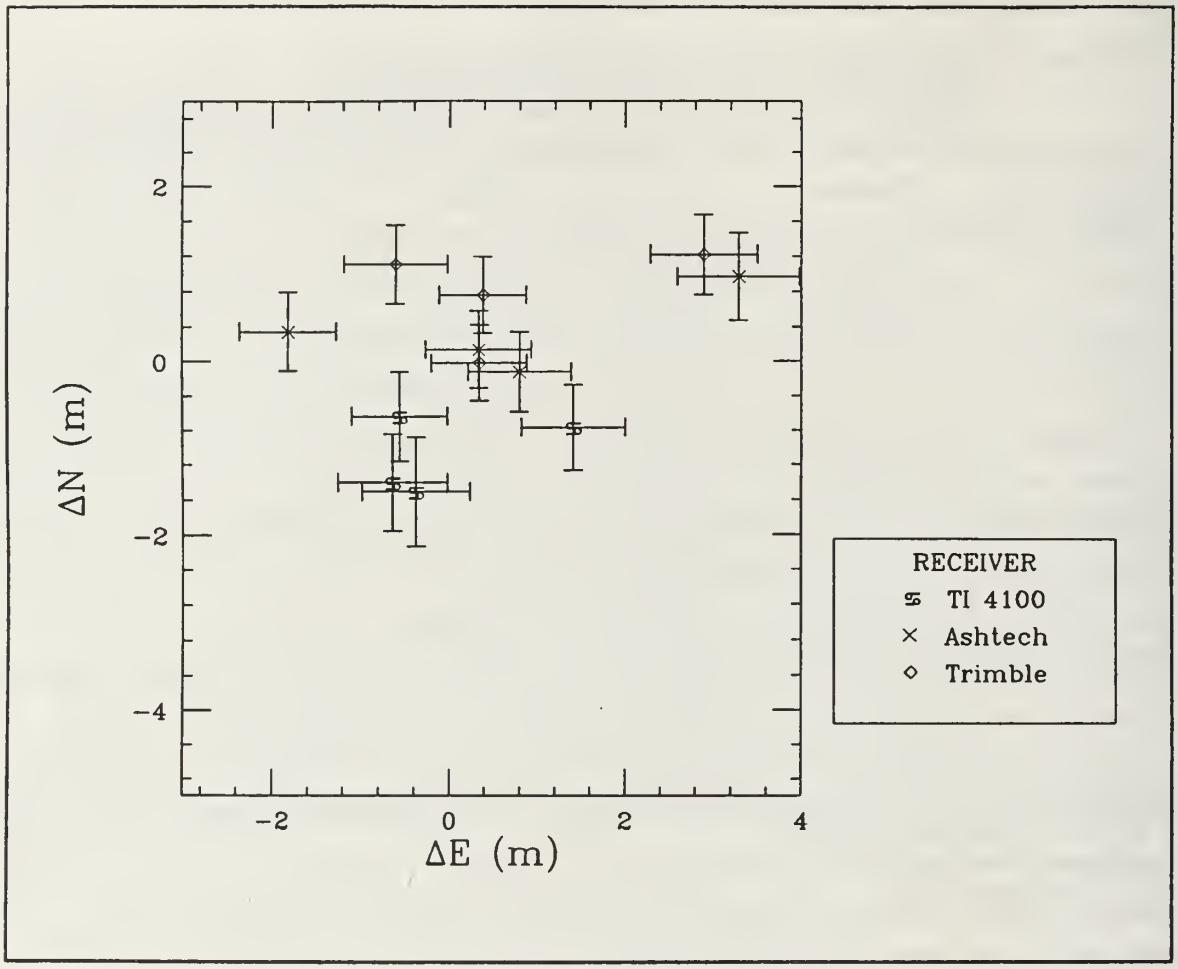

Figure 19. ΔEast versus ΔNorth for Beach Lab, Broadcast Ephemeris Data

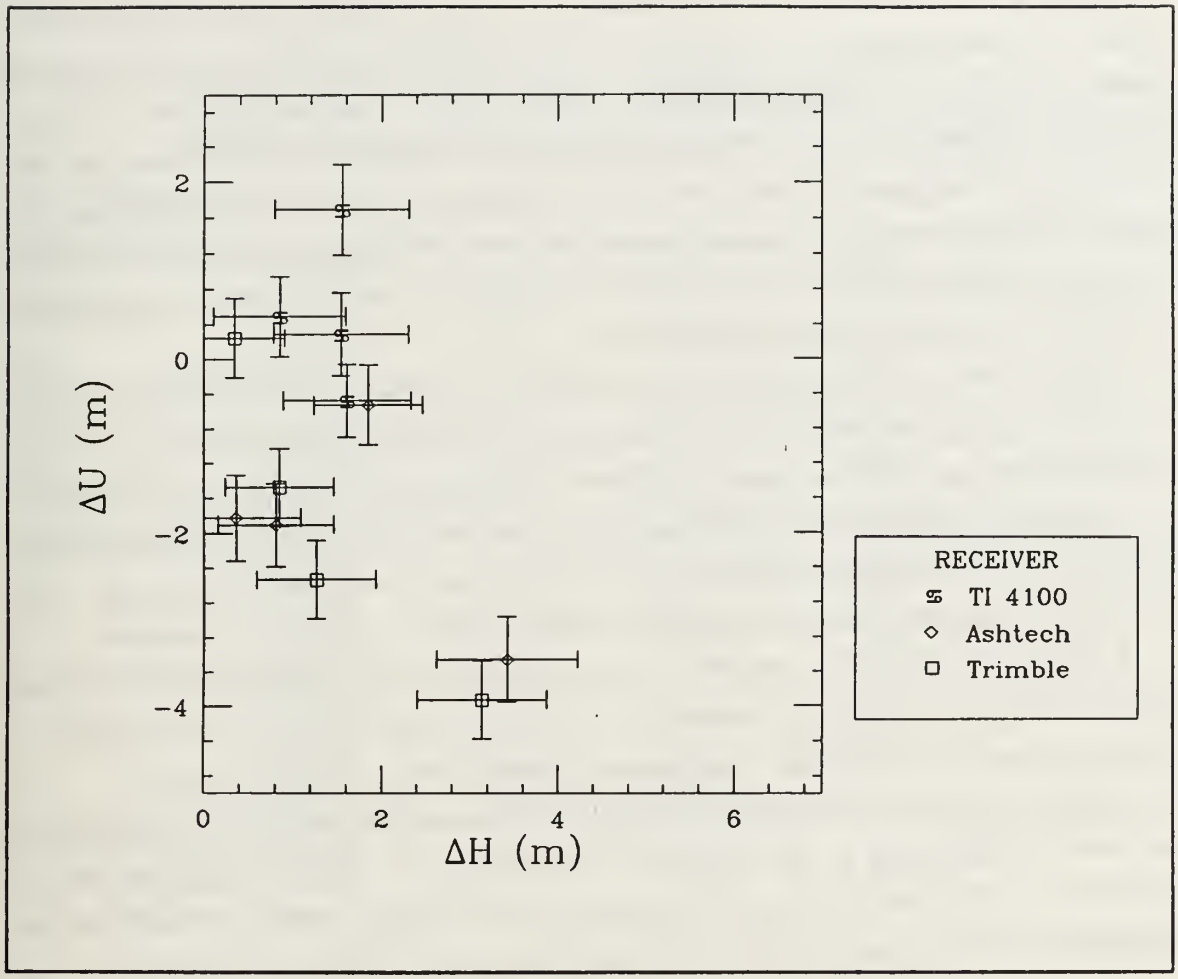

Figure 20. ΔHor versus ΔUp for Beach Lab, Broadcast Ephemeris Data

Table 9 and Figures 21 and 22 present the accuracy results of the three receivers using the precise ephemeris. It can be seen that the position estimates produced with the precise ephemeris give better agreement to the Transit Doppler positions than the broadcast ephemeris. Overall, the precise ephemeris results are more accurate and precise in every component difference as demonstrated by comparison of the mean component differences and the standard deviations computed about the mean differences. The overall RSS is at about the 1.5 meter level. Again, the origin is within the ensemble of all position differences and formal errors.

The estimates produced by the three receivers are all comparable, with the Ashtech and Trimble giving somewhat better results than the TI 4100 receiver over the four days of observations especially in terms of difference dispersion. The component differences for the Ashtech receiver are all fairly tightly clustered about the origin while the Trimble and TI 4100 receivers show greater dispersion especially in the east component. The TI 4100 receiver also shows the greatest dispersion in the north and up directions.

As seen in the broadcast ephemeris results, comparisons of dispersion between the north and the east reveal that dispersion is greater in the east than in the north direction. Also conspicuous is the greater dispersion in the vertical than in the horizontal.

Again, we see that the GASP estimated formal errors have underestimated the actual error as determined by the dispersion of the differences. For the precise ephemeris estimates, GASP formal error underestimates the actual error more in the east and up components. It represents the error in the north component fairly well. The actual error on the east and up components is underestimated by a factor of about two. The relationship for the error in the north component is almost one-to-one.

Table 9. BEACH LAB COMPONENT DIFFERENCES (ΔE, ΔN, ΔU) USING PRECISE EPHEMERIS: Solution Differences Between GPS and Transit Doppler Methods, Second Term is GASP Estimated Formal Error, RSS is Magnitude of the Difference Vector

Day of Year 1990	Receiver	ΔE (m)	ΔN (m)	ΔU (m)	ΔH (m)	RSS (m)
338	TI 4100	1.3 ± .6	1.3 ± .6	−1.6 ± .5	1.9 ± .8	2.4
	Ashtech	−1.2 ± .6	−0.6 ± .4	−0.7 ± .5	1.4 ± .7	1.5
	Trimble	−1.9 ± .6	0.3 ± .4	−0.8 ± .4	1.9 ± .6	2.1
339	TI 4100	−0.5 ± .6	−0.1 ± .6	−0.6 ± .5	0.5 ± .7	0.7
	Ashtech	−0.3 ± .6	−0.6 ± .5	−0.0 ± .5	0.7 ± .7	0.7
	Trimble	−0.0 ± .6	−0.1 ± .4	−1.4 ± .4	0.1 ± .5	1.4
340	TI 4100	−1.6 ± .5	−0.0 ± .5	−1.6 ± .5	1.6 ± .6	2.3
	Ashtech	−0.0 ± .6	−0.4 ± .5	−2.3 ± .5	0.4 ± .5	2.3
	Trimble	−0.4 ± .5	0.2 ± .4	−1.3 ± .4	0.4 ± .6	1.4
341	TI 4100	2.1 ± .6	0.8 ± .5	1.6 ± .5	2.2 ± .7	2.8
	Ashtech	−0.2 ± .6	0.6 ± .5	−0.1 ± .5	0.7 ± .6	0.7
	Trimble	1.4 ± .6	0.2 ± .4	0.5 ± .5	1.4 ± .6	1.5
Mean Component Difference and Standard Deviation about Mean		−0.1 ± 1.2	0.1 ± .6	−0.7 ± 1.1	1.1 ± .7	1.6 ± .7

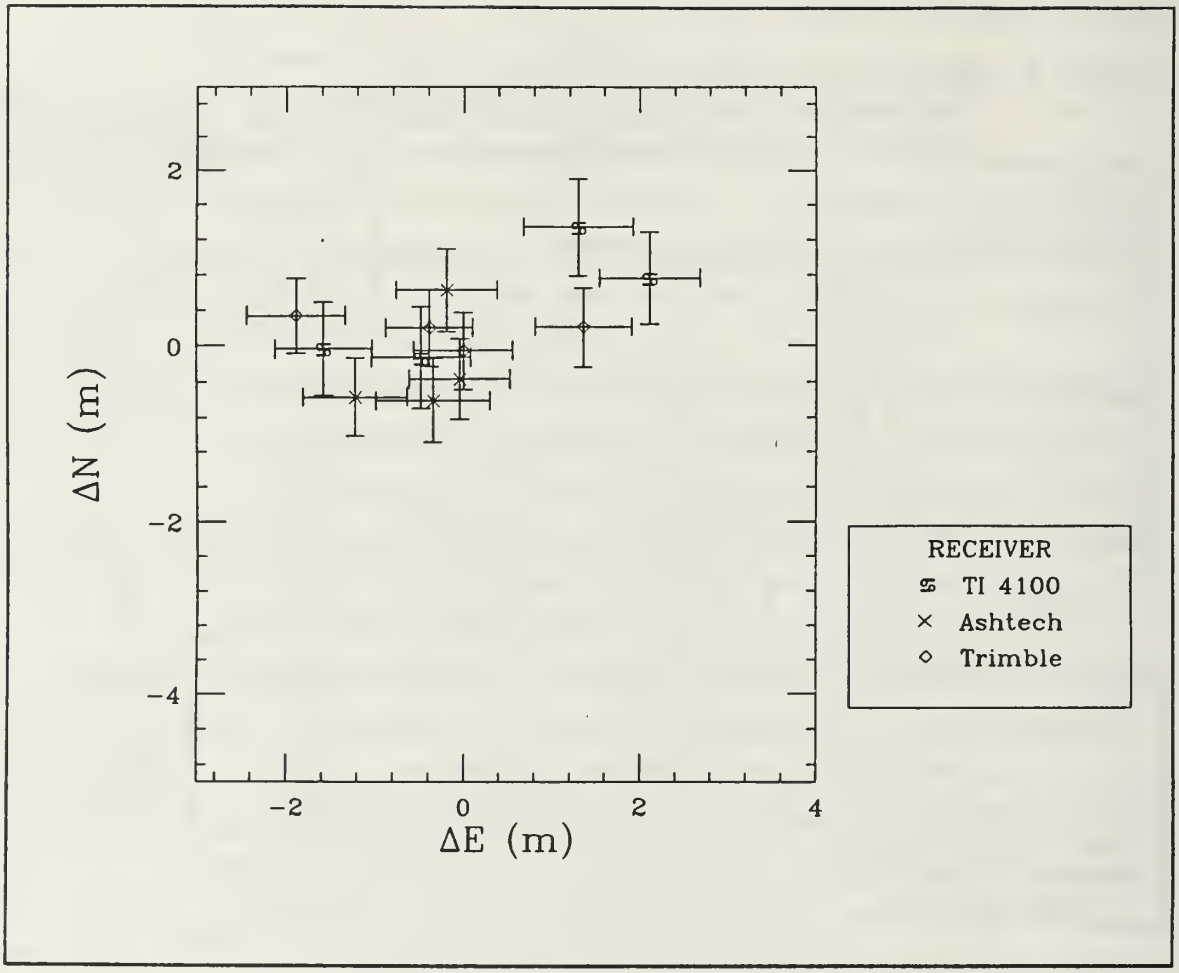

Figure 21. ΔEast versus ΔNorth for Beach Lab, Precise Ephemeris Data

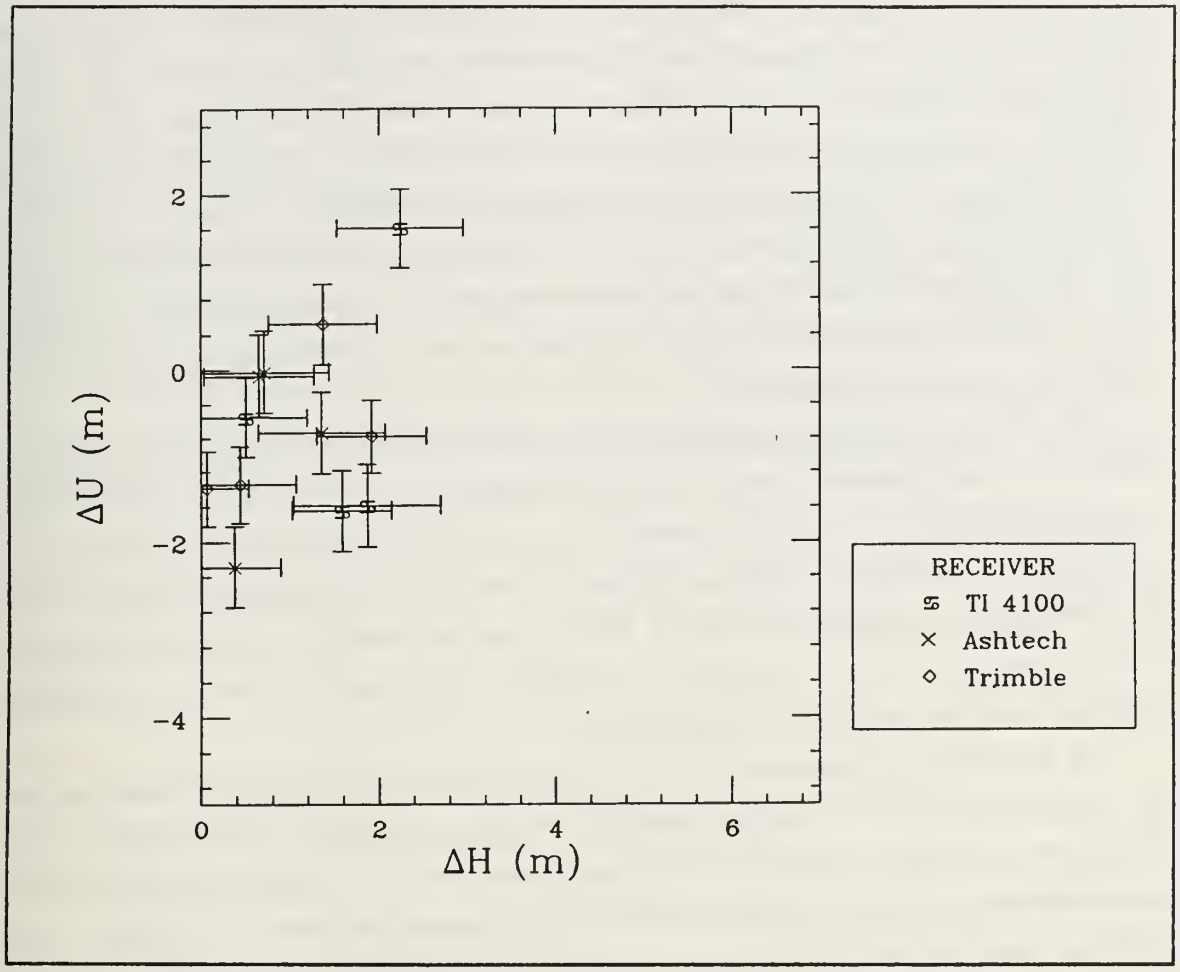

Figure 22. ΔHor versus ΔUp for Beach Lab, Precise Ephemeris Data

Table 10 and Figures 23 and 24 display the Beach Lab repeatability results that average over days by receiver for both the precise and broadcast ephemerides. The means and standard deviations on the means show that geodetic-quality point positions are achieved using the precise ephemeris. This is especially true for the results produced with the Ashtech and Trimble receivers. The standard deviations i.e., observed errors are typically within or around one meter on all components for these receivers. The accuracies, as determined by the RSS of the mean component differences, are within one meter for all receivers demonstrating that agreement to the Transit Doppler estimates are within the computed noise levels.

The TI 4100 precise ephemeris results are less precise than either the Ashtech or Trimble precise ephemeris results and, interestingly, are less precise than the TI 4100 broadcast ephemeris results. The reason for this is not known. However, examination of the RSS of the mean component differences reveals that the overall accuracy of the TI 4100 precise ephemeris estimates is better than the broadcast ephemeris estimates. This is presumably due to increased systematic error associated with the broadcast ephemeris satellite positions and clock states.

The broadcast ephemeris estimates show that geodetic-quality point positions are not obtained using the broadcast satellite positions and clock states. Higher values computed for the RSS of the mean differences show reduced accuracy compared to the precise ephemeris estimates. Also, the broadcast ephemeris estimates are generally more imprecise than the precise ephemeris estimates. As previously mentioned, this was not true for the TI 4100 receiver however.

It is also clear that averaging the component differences over days has significantly improved the accuracy and precision for all receivers for both ephemerides. The individual components show improvement and, as a consequence, the RSS of the averaged components is also improved. This demonstrates the importance of averaging over many independent position estimates to suppress the effects of random error.

The error bars, representing the actual observed error (the standard deviations about the mean component differences), show significant asymmetry. This dramatically illustrates the reduced precision in the east component as compared to the north component and in the vertical component when compared to the horizontal. It also illustrates that the GASP estimated formal errors substantially underestimated the observed or true errors. For the precise ephemeris estimates, errors on the north component for all three receivers displayed close agreement to the GASP estimated errors. The Ashtech receiver showed the best agreement in the east component and the Trimble receiver in the up. The broacast ephemeris estimates also displayed close agreement in the north for all receivers, but the east and up components showed even poorer agreement than the precise ephemeris.

Table 10. **BEACH LAB REPEATABILITY (ΔE, ΔN, ΔU): AVERAGE OVER DAYS BY CEIVER:** Mean RSS is Magnitude of the Mean Difference Vector

Ephemeris	Receiver	Mean ΔE (m)	Mean ΔN (m)	Mean ΔU (m)	Mean ΔH (m)	Mean H (m)
Broadcast	TI 4100	0.0 ± 1.0	−1.1 ± .4	0.5 ± .9	1.1 ± .5	1.2 ±
	Ashtech	0.7 ± 2.1	0.3 ± .5	−1.9 ± 1.2	0.7 ± 2.1	2.1 ±
	Trimble	0.8 ± 1.5	0.8 ± .6	−1.9 ± 1.8	1.1 ± 1.4	2.2 ±
Precise	TI 4100	0.3 ± 1.7	0.5 ± .7	− 0.5 ± 1.5	0.6 ± 1.5	0.8 ±
	Ashtech	−0.5 ± .5	−0.2 ± .6	− 0.8 ± 1.1	0.5 ± .7	0.9 ±
	Trimble	− 0.2 ± 1.3	0.2 ± .2	−0.7 ± .9	0.3 ± 1.2	0.8 ±

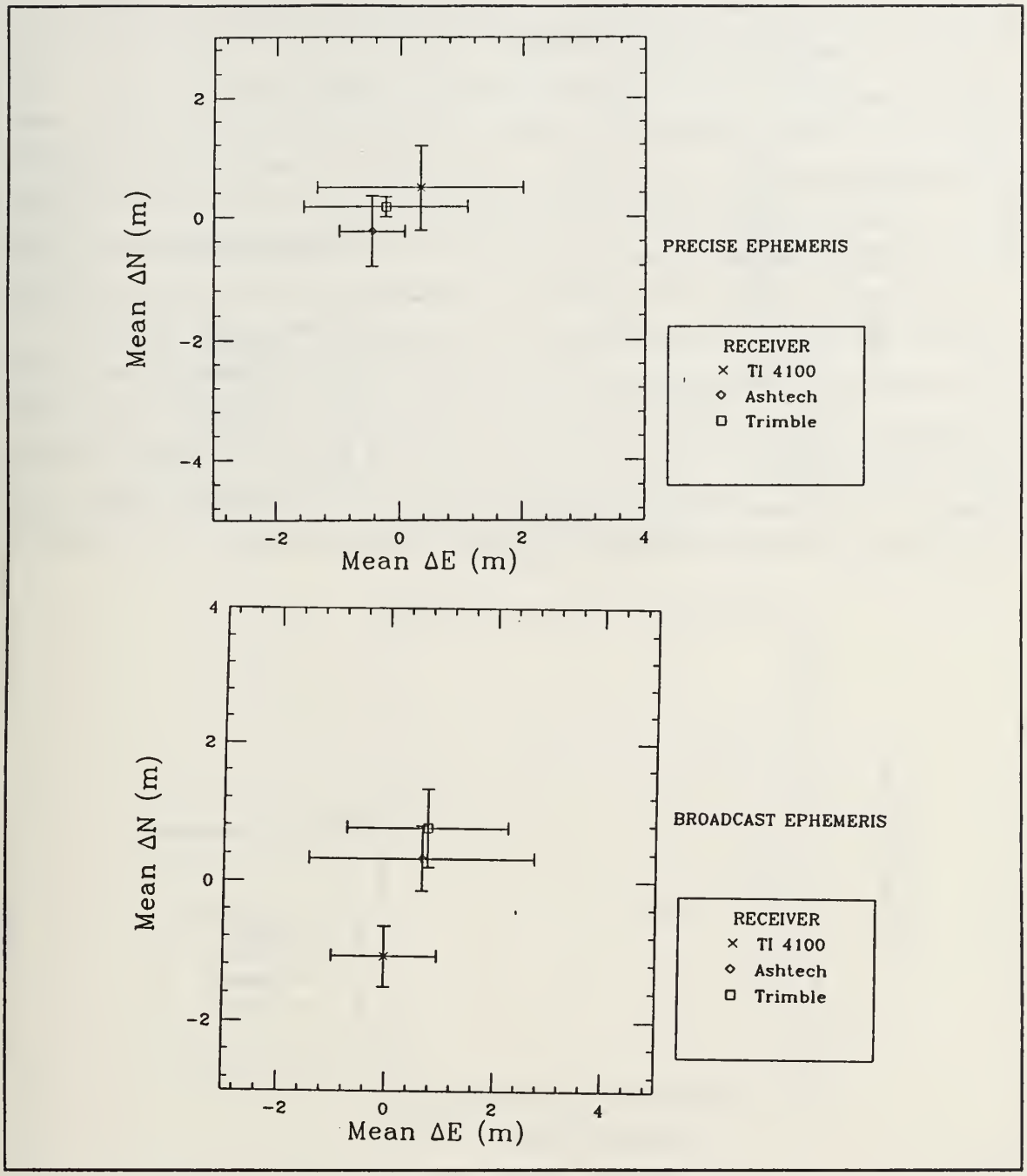

Figure 23. Mean ΔEast versus Mean ΔNorth for Beach Lab Repeatability: Average Over Days by Receiver

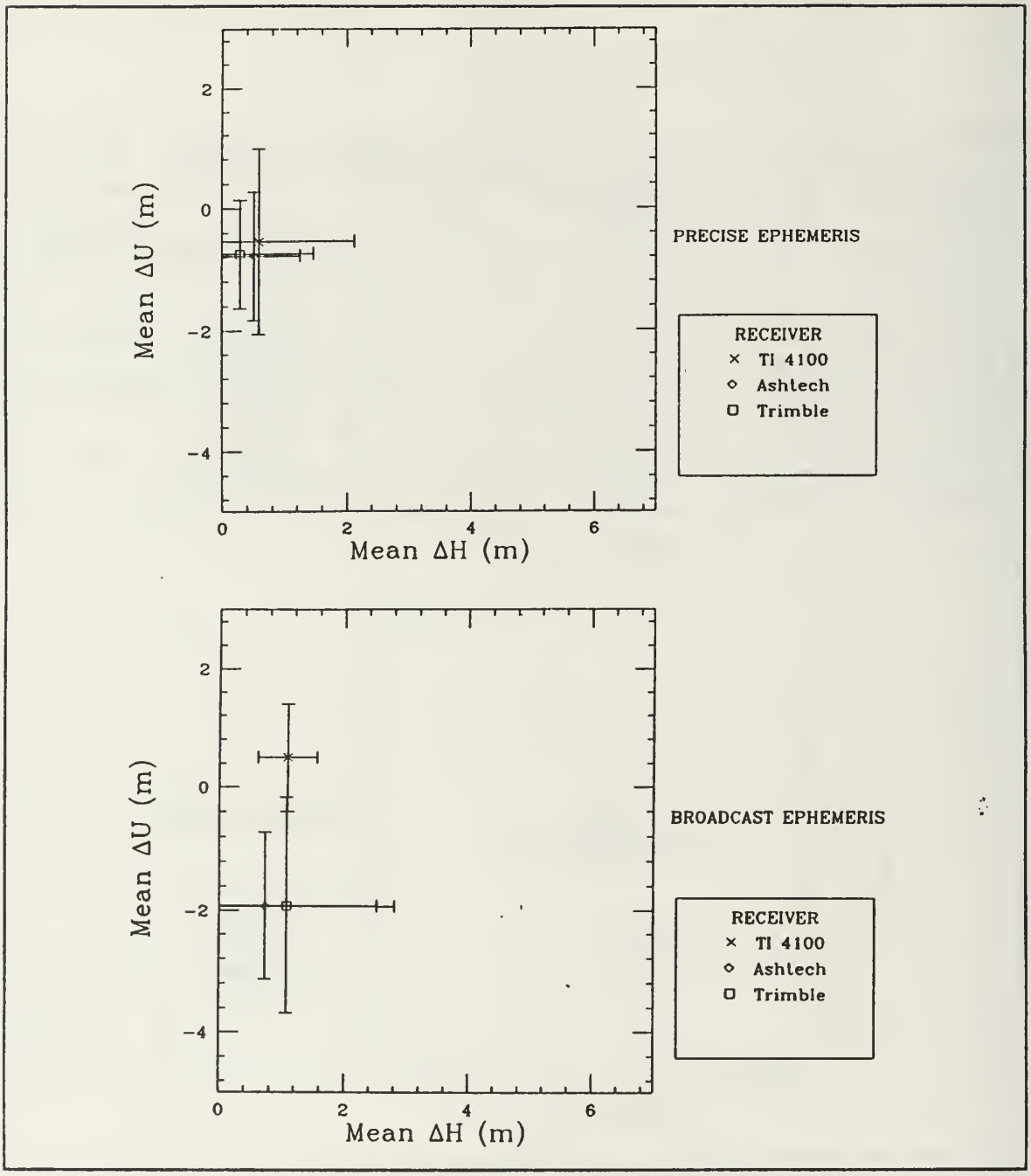

Figure 24. Mean ΔHor versus Mean ΔUp for Beach Lab Repeatability: Average Over Days by Receiver

Table 11 and Figures 25 and 26 display the Beach Lab repeatability results that average over receivers by day for both the precise and broadcast ephemerides. The table and the plots show that the day 339 results, produced using the broadcast ephemeris, were the most inaccurate and imprecise of all the daily estimates. Overall, the broadcast ephemeris results showed much less precision than the precise ephemeris estimates. The precision on the positions estimated with the precise ephemeris was roughly two times better than those estimated with the broadcast ephemeris. This demonstrates the inconsistency of the broadcast ephemeris in estimating geodetic-quality point positions.

Again, the plots show asymmetry in the magnitudes of the error bars. The east component displays greater imprecision than the north component. Comparison of the vertical and horizontal components does not reveal any obvious overall asymmetry except in a few individual cases. This also shows that, again, the GASP estimated formal errors underestimate the true errors. The computed values demonstrate, for the precise ephemeris, the north and up formal errors best estimate the observed errors for all days.

Table 11. BEACH LAB REPEATABILITY (ΔE, ΔN, ΔU): AVERAGE OVER RECEIVERS
DAY: Mean RSS is Magnitude of the Mean Difference Vector

Ephemeris	Day	Mean ΔE (m)	Mean ΔN (m)	Mean ΔU (m)	Mean ΔH (m)	Mean R (m)
Broadcast	338	−0.3 ± .6	− 0.1 ± 1.3	− 1.4 ± 1.5	0.3 ± .8	1.4 ± 1
	339	1.9 ± 2.0	0.2 ± 1.5	− 1.9 ± 3.1	1.9 ± 2.2	2.7 ± 3
	340	0.2 ± .7	−0.0 ± .7	− 1.0 ± 1.3	0.2 ± .7	1.0 ± 1
	341	− 0.0 ± 1.6	−0.1 ± .6	−0.3 ± .4	0.2 ± .8	0.3 ± .
Precise	338	− 0.6 ± 1.7	0.4 ± 1.0	−1.0 ± .5	0.7 ± 1.9	1.3 ± 1
	339	−0.3 ± .2	−0.3 ± .3	−0.7 ± .7	0.4 ± .4	0.8 ± .
	340	−0.7 ± .8	−0.1 ± .3	−1.8 ± .5	0.7 ± .8	1.9 ± .
	341	1.1 ± 1.2	0.5 ± .3	0.7 ± .9	1.2 ± 1.2	1.4 ± 1

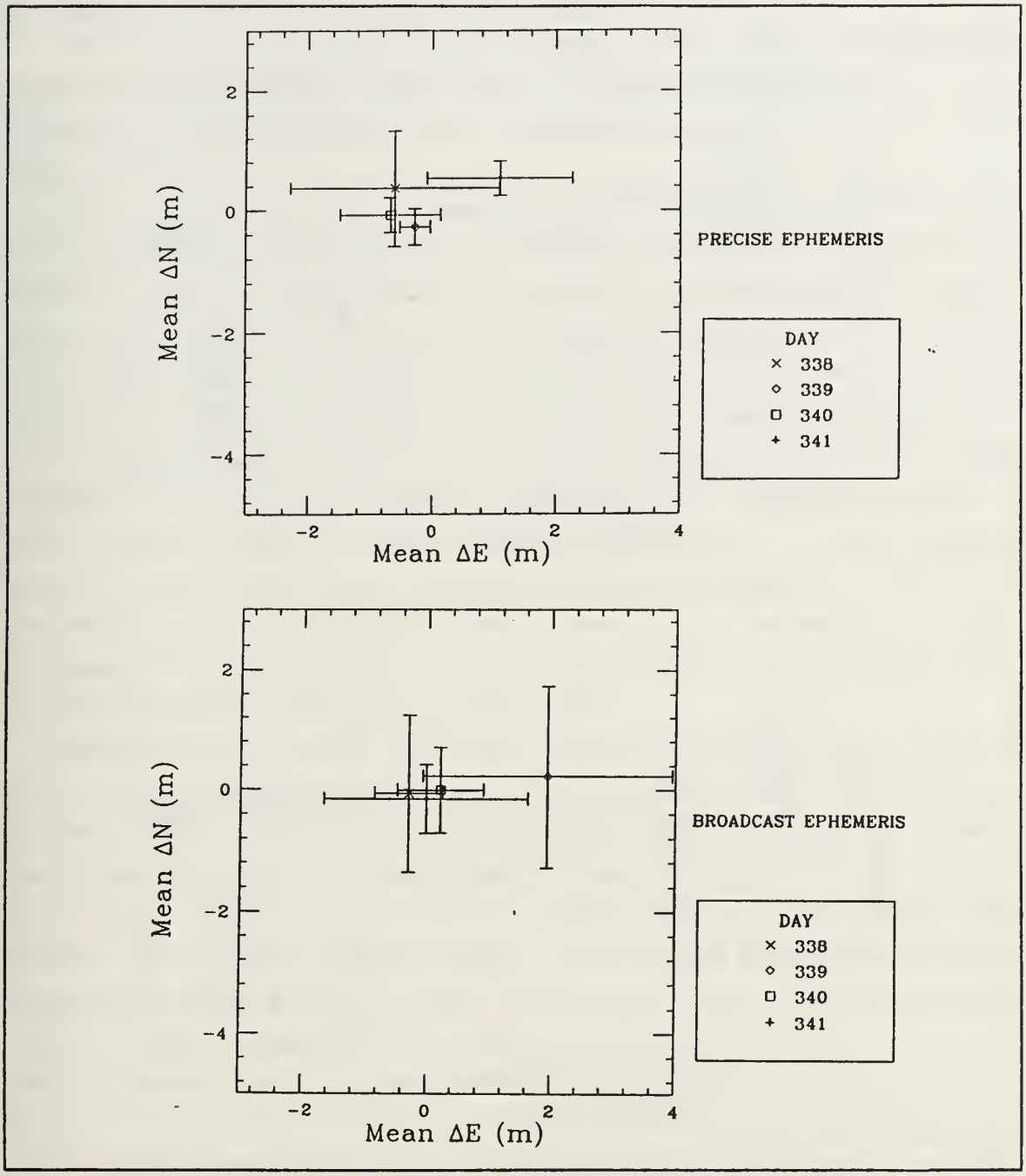

Figure 25. Mean ΔEast versus Mean ΔNorth for Beach Lab Repeatability: Average Over Receivers by Day

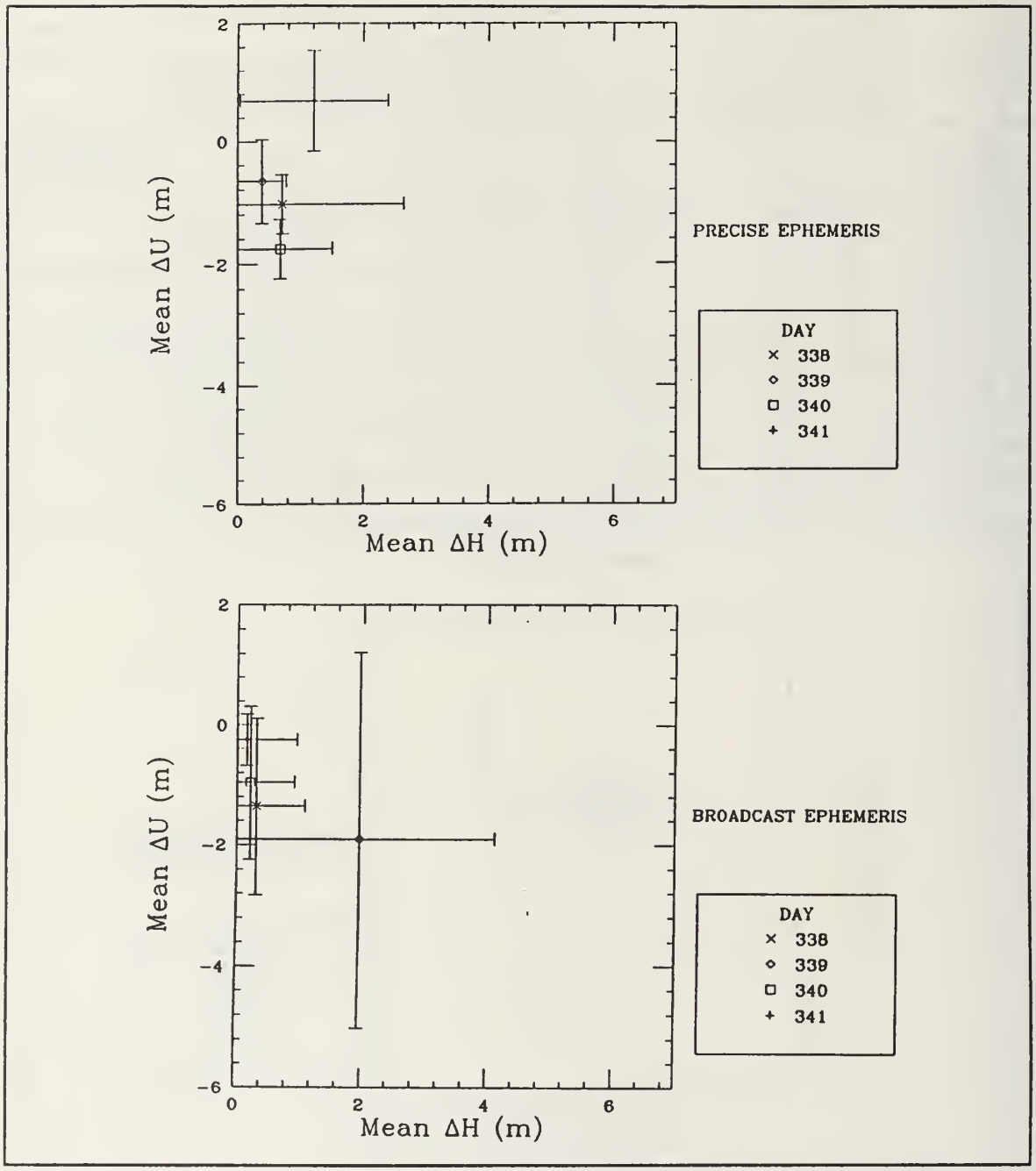

Figure 26. Mean ΔHor versus Mean ΔUp for Beach Lab Repeatability: Average Over Receivers by Day

B. LOBOS3 RESULTS

The TI 4100 receiver was the only model used to collect data at the LOBOS3 site. Independent data sets were created for each of the three days of site occupation. Results produced by the broadcast and precise ephemeris are compared for each of the independent data sets.

Table 12 and Figures 27 and 28 displaying the LOBOS3 component differences for both ephemerides clearly demonstrate the advantage of using the precise ephemeris to determine the point position. Accuracy is improved in every component. The broadcast ephemeris estimates show much lower levels of accuracy and precision and there appears to be a bias present in the south-east and up directions. Errors in the predicted satellite positions or in the broadcast satellite clock models are the probable cause of this bias.

The precise ephemeris results show very good agreement with the Transit Doppler estimates and can definitely be considered geodetic-quality. As with the Beach Lab results, the precise ephemeris estimates show greater dispersion in the east component than in the north. Any difference in dispersion between the vertical and the horizontal does not appear to be significant for either ephemeris. Also noteworthy, the TI 4100 gave much better precise ephemeris results at this site than at the Beach Lab and the broadcast ephemeris results are much worse overall.

Because of the peculiar TI 4100, precise ephemeris results obtained at the Beach Lab, it would be desirable to compare the precise ephemeris results obtained with the TI 4100 receiver at LOBOS3 to those obtained by the other two receivers at the Beach Lab. Direct comparison of the results requires some caution, however, because of the longer lengths of the data sets processed for LOBOS3. With this caveat in mind, comparison of the LOBOS3 TI 4100 estimates to the Ashtec and Trimble Beach Lab estimates reveals that better results, in terms of both accuracy and precision, were produced with the TI 4100 receiver for all components at LOBOS3. This may be due to better precise ephemeris satellite positions provided for this particular week. Again, it should be stressed, although the LOBOS3 precise ephemeris results with the TI 4100 were best overall, all three receivers produced geodetic-quality point positions with the precise ephemeris.

Table 12. **LOBOS3 COMPONENT DIFFERENCES (ΔE, ΔN, ΔU):** Solution Differences tween GPS and Transit Doppler Methods for Broadcast and Precise Ephemerides, ond Term is GASP Estimated Formal Error, RSS is Magnitude of the Difference Ve

Ephemeris	Day of Year 1991	ΔE (m)	ΔN (m)	ΔU (m)	ΔH (m)	RSS (m
Broadcast	36	1.4 ± .6	−1.6 ± .5	1.7 ± .5	2.1 ± .8	2.7
	37	3.4 ± .8	−4.6 ± .6	4.9 ± .6	5.7 ± 1.0	7.5
	38	1.3 ± .7	−3.3 ± .5	5.8 ± .5	3.6 ± .7	6.8
Precise	36	−0.4 ± .6	−0.4 ± .5	0.6 ± .5	0.6 ± .8	0.9
	37	0.4 ± .6	−0.2 ± .4	−0.6 ± .4	0.5 ± .8	0.7
	38	1.3 ± .6	0.1 ± .5	0.2 ± .5	1.3 ± .7	1.3

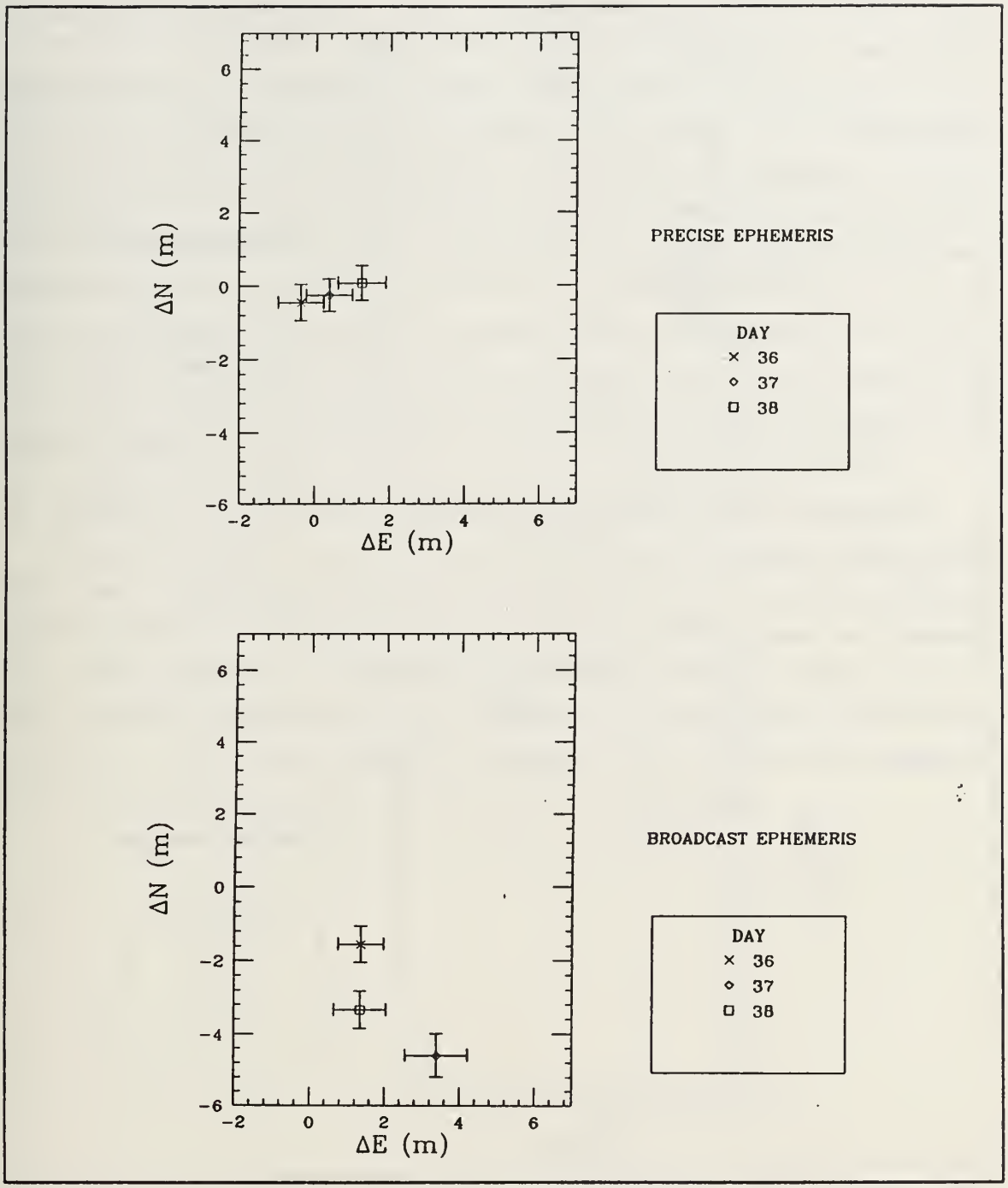

Figure 27. ΔEast versus ΔNorth for LOBOS3

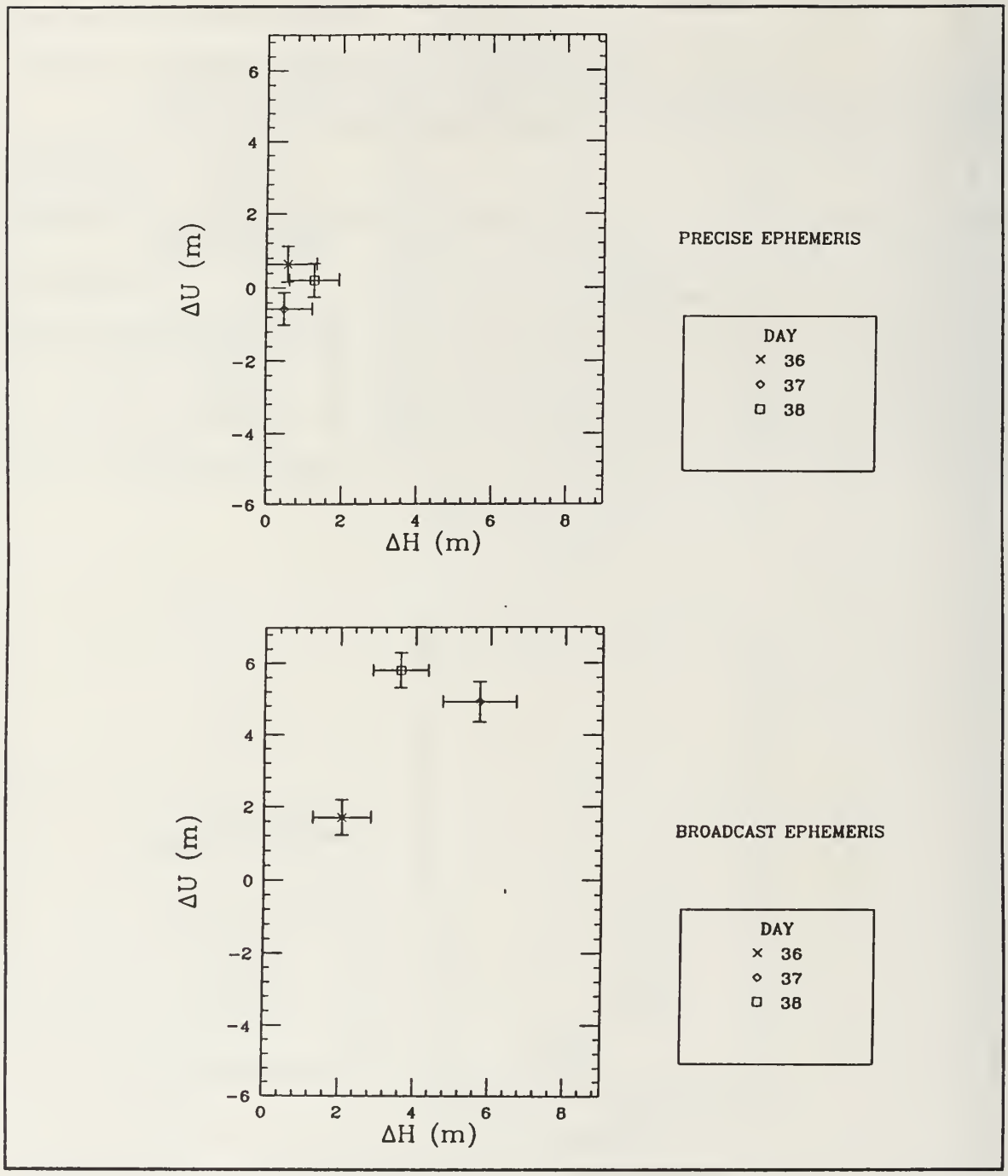

Figure 28. ΔHor versus ΔUp for LOBOS3

The LOBOS3 repeatability results averaging over days, displayed in Table 13 and Figures 29 and 30, clearly shows the inaccuracy and imprecision of the broadcast ephemeris results. The south-east-up bias alluded to earlier can also be clearly seen in the broadcast ephemeris estimates. Comparison of the error bars on the averaged precise ephemeris estimates shows the characteristic east versus north asymmetry. No significant vertical versus horizontal asymmetry is evident, however. The magnitudes of the error bars on the precise ephemeris estimates show that, in this case, the GASP estimated formal errors more closely represented the true errors. However, the formal error estimates produced for the broadcast ephemeris results underestimated the true errors by a factor of approximately two for the east component, three for the north, and four in the vertical. The precise ephemeris statistics demonstrate that by averaging over independent estimates, the accuracy and precision can be significantly improved.

C. REGIONAL AGREEMENT BETWEEN GPS AND TRANSIT DOPPLER

In order to establish a regional reference for the expected agreement between GPS and Transit Doppler position estimates in the Central California area, the overall accuracy and precision of the position differences using the precise ephemeris are evaluated. The precise ephemeris mean component differences and standard deviations over all Beach Lab and LOBOS3 data sets were computed to provide values for this expected agreement. These values, obtained by averaging over 15 data sets, are mean $\Delta E = 0.21 \pm 1.1$, mean $\Delta N = 0.09 \pm .52$, and mean $\Delta U = -0.54 \pm 1.03$.

Table 13. **LOBOS3 REPEATABILITY (ΔE, ΔN, ΔU) AVERAGE OVER DAYS FOR TI 4** RECEIVER: Mean RSS is Magnitude of the Mean Difference Vector

Ephemeris	Mean ΔE (m)	Mean ΔN (m)	Mean ΔU (m)	Mean ΔH (m)	Mean RS (m)
Broadcast	2.0 ± 1.2	-3.2 ± 1.5	4.1 ± 2.2	3.8 ± 1.9	5.6 ± 2.9
Precise	$0.4 \pm .8$	$-0.2 \pm .3$	$0.1 \pm .6$	$0.5 \pm .8$	$0.5 \pm .9$

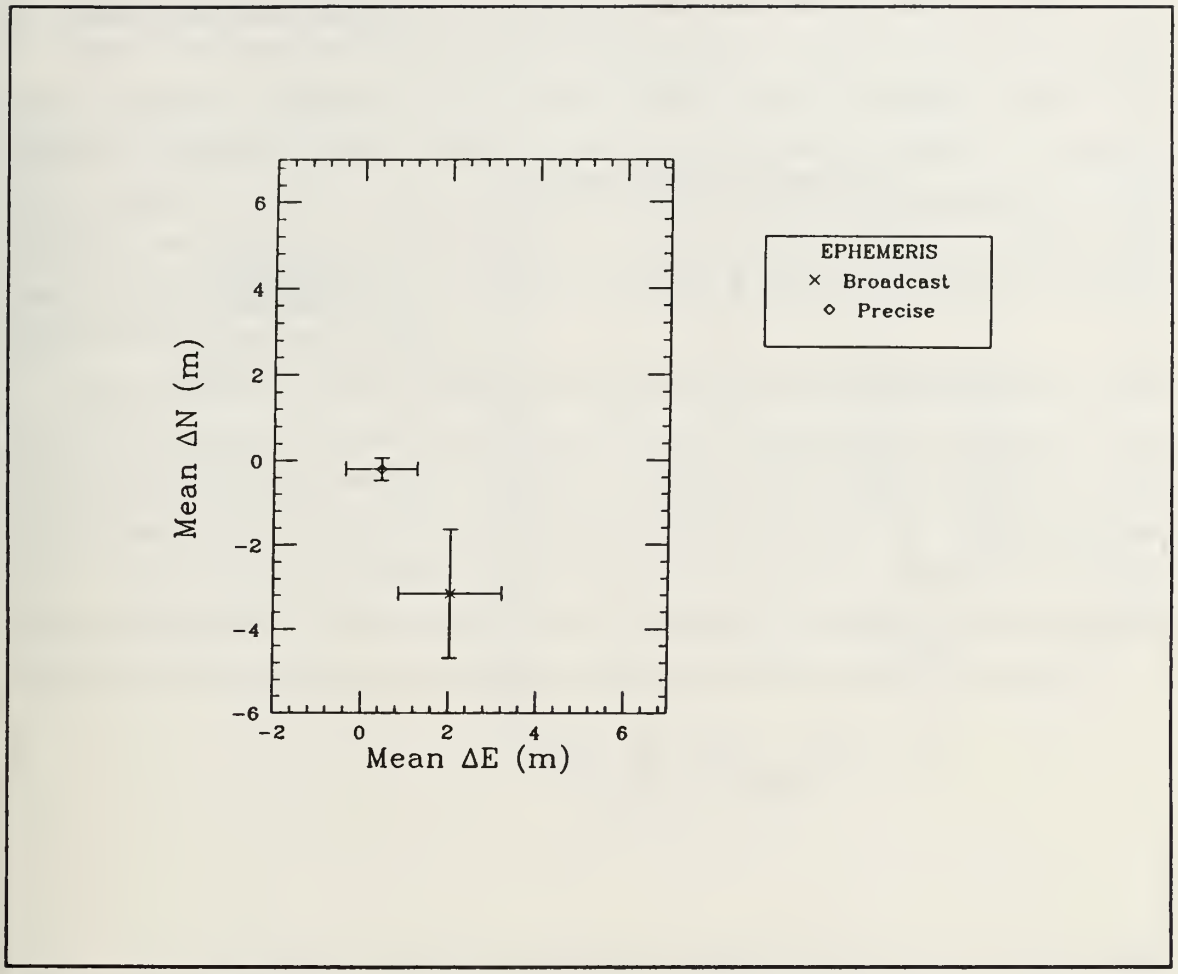

Figure 29. Mean ΔEast versus Mean ΔNorth for LOBOS3 Repeatability: Average Over Days

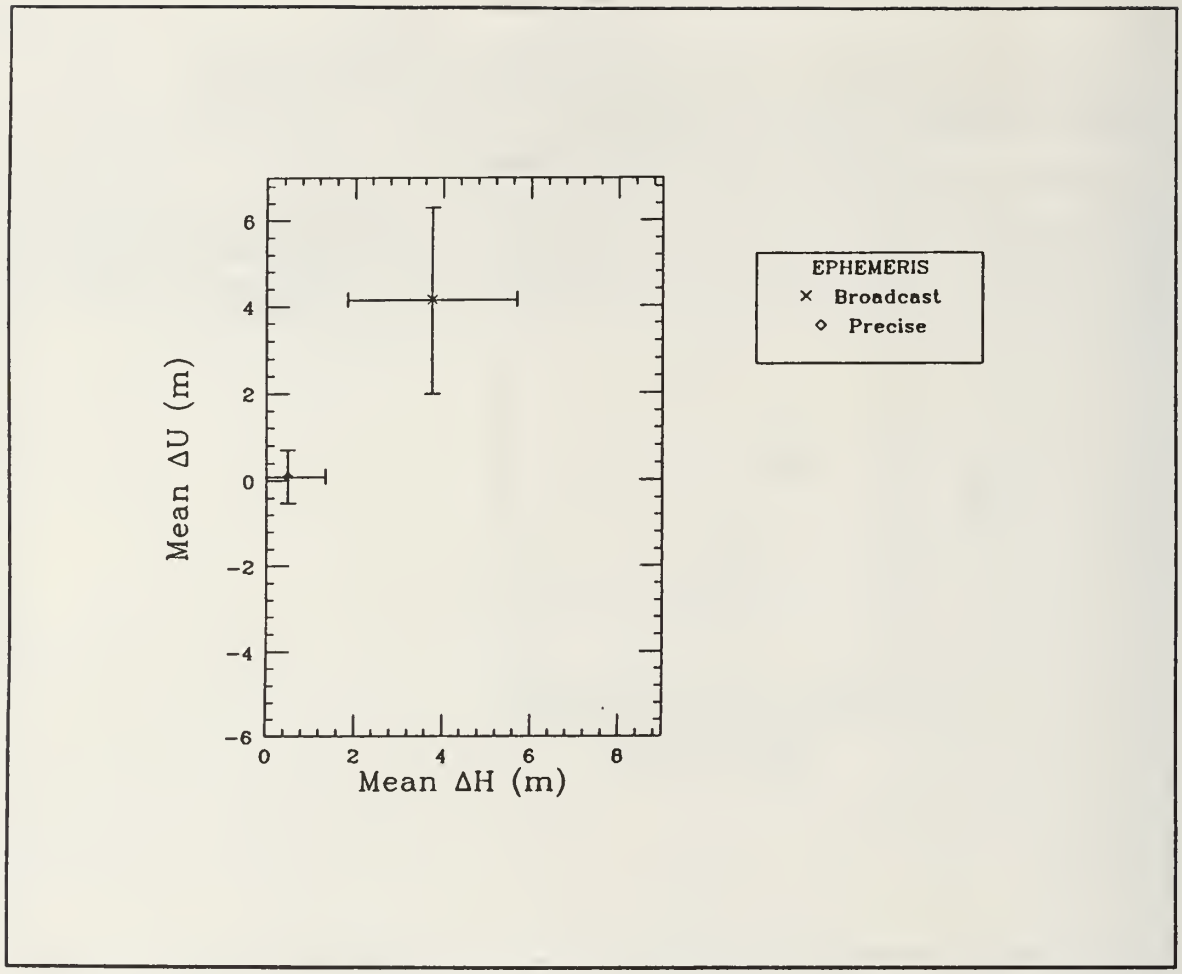

Figure 30. Mean ΔHor versus Mean ΔUp for LOBOS3 Repeatability: Average Over Days

D. POSITIONING RESULTS - SELECTIVE AVAILABILITY ACTIVATED

Table 14 and Figures 31 and 32 present the solution differences between the coordinates previously established for mark BLDG 224.3 and the coordinates estimated for the mark using the broadcast ephemeris after the activation of Selective Availability. From comparison of the broadcast ephemeris results obtained at the Beach Lab and LOBOS3 sites to the results displayed here, it is quite obvious that the activation of SA has severely impacted the position estimate. Both the accuracy and precision of the results have been adversely affected.

The average RSS of the estimated positions over the five data sets is about 16 meters. When contrasted to the approximately six meter average RSS computed for the LOBOS3 site using the broadcast ephemeris, some indication of the magnitude of this effect is realized. The east and up components are most affected. The north component seems to be much less effected by SA than the other two components. Precise ephemerides were not obtained for this survey period so a comparison of the broadcast ephemeris results to the precise ephemeris estimated position cannot be performed.

Table 14. **BLDG 224.3 COMPONENT DIFFERENCES (ΔE, ΔN, ΔU):** Selective Availabi Test - GPS Solution Differences Between Previously Determined Coordinates and ordinates Determined After Activation of S/A (Using Broadcast Ephemeris), RS Magnitude of the Difference Vector

Day of Year 1991	Segment	ΔE (m)	ΔN (m)	ΔU (m)	ΔH (m)	RSS (n
197	A	-23.4 ± 1.8	-3.6 ± 1.1	20.5 ± 1.0	23.7 ± 1.9	31.3
	B	$-1.8 \pm .7$	$2.9 \pm .8$	$12.0 \pm .8$	3.4 ± 1.1	12.5
198	C	8.8 ± 2.0	-2.7 ± 1.0	$0.7 \pm .8$	9.2 ± 2.2	9.3
	D	$-5.4 \pm .8$	$2.3 \pm .9$	17.8 ± 1.3	5.9 ± 1.1	18.7
	E	-7.9 ± 1.0	$-0.3 \pm .8$	$1.6 \pm .8$	7.9 ± 1.0	8.0

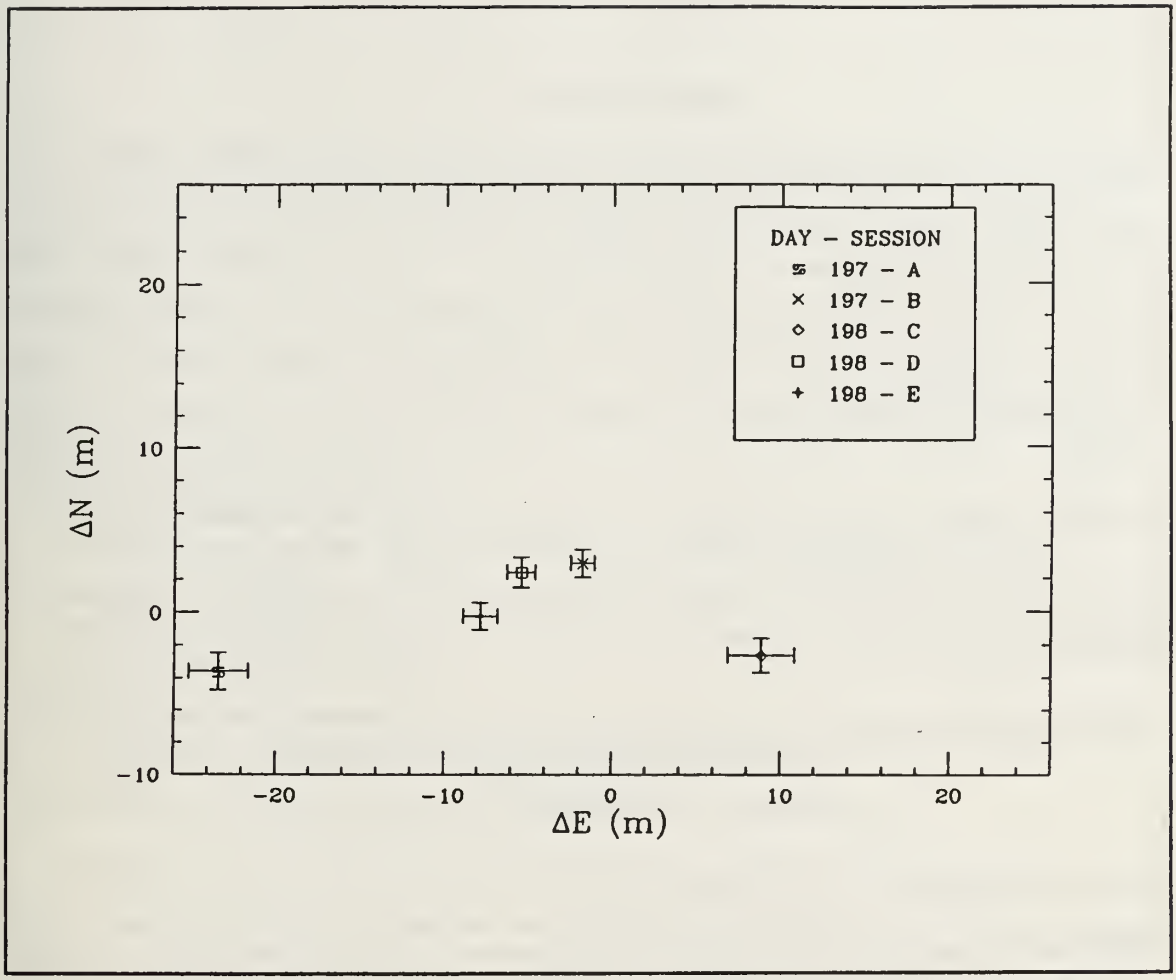

Figure 31. ΔEast versus ΔNorth for BLDG 224.3, Broadcast Ephemeris Data

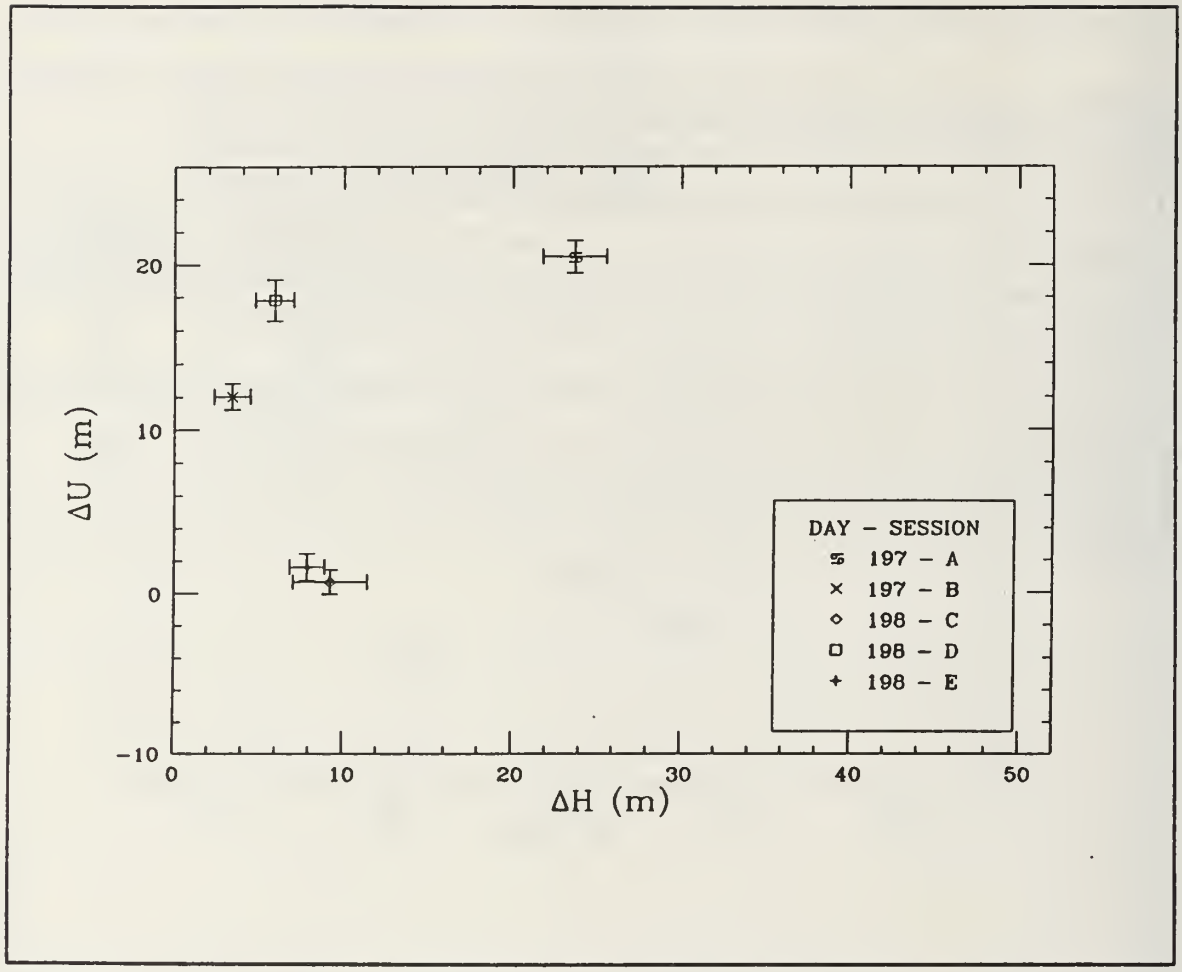

Figure 32. ΔHor versus ΔUp for BLDG 224.3, Broadcast Ephemeris Data

V. CONCLUSIONS

GASP estimated point positions, produced with data collected from three GPS receivers over seven days, are compared to independent Transit Doppler estimated positions. The differences between the positions provide a measure of accuracy for the computed GPS positions. Both broadcast and precise ephemerides were used to estimate the GASP point positions. The precision for a group of estimated positions is determined by calulating the mean of the differences and standard deviations on the means for the group. Major conclusions are:

1. GASP point position estimates generated with the precise ephemeris agree to Transit Doppler point position estimates to within one meter on each axis.
2. All three GPS receivers used in this study are capable of producing point positions with observed errors on the RSS of less than 1.5 meters, when the precise ephemeris and clock states are utilized.
3. Point positions estimated with the precise ephemeris are more accurate and precise than positions estimated with the broadcast ephemeris.
4. Selective Availability has had a dramatic effect on positions.

The GPS point positions estimated by GASP using the precise ephemeris and clock states demonstrated good agreement with positions estimated by the Transit Doppler positioning system. The level of agreement was within the one meter noise level established for both systems. In general, the Transit Doppler positions were within the ensemble of corresponding GPS position estimates. This would seem to indicate that many of the systematic errors that effect the GPS measurements had been successfully modeled or removed by the GASP algorithm. Of course, systematic errors common to both positioning systems may remain.

Accuracy and precision indicate that all three GPS receivers examined in this study are capable of producing geodetic-quality point positions. Between-receiver comparisons of the estimated positions using both the precise and broadcast ephemeris reveal that the Trimble and Ashtech receivers provide results that compare favorably to those produced by the TI 4100 receiver. This is not surprising considering that all three receivers record the carrier phase measurements essential to GASP processing and high-precision point positioning. Although the carrier phase observable recorded by the three receivers is the same, the pseudorange observable exhibits some important differences.

Pseudoranges are observed from the L1 signal using the C/A-code for the Ashtech and Trimble receivers. The TI 4100 receiver observes pseudoranges on both the L1 and L2 signals using the P-code. Consequently, a dual frequency ionospheric correction can not be computed for pseudoranges observed with the Ashtech and Trimble receivers. This, along with higher noise levels associated with C/A code measurements, caused a high incidence of data rejection in preliminary processing runs. Relaxing the pseudorange edit tolerance to ten meters allowed the acceptance of a much higher percentage of observations. Even so, rejection figures for these receivers were still higher than the TI 4100 receiver.

Though a higher percentage of observations were rejected with the Ashtech and Trimble receivers, a high degree of accuracy and precision was maintained. The high accuracy and precision levels observed with these receivers may be attributed to their increased channel capacity. The ability to collect and subsequently to process more simultaneous satellite carrier phase measurements provides greater geometric diversity. More measurements per epoch and the incorporation of more satellites into the processing run provides increased system redundancy. These two factors act to strengthen the estimated position solution. Position solutions produced by the TI 4100 receiver should also be improved now that more satellites are allowed per processing run. The benefits gained from these additional measurements will be nullified if too many observations are rejected in the data editing process. Thus, it may be desirable in future tests to determine an optimal pseudorange edit tolerance.

Point positions estimated using precise ephemerides and clock states are superior to the solutions produced with the broadcast ephemeris and clock states. The results obtained with the three receivers at the Beach Lab demonstrate that, overall, better positions estimates were provided with the precise ephemeris and clock states. This is clearly the case at the LOBOS3 site where significantly better results were achieved with the precise ephemeris. These results, together with results produced in past studies, demonstrate that positions produced with the precise ephemeris are generally more reliable, accurate, and consistent than those produced with the broadcast ephemeris [Ref. 2: p. 497].

The recent reactivation of Selective Availabilty has accomplished its intended purpose. For the results reported in this study, SA has severely degraded the accuracy and repeatability of point position estimates that were produced with the broadcast ephemeris. The effects of SA on position estimates using the precise ephemeris were not assessed in this investigation. This may be a topic for future consideration.

The RINEX modifications to the GASP program now allow it to utilize data collected with a greater variety of GPS receivers. This will permit point position determinations from a multitude of additional sources and will enable DMA to augment its point positioning data base. Only data that was converted to the original RINEX format was used in these tests. Additional tests should be conducted with data presented in the RINEX 2 format to ensure that the program code designed to process this data is free of error.

Additional tests should be conducted to verify the validity of the conclusions presented here. Tests, similiar in design but extending over longer time periods (weeks as opposed to days), would provide a more satisfactory indication of the long-term repeatability for the different receivers.

APPENDIX A. KEPLERIAN ELEMENTS

Six Keplerian elements and a reference time are necessary to completely describe the satellite orbit and the position of the satellite in the orbit. The six Keplerian elements given in the broadcast ephemeris are:

- Right ascension of the ascending node (Ω)
- Inclination (i)
- Argument of perigee (ω)
- Semi-major axis of the elliptical orbit (a)
- Eccentricity of the orbit (e)
- An element describing the position of the satellite on the orbital ellipse (e.g., Mean anomaly (M)) which is a function of time

The ephemeris reference time is designated (t_{oe}). The five Keplerian elements that describe the orbit are Ω, i, ω, a, and e. M gives the position of the satellite in its orbit at a time t. See Figure 33 for a graphic representation.

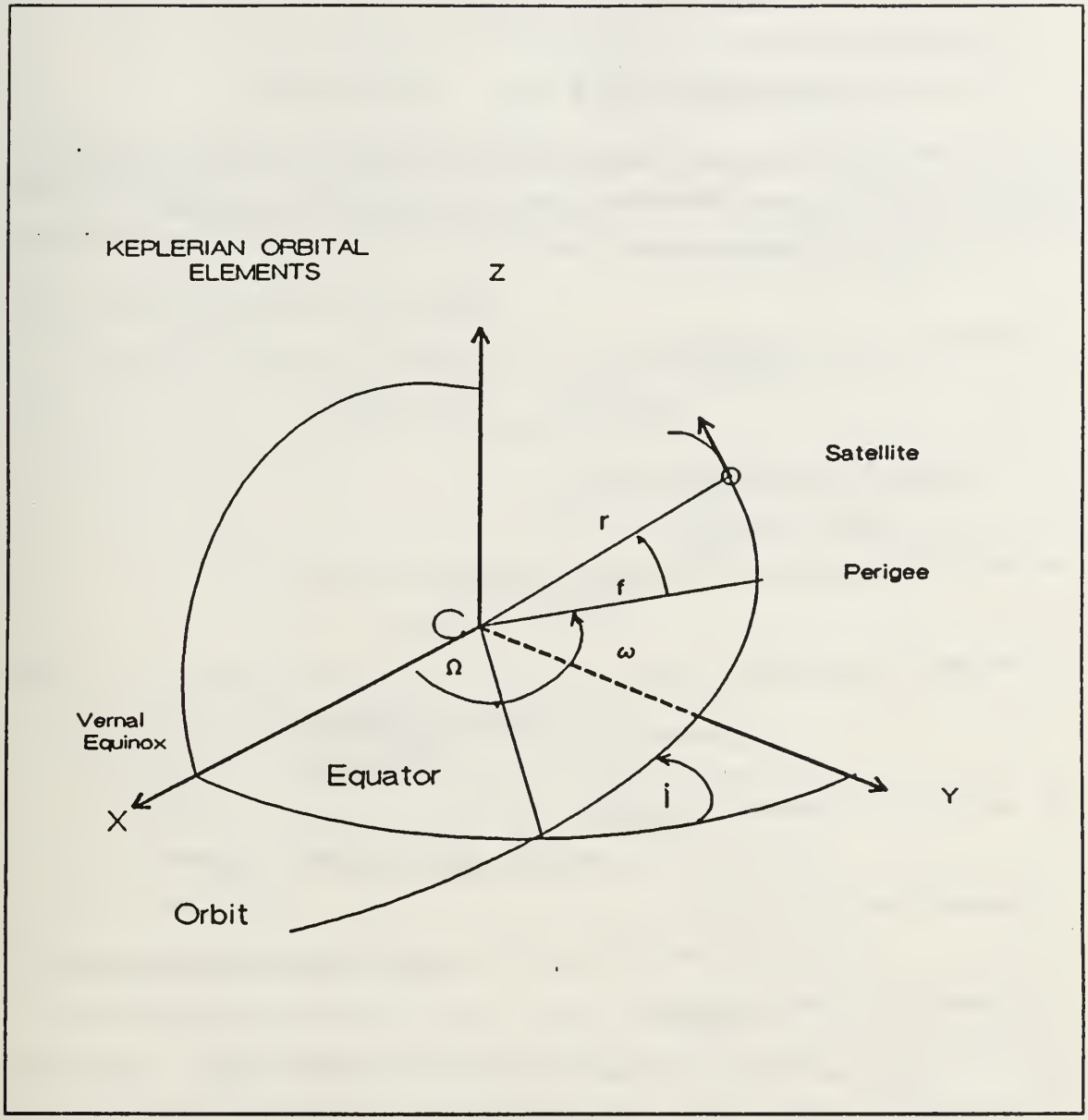

Figure 33. The Keplerian Orbital Elements: Symbols are Explained in the Text

Other Broadcast Ephemeris parameters that are transmitted in the Navigation Message describe the deviations of the satellite motion from the smooth ellipse defined by the six Keplerian elements refered to above. These perturbing terms include:

- Mean motion difference (Δn)
- Rate of right ascension ($\dot{\Omega}$)
- Rate of inclination ($\dot{i}$)

- Corrections to argument of latitude (C_{uc}, C_{us})
- Corrections to orbital radius (C_{rc}, C_{rs})
- Corrections to inclination (C_{ic}, C_{is})

In order to transform the Keplerian orbital parameters to coordinates in the conventional terrestrial system, the following computations must be performed:

- find time since reference epoch

$$t_k = t - t_{oe}$$

- solve for mean anomaly at t_k

$$M_k = M_0 + \left[\sqrt{\frac{\mu}{a^3}} + \Delta n\right] t_k$$

where the gravitational constant

$\mu = 3.986005 \times 10^{14} \frac{m^3}{sec^2}$

- solve Kepler's equation iteratively for eccentric anomaly, E_k

$$M_k = E_k - e \sin E_k$$

- compute true anomaly,

$$f_k = \tan^{-1}\left[\sqrt{(1-e^2)}\ \frac{(\sin E_k)}{(\cos E_k - e)}\right]$$

- compute the argument of latitude,

$$u_k = \omega + f_k + C_{uc} \cos 2(\omega + f_k) + C_{us} \sin 2(\omega + f_k)$$

- compute the orbital radius,

$$r_k = a(1 - e \cos E_k) + C_{rc} \cos 2(\omega + f_k) + C_{rs} \sin 2(\omega + f_k)$$

- compute the orbital inclination,

$$i_k = i_0 + \dot{i} t_k + C_{ic} \cos 2(\omega + f_k) + C_{is} \sin 2(\omega + f_k)$$

- compute the longitude of the ascending node,

$$\lambda_k = \Omega_0 + (\dot{\Omega} - \omega_e) t_k - \omega_e t_{oe}$$

where the mean earth rotation rate is

$\omega_e = 7.292115147 \times 10^{-5} \frac{rad}{sec}$

- then compute the CT (earth-fixed) coordinates,

$$X_k = r_k \cos u_k \cos \lambda_k - r_k \sin u_k \cos i_k \sin \lambda_k$$

$$Y_k = r_k \cos u_k \sin \lambda_k + r_k \sin u_k \cos i_k \cos \lambda_k$$

$$Z_k = r_k \sin u_k \sin i_k$$

APPENDIX B. LEAST SQUARES IN GPS

The contents of this appendix follow the development in Uotila [Ref. 16]. This development focuses on the general, nonlinear, observation equation model. This is the model utilized by GASP in performing its batch least squares adjustment.

A. THE MATHEMATICAL MODEL

Using matrix notation the mathematical model is given by,

$$L^a = F(X^a)$$

$$\hat{L}^a = F(\hat{X}^a)$$

$$L^b - \varepsilon = F(X^a)$$

where, L^a = Theoretical values of the observed quantities

X = Theoretical values of the paramters

$\hat{L}^a$ = Estimates or adjusted values of the observed quantities

$\hat{X}$ = Estimates or adjusted values of the parameters

L^b = Observed values of the observables

ε = "True" errors

B. OBSERVATION EQUATIONS

Prior to employing the least squares method, a nonlinear function is linearized by expanding in a Taylor series and eliminating terms second order and higher. For a set of nonlinear functions in matrix form we get,

$$L^b - \varepsilon = F(X^a) = F(X^0) + \frac{\partial F}{\partial X}\Big|_{X^a = X^0}(X^a - X^0) + \cdots = F(X^0) + \frac{\partial F}{\partial X^a}\Big|_{X^a = X^0} X + \cdots$$

$$A = \frac{\partial F}{\partial X^a}\Big|_{X^a = X^0}$$

where, X^0 are approximate values for the parameters and is the point about which expansion is done, and

A is called the design matrix and it has the form

$$A = \begin{bmatrix} \frac{\partial f_1}{\partial x_1} & \frac{\partial f_1}{\partial x_2} & \cdots & \frac{\partial f_1}{\partial x_u} \\ \frac{\partial f_2}{\partial x_1} & \frac{\partial f_2}{\partial x_2} & \cdots & \frac{\partial f_2}{\partial x_u} \\ \vdots & \vdots & \vdots & \vdots \\ \frac{\partial f_n}{\partial x_1} & \frac{\partial f_n}{\partial x_2} & \cdots & \frac{\partial f_n}{\partial x_u} \end{bmatrix}$$

where, n is the number of observations, and

u is the number of equation parameters. We will assume that redundancy exists, i.e., the number of observations is greater than the number of unknown parameters.

Using the relations:

$$\varepsilon = A\,X + F(X^0) - L^b$$

$$V = A\,\hat{X} + F(X^0) - L^b$$

where, V is a vector of differences between the observed values and the estimated values (V is refered to as the residual vector) and

$$X = X^a - X^0$$

$$\hat{X} = \hat{X}^a - X^0$$

and from,

$$F(X^0) = L^0$$

$$L^0 - L^b = L$$

where, L^0 are the computed observations evaluated at X^0 we get,

$$V = A\,\hat{X} + L$$

These are the observation equations.

C. MINIMUM VARIANCE SOLUTION

To find a unique set of parameter estimates some condition must be imposed on the residuals. By minimizing the sum of the squares of the weighted residuals, we obtain a best estimate for the parameters in a least squares sense.

The weight matrix denoted P is given as,

$$P = \sigma_0^2 \Sigma_L^{-1}$$

where, Σ_L^{-1} is the inverse of the observation variance-covariance matrix and

σ_0 is the *a priori* variance of unit weight.

The weight matrix provides a way to assign relative importance to various observations. The observation variance-covariance matrix lets us express random errors or noise associated with the observations as variances and relationships between observations as covariances. It is through the variance-covariance matrix that knowledge about the observations is propagated. This allows the variances and covariances for the estimated parameters to be determined (i.e., it gives an estimate of the noise in the solution). The variances make up the diagonal elements of the matrix and the off-diagonal elements are the covariances. The variance-covariance matrix may be written,

$$\Sigma_L = \begin{bmatrix} \sigma_{L1}^2 & \sigma_{L1\,L2} & \cdots & \sigma_{L1\,Ln} \\ \sigma_{L2\,L1} & \sigma_{L2}^2 & \cdots & \sigma_{L2\,Ln} \\ \cdot & \cdot & \cdots & \cdot \\ \cdot & \cdot & \cdots & \cdot \\ \cdot & \cdot & \cdots & \cdot \\ \sigma_{Ln\,L1} & \sigma_{Ln\,L2} & \cdots & \sigma_{Ln}^2 \end{bmatrix}$$

where, $\sigma_{ij} \equiv \sigma_{ji}$ i.e., a symmetric matrix. The variance-covariance matrix is diagonal if the observations are uncorrelated.

For the minimum variance solution, we want to minimize $V^T P V$ which is the sum of the squares of the weighted residuals in matrix notation. By some algebraic manipulation we can show,

$$V^T P V = \hat{X} A^T P A \hat{X} + 2 L^T P A \hat{X} + L^T P L$$

Minimizing by partially differentiating with respect to $\hat{X}$ gives,

$$\frac{1}{2} \frac{\partial (V^T P V)}{\partial \hat{X}} = A^T P A \hat{X} + A^T P L = 0$$

This is known as the normal equation. Now solving for $\hat{X}$ we get,

$$\hat{X} = -(A^T P A)^{-1} A^T P L$$

where, $\hat{X}$ is the adjustment vector that is applied to X^0 giving an improved estimate for the parameters. A number of iterations may be necessary before $\hat{X}$ reaches some acceptable level, that is it sufficiently converges.

D. A POSTERIORI VARIANCE OF UNIT WEIGHT

The sum of the squares of the residuals $V^T P V$ are found by,

$$V^T P V = L^T P L + \hat{X}^T A^T P L$$

The *a posteriori* variance of unit weight may be calculated,

$$\hat{\sigma}_0^2 = \frac{V^T P V}{n - u}$$

where, $n - u$ is the degree of freedom.

E. VARIANCE-COVARIANCE MATRIX OF ADJUSTED PARAMETERS

The variance-covariance matrix for the adjusted parameters is given by,

$$\Sigma_{\hat{X}^a} = (A^T P A)^{-1} A^T P \Sigma_L P A (A^T P A)^{-1}$$

but with $P = \sigma_0^2 \Sigma_L^{-1}$ this reduces to,

$$\Sigma_{\hat{X}^a} = \sigma_0^2 (A^T P A)^{-1}$$

F. VARIANCE-COVARIANCE MATRIX OF THE ADJUSTED, OBSERVED QUANTITIES

This matrix is given by,

$$\Sigma_{\hat{L}^a} = \sigma_0^2 A (A^T P A)^{-1} A^T$$

G. SUMMARY

To summarize the theoretical aspects of the least squares method using the nonlinear, observation equation model,

- The nonlinear system of equations is linearized by expanding in a Taylor series and nonlinear terms are truncated (Note: the number of equations must be greater than or equal to the number of parameters),

- A suitable noise model is chosen as represented by the observation variance-covariance matrix and *a priori* variance of unit weight, and
- the sum of the squares of the residuals are minimized to yield a minimum variance solution

The operational procedures to estimate values for the unknown parameters are,

- Develop a mathematical model that expresses the observations as a function of some unknown parameters,
- select appropriate approximate values for the parameters X^0 (e.g., the receiver co-ordinates),
- Form the vector of computed observations L^0 by evaluating the mathematical model at X^0,
- Determine L, which is the difference vector of the computed observations minus the actual observations,
- Form the weight matrix P from the observation variance-covariance matrix and the *a priori* variance of unit weight
- take the partial derivatives of the mathematical model with respect to the unknowns and evalute at X^0 to form the elements of the design matrix A,
- solve for the change in parameters, $\hat{X}$,
- Compute the parameter variance-covariance matrix, *a posteriori* variance, the residual vector, etc.,
- apply $\hat{X}$ to the initial approximations and stop if $\hat{X}$ has sufficiently converged, otherwise repeat the process using $\hat{X}^a$ as the new X^0 (i.e., iterate)

APPENDIX C. CONSTANTS USED IN GASP

Table 21 presents the constants used in the GASP program. The constants are identified; and the common symbols, the units (if applicable), and the values are given.

Table 15. CONSTANTS USED IN GASP

Constant	Symbol	Units	Value
WGS-84 Earth's Semi-major Axis	a	km	6378.137
WGS-84 Inverse Earth Flattening	$1/f$		298.257223563
Product of Gravitational Constant and Earth's Mass	GM	$km^3/\ sec^2$	3.986005×10^5
Earth's Rotation Rate	ω	$rad/$ sec	$7.2921151467 \times 10^{-}$
Pi	π		3.1415926535897932
Speed of Light	c	$km/$ sec	299,792.458
Satellite Base Frequency	f_0	Hz	10.23×10^6
L1 Signal Frequency	f_{L1}	Hz	$154 f_0$
L2 Signal Frequency	f_{L2}	Hz	$120 f_0$
L1 Signal Wavelength	λ_{L1}	cm	19.029
L2 Signal Wavelength	λ_{L2}	cm	24.421
TI 4100 Receiver L1 Frequency Offset		Hz	-6000
TI 4100 Receiver L2 Frequency Offset		Hz	7600

APPENDIX D. TABLES OF RESULTS IN CT COORDINATES

A. BEACH LAB RESULTS

The results previously expressed in terms of local east, north, and up coordinates are presented here as component differences in conventional terrestrial coordinates (X, Y, and Z) for the reader more comfortable with this reference frame. Tables 15 through 17 display these results. No corresponding target plots are shown.

Table 16. BEACH LAB COMPONENT DIFFERENCES (ΔX, ΔY, ΔZ) USING BROADCAST EPHEMERIS: Solution Differences Between GPS and Transit Doppler Methods, Second Term is GASP Estimated Formal Error

Day of Year 1990	Receiver	ΔX (m)	ΔY (m)	ΔZ (m)
338	TI 4100	$-1.1 \pm .6$	$-0.6 \pm .6$	$-1.0 \pm .4$
	Ashtech	$1.1 \pm .7$	$1.1 \pm .4$	$-1.0 \pm .4$
	Trimble	$1.0 \pm .6$	$2.6 \pm .4$	$-0.6 \pm .4$
339	TI 4100	$-1.5 \pm .6$	$-1.7 \pm .7$	$-0.2 \pm .4$
	Ashtech	$4.6 \pm .7$	$1.1 \pm .5$	$-1.3 \pm .4$
	Trimble	$4.5 \pm .7$	$1.8 \pm .4$	$-1.4 \pm .4$
340	TI 4100	$-0.9 \pm .6$	$-0.4 \pm .6$	$-0.2 \pm .4$
	Ashtech	$1.4 \pm .6$	$0.8 \pm .4$	$-1.2 \pm .4$
	Trimble	$1.2 \pm .6$	$1.2 \pm .4$	$-0.3 \pm .4$
341	TI 4100	$1.2 \pm .5$	$-0.9 \pm .5$	$-0.9 \pm .4$
	Ashtech	$-1.2 \pm .6$	$1.5 \pm .4$	$-0.0 \pm .4$
	Trimble	$0.2 \pm .6$	$-0.4 \pm .4$	$0.1 \pm .4$

Table 17. **BEACH LAB COMPONENT DIFFERENCES (ΔX, ΔY, ΔZ) USING PRECI EPHEMERIS:** Solution Differences Between GPS and Transit Doppler Metho Second Term is GASP Estimated Formal Error

Day of Year 1990	Receiver	ΔX (m)	ΔY (m)	ΔZ (m)
338	TI 4100	2.2 ± .6	1.1 ± .6	0.1 ± .4
	Ashtech	−0.9 ± .6	0.9 ± .4	−0.9 ± .4
	Trimble	−1.2 ± .6	1.7 ± .4	−0.2 ± .4
339	TI 4100	−0.2 ± .6	0.6 ± .6	−0.4 ± .4
	Ashtech	−0.5 ± .7	−0.1 ± .5	−0.5 ± .4
	Trimble	0.6 ± .6	0.9 ± .4	−0.9 ± .4
340	TI 4100	−0.7 ± .6	1.9 ± .6	−1.0 ± .4
	Ashtech	0.8 ± .6	1.4 ± .4	−1.7 ± .4
	Trimble	0.3 ± .6	1.2 ± .4	−0.6 ± .4
341	TI 4100	1.3 ± .6	−1.8 ± .6	1.6 ± .4
	Ashtech	0.1 ± .6	0.5 ± .5	0.5 ± .4
	Trimble	1.0 ± .6	−1.0 ± .4	0.5 ± .4

Table 18. BEACH LAB REPEATABILITY (ΔX, ΔY, ΔZ): AVERAGE OVER DAYS BY RECEIVER

Ephemeris	Receiver	Mean ΔX (m)	Mean ΔY (m)	Mean ΔZ (m)
Broadcast	TI 4100	-0.6 ± 1.2	$-0.9 \pm .6$	$-0.6 \pm .4$
	Ashtech	1.5 ± 2.4	$1.1 \pm .3$	$-0.9 \pm .6$
	Trimble	1.7 ± 1.9	1.3 ± 1.3	$-0.5 \pm .6$
Precise	TI 4100	0.7 ± 1.3	0.4 ± 1.6	0.1 ± 1.1
	Ashtech	$-0.1 \pm .7$	$0.7 \pm .6$	$-0.7 \pm .9$
	Trimble	$0.2 \pm .9$	0.7 ± 1.2	$-0.3 \pm .6$

B. LOBOS3 RESULTS

Tables 18 and 19 display the LOBOS3 results in conventional terrestrial X, Y, and Z coordinates. Associated target plots are not presented.

Table 19. LOBOS3 COMPONENT DIFFERENCES (ΔX, ΔY, ΔZ): Solution Differences tween GPS and Transit Doppler Methods for Broadcast and Precise Ephemerides, S ond Term is GASP Estimated Formal Error

Ephemeris	Day of Year 1991	ΔX (m)	ΔY (m)	ΔZ (m)
Broadcast	36	$-0.1 \pm .7$	$-2.7 \pm .5$	$-0.2 \pm .4$
	37	$-0.6 \pm .9$	$-7.5 \pm .6$	$-0.8 \pm .5$
	38	$-2.4 \pm .8$	$-6.4 \pm .5$	$0.8 \pm .4$
Precise	36	$-0.7 \pm .7$	$-0.5 \pm .5$	$0.0 \pm .4$
	37	$0.5 \pm .7$	$0.1 \pm .4$	$-0.5 \pm .3$
	38	$1.0 \pm .7$	$-0.8 \pm .5$	$0.2 \pm .4$

Table 20. LOBOS3 REPEATABILITY (ΔX, ΔY, ΔZ): AVERAGE OVER DAYS

Ephemeris	Mean ΔX (m)	Mean ΔY (m)	Mean ΔZ (m)
Broadcast	-1.0 ± 1.2	-5.5 ± 2.5	$-0.1 \pm .8$
Precise	$0.3 \pm .9$	$-0.4 \pm .5$	$-0.1 \pm .4$

C. BLDG 224.3 RESULTS

Table 20 presents the solution differences for BLDG 224.3 in the CT coordinate system.

Table 21. BLDG 224.3 COMPONENT DIFFERENCES (ΔX, ΔY, ΔZ): Selective Availab Test - GPS Solution Differences Between Previously Determined Coordinates and ordinates Determined After Activation of S/A (Using Broadcast Ephemeris)

Day of Year 1991	Segment	ΔX (m)	ΔY (m)	ΔZ (m)
197	A	-29.7 ± 1.9	-4.5 ± 1.1	$5.8 \pm .6$
	B	$-5.7 \pm .8$	$-5.8 \pm .9$	$9.5 \pm .5$
198	C	6.4 ± 2.1	$-6.5 \pm .9$	$-1.7 \pm .7$
	D	-11.4 ± 1.0	-8.1 ± 1.3	$12.4 \pm .7$
	E	-7.5 ± 1.0	2.9 ± 1.1	$0.7 \pm .5$

APPENDIX E. SUMMARIES OF POSITIONING RESULTS

A. SUMMARY OF TRANSIT POSITION RESULTS

Station name:	DOP5
Method:	Transit Doppler Observations (@DOP3) and Conventional Terrestrial Surveying
Period of Occupation:	January 26-30, 1991
Transit Receiver:	Magnavox MX-1502
Satellites Observed:	77,105,115,124,126,128
Passes Accepted:	57
RMS of Residuals:	8.0 cm

WGS 84 Estimated Station Coordinates

Monument (X,Y,Z) (meters): -2707273.74 -4353292.80 3781989.36

Geodetic Coordinates (monument):

$\Phi = 36°36'06.2347 \quad \Lambda = 238°07'22.404 \quad h = -23.55$ *meters*

Standard Deviations (Φ,Λ,h) (meters):

1.0 1.0 1.0 -- 1 Sigma

Station name:	DOP1
Method:	Transit Doppler Observations (@DOP3) and Conventional Terrestrial Surveying
Period of Occupation:	January 26-30, 1991
Transit Receiver:	Magnavox MX-1502
Satellites Observed:	77,105,115,124,126,128
Passes Accepted:	57
RMS of Residuals:	8.0 cm

WGS 84 Estimated Station Coordinates

Monument (X,Y,Z) (meters): -2707255.23 -4353301.05 3781993.34

Geodetic Coordinates (monument):

$\Phi = 36°36'06.3917 \quad \Lambda = 238°07'23.211 \quad h = -23.40$ *meters*

Standard Deviations (Φ,Λ,h) (meters):

1.0 1.0 1.0 -- 1 Sigma

Station name:	DOP2
Method:	Transit Doppler Observations (@DOP3) and Conventional Terrestrial Surveying
Period of Occupation:	January 26-30, 1991
Transit Receiver:	Magnavox MX-1502
Satellites Observed:	77,105,115,124,126,128
Passes Accepted:	57
RMS of Residuals:	8.0 cm

WGS 84 Estimated Station Coordinates

Monument (X,Y,Z) (meters): -2707259.43 -4353297.54 3781994.29

Geodetic Coordinates (monument):

$\Phi = 36°36'06.4311 \quad \Lambda = 238°07'22.9936 \quad h = -23.45$ *meters*

Standard Deviations (Φ,Λ,h) (meters):

1.0 1.0 1.0 -- 1 Sigma

Station name:	LOBOS3
Method:	Transit Doppler Observations
Period of Occupation:	January 31- February 4, 1991
Transit Receiver:	Magnavox MX-1502
Satellites Observed:	77,105,115,124,126,128
Passes Accepted:	62
RMS of Residuals:	9.0 cm

WGS 84 Estimated Station Coordinates

Monument (X,Y,Z) (meters): -2693399.38 -4346211.98 3799864.81

Geodetic Coordinates (monument):

$$\Phi = 36°48'09.683 \quad \Lambda = 238°12'46.841 \quad h = -30.45 \textit{ meters}$$

Standard Deviations (Φ,Λ,h) (meters):

1.0 1.0 1.0 -- 1 Sigma

B. SUMMARY OF GPS POSITION RESULTS

1. Beach Lab Sites

Station name:	DOP5
Method:	GPS WGS 84 Absolute Point Positioning
Software:	STARPREP (version 1.1), GASP (version 2.0)
Ephemerides:	Broadcast
Satellite Clock States:	Broadcast
Date of Occupation:	Day 338, 1990
GPS Receiver:	TI 4100 BEPP/CORE (versions 3.7/5.1)
Date of Point Position Estimation:	June 1991
Data Collection Span:	6.2 Hours
PRN Numbers Tracked:	2,6,9,11,12,13,18,19
Final Number of GASP Observables:	1030
Percentage of Data Rejected:	2.2 %
RMS of Residuals:	4.709 cm
WGS 84 Estimated Station Coordinates	
Monument (X,Y,Z) (meters):	-2707274.8418 -4353293.3659 3781988.4006
Standard Deviations (X,Y,Z) (meters):	
	0.6310 0.5967 0.4054

Geodetic Coordinates (monument):

$\Phi = 36°36'06.1889 \quad \Lambda = 238°07'22.3782 \quad h = -23.268$ *meters*

Antenna height (monument to electrical center of antenna):

1.5403 *meters*

Station name:	DOP1
Method:	GPS WGS 84 Absolute Point Positioning
Software:	STARPREP (version 1.1), GASP (version 2.0)
Ephemerides:	Broadcast
Satellite Clock States:	Broadcast
Date of Occupation:	Day 339, 1990
GPS Receiver:	TI 4100 BEPP/CORE (versions 3.7/5.1)
Date of Point Position Estimation:	June 1991
Data Collection Span:	6.2 Hours
PRN Numbers Tracked:	2,6,9,11,12,13,18,19
Final Number of GASP Observables:	1017
Percentage of Data Rejected:	1.2 %
RMS of Residuals:	4.794 cm
WGS 84 Estimated Station Coordinates	
Monument (X,Y,Z) (meters):	-2707256.7432 -4353302.7647 3781993.1333
Standard Deviations (X,Y,Z) (meters):	
	0.6480 0.6657 0.4016

Geodetic Coordinates (monument):

$$\Phi = 36°36'06.3426 \quad \Lambda = 238°07'23.1963 \quad h = -21.712 \textit{ meters}$$

Antenna height (monument to electrical center of antenna):

1.3673 *meters*

Station name:	DOP5
Method:	GPS WGS 84 Absolute Point Positioning
Software:	STARPREP (version 1.1), GASP (version 2.0)
Ephemerides:	Broadcast
Satellite Clock States:	Broadcast
Date of Occupation:	Day 340, 1990
GPS Receiver:	TI 4100 BEPP/CORE (versions 3.7/5.1)
Date of Point Position Estimation:	June 1991
Data Collection Span:	7.1 Hours
PRN Numbers Tracked:	2,6,9,11,12,13,18,19
Final Number of GASP Observables:	1185
Percentage of Data Rejected:	2.3 %
RMS of Residuals:	4.584 cm
WGS 84 Estimated Station Coordinates	
Monument (X,Y,Z) (meters):	-2707276.6237 -4353293.1626 3781989.1370
Standard Deviations (X,Y,Z) (meters):	
	0.5496 0.5643 0.3848

Geodetic Coordinates (monument):

$\Phi = 36°36'06.1932 \quad \Lambda = 238°07'22.3130 \quad h = -22.212$ *meters*

Antenna height (monument to electrical center of antenna):

1.5873 *meters*

Station name:	DOP5
Method:	GPS WGS 84 Absolute Point Positioning
Software:	STARPREP (version 1.1), GASP (version 2.0)
Ephemerides:	Broadcast
Satellite Clock States:	Broadcast
Date of Occupation:	Day 341, 1990
GPS Receiver:	TI 4100 BEPP/CORE (versions 3.7/5.1)
Date of Point Position Estimation:	June 1991
Data Collection Span:	6.5 Hours
PRN Numbers Tracked:	2,6,9,11,12,13,18,19
Final Number of GASP Observables:	690
Percentage of Data Rejected:	38.2 %
RMS of Residuals:	3.306 cm
WGS 84 Estimated Station Coordinates	
Monument (X,Y,Z) (meters):	-2707272.5806 -4353293.6093 3781988.4578
Standard Deviations (X,Y,Z) (meters):	
	0.5463 0.5307 0.3803

Geodetic Coordinates (monument):

$$\Phi = 36°36'06.2095 \quad \Lambda = 238°07'22.4606 \quad h = -24.027 \textit{ meters}$$

Antenna height (monument to electrical center of antenna):

1.5103 *meters*

Station name:	DOP1
Method:	GPS WGS 84 Absolute Point Positioning
Software:	STARPREP (version 1.1), GASP (version 2.0)
Ephemerides:	Broadcast
Satellite Clock States:	Broadcast
Date of Occupation:	Day 338, 1990
GPS Receiver:	Ashtech LD XII
	Receiver software version
Date of Point Position Estimation:	June 1991
Data Collection Span:	5.6 Hours
PRN Numbers Tracked:	2,6,9,11,12,15,16,18,19
Final Number of GASP Observables:	1733
Percentage of Data Rejected:	9.3 %
RMS of Residuals:	3.336 cm
WGS 84 Estimated Station Coordinates	
Monument (X,Y,Z) (meters):	-2707254.1323 -4353299.9074 3781992.3652
Standard Deviations (X,Y,Z) (meters):	
	0.6568 0.4494 0.4107

Geodetic Coordinates (monument):

$$\Phi = 36°36'06.3962 \quad \Lambda = 238°07'23.2248 \quad h = -25.225 \textit{ meters}$$

Antenna height (monument to electrical center of antenna):

1.3313 *meters*

Station name:	DOP5
Method:	GPS WGS 84 Absolute Point Positioning
Software:	STARPREP (version 1.1), GASP (version 2.0)
Ephemerides:	Broadcast
Satellite Clock States:	Broadcast
Date of Occupation:	Day 339, 1990
GPS Receiver:	Ashtech LD XII
	Receiver software version
Date of Point Position Estimation:	June 1991
Data Collection Span:	6 Hours
PRN Numbers Tracked:	2,6,9,11,12,15,16,18,19
Final Number of GASP Observables:	1079
Percentage of Data Rejected:	19.8%
RMS of Residuals:	4.590 cm
WGS 84 Estimated Station Coordinates	
Monument (X,Y,Z) (meters):	-2707269.1762 -4353291.6786 3781988.0816
Standard Deviations (X,Y,Z) (meters):	
	0.7447 0.4817 0.4241

Geodetic Coordinates (monument):

$\Phi = 36°36'06.2662 \quad \Lambda = 238°07'22.5359 \quad h = -27.011$ *meters*

Antenna height (monument to electrical center of antenna):

1.3373 *meters*

Station name:	DOP1
Method:	GPS WGS 84 Absolute Point Positioning
Software:	STARPREP (version 1.1), GASP (version 2.0)
Ephemerides:	Broadcast
Satellite Clock States:	Broadcast
Date of Occupation:	Day 340, 1990
GPS Receiver:	Ashtech LD XII
	Receiver software version
Date of Point Position Estimation:	June 1991
Data Collection Span:	6.8 Hours
PRN Numbers Tracked:	2,6,9,11,12,15,16,18,19
Final Number of GASP Observables:	1297
Percentage of Data Rejected:	9.7 %
RMS of Residuals:	4.481 cm
WGS 84 Estimated Station Coordinates	
Monument (X,Y,Z) (meters):	-2707253.7859 -4353300.2267 3781992.1104
Standard Deviations (X,Y,Z) (meters):	
	0.6444 0.4487 0.4048

Geodetic Coordinates (monument):

$$\Phi = 36°36'06.3879 \quad \Lambda = 238°07'23.2434 \quad h = -25.306 \textit{ meters}$$

Antenna height (monument to electrical center of antenna):

1.2483 *meters*

Station name:	DOP1
Method:	GPS WGS 84 Absolute Point Positioning
Software:	STARPREP (version 1.1), GASP (version 2.0)
Ephemerides:	Broadcast
Satellite Clock States:	Broadcast
Date of Occupation:	Day 341, 1990
GPS Receiver:	Ashtech LD XII
	Receiver software version
Date of Point Position Estimation:	June 1991
Data Collection Span:	6.9 Hours
PRN Numbers Tracked:	2,6,9,11,12,15,16,18,19
Final Number of GASP Observables:	1255
Percentage of Data Rejected:	13.6%
RMS of Residuals:	4.259 cm
WGS 84 Estimated Station Coordinates	
Monument (X,Y,Z) (meters):	-2707256.4461 -4353299.5540 3781993.3044
Standard Deviations (X,Y,Z) (meters):	
	0.6027 0.4345 0.3941

Geodetic Coordinates (monument):

$$\Phi = 36°36'06.4029 \quad \Lambda = 238°07'23.1382 \quad h = -23.925 \textit{ meters}$$

Antenna height (monument to electrical center of antenna):

1.4823 *meters*

Station name:	DOP2
Method:	GPS WGS 84 Absolute Point Positioning
Software:	STARPREP (version 1.1), GASP (version 2.0)
Ephemerides:	Broadcast
Satellite Clock States:	Broadcast
Date of Occupation:	Day 338, 1990
GPS Receiver:	Trimble 4000ST
	Receiver software version 4.3X
Date of Point Position Estimation:	June 1991
Data Collection Span:	6 Hours
PRN Numbers Tracked:	2,6,9,11,12,15,16,18,19
Final Number of GASP Observables:	1151
Percentage of Data Rejected:	11.1%
RMS of Residuals:	4.014 cm
WGS 84 Estimated Station Coordinates	
Monument (X,Y,Z) (meters):	-2707258.5156 -4353294.9312 3781993.6745
Standard Deviations (X,Y,Z) (meters):	
	0.6452 0.4227 0.3927

Geodetic Coordinates (monument):

$\Phi = 36°36'06.4673 \quad \Lambda = 238°07'22.9693 \quad h = -25.978$ *meters*

Antenna height (monument to electrical center of antenna):

1.3313 *meters*

Station name:	DOP2
Method:	GPS WGS 84 Absolute Point Positioning
Software:	STARPREP (version 1.1), GASP (version 2.0)
Ephemerides:	Broadcast
Satellite Clock States:	Broadcast
Date of Occupation:	Day 339, 1990
GPS Receiver:	Trimble 4000ST
	Receiver software version 4.3X
Date of Point Position Estimation:	June 1991
Data Collection Span:	6 Hours
PRN Numbers Tracked:	2,6,9,11,12,15,16,18,19
Final Number of GASP Observables:	1073
Percentage of Data Rejected:	18.0%
RMS of Residuals:	3.929 cm
WGS 84 Estimated Station Coordinates	
Monument (X,Y,Z) (meters):	-2707254.9181 -4353295.7659 3781992.9337
Standard Deviations (X,Y,Z) (meters):	
	0.6625 0.4241 0.3944

Geodetic Coordinates (monument):

$$\Phi = 36°36'06.4710 \quad \Lambda = 238°07'23.1099 \quad h = -27.376 \textit{ meters}$$

Antenna height (monument to electrical center of antenna):

1.3023 *meters*

Station name:	DOP2
Method:	GPS WGS 84 Absolute Point Positioning
Software:	STARPREP (version 1.1), GASP (version 2.0)
Ephemerides:	Broadcast
Satellite Clock States:	Broadcast
Date of Occupation:	Day 340, 1990
GPS Receiver:	Trimble 4000ST
	Receiver software version 4.3X
Date of Point Position Estimation:	June 1991
Data Collection Span:	7.5 Hours
PRN Numbers Tracked:	2,6,9,11,12,15,16,18,19
Final Number of GASP Observables:	1282
Percentage of Data Rejected:	18.8%
RMS of Residuals:	3.896 cm
WGS 84 Estimated Station Coordinates	
Monument (X,Y,Z) (meters):	-2707258.2384 -4353296.3532 3781994.0224
Standard Deviations (X,Y,Z) (meters):	
	0.5624 0.4229 0.3724

Geodetic Coordinates (monument):

$$\Phi = 36°36'06.4558 \quad \Lambda = 238°07'23.0090 \quad h = -24.919 \textit{ meters}$$

Antenna height (monument to electrical center of antenna):

1.2743 *meters*

Station name:	DOP2
Method:	GPS WGS 84 Absolute Point Positioning
Software:	STARPREP (version 1.1), GASP (version 2.0)
Ephemerides:	Broadcast
Satellite Clock States:	Broadcast
Date of Occupation:	Day 341, 1990
GPS Receiver:	Trimble 4000ST
	Receiver software version 4.3X
Date of Point Position Estimation:	June 1991
Data Collection Span:	6.7 Hours
PRN Numbers Tracked:	2,6,9,11,12,15,16,18,19
Final Number of GASP Observables:	1280
Percentage of Data Rejected:	13.5%
RMS of Residuals:	4.096 cm
WGS 84 Estimated Station Coordinates	
Monument (X,Y,Z) (meters):	-2707259.2464 -4353297.8957 3781994.4146
Standard Deviations (X,Y,Z) (meters):	
	0.6003 0.4309 0.3825

Geodetic Coordinates (monument):

$\Phi = 36°36'06.4304 \quad \Lambda = 238°07'23.0073 \quad h = -23.206$ *meters*

Antenna height (monument to electrical center of antenna):

1.3933 *meters*

Station name:	DOP5
Method:	GPS WGS 84 Absolute Point Positioning
Software:	STARPREP (version 1.1), GASP (version 2.0)
Ephemerides:	Precise WGS 84 EF##90336
Satellite Clock States:	Precise PC90336
Date of Occupation:	Day 338, 1990
GPS Receiver:	TI 4100 BEPP/CORE (versions 3.7/5.1)
Date of Point Position Estimation:	June 1991
Data Collection Span:	6.2 Hours
PRN Numbers Tracked:	2,6,9,11,12,13,18,19
Final Number of GASP Observables:	1033
Percentage of Data Rejected:	1.9 %
RMS of Residuals:	4.717 cm
WGS 84 Estimated Station Coordinates	
Monument (X,Y,Z) (meters):	-2707271.5459 -4353291.7286 3781989.5013
Standard Deviations (X,Y,Z) (meters):	
	0.6306 0.5974 0.4060

Geodetic Coordinates (monument):

$\Phi = 36°36'06.2781 \quad \Lambda = 238°07'22.4560 \quad h = -25.125$ *meters*

Antenna height (monument to electrical center of antenna):

1.5403 *meters*

Station name:	DOP1
Method:	GPS WGS 84 Absolute Point Positioning
Software:	STARPREP (version 1.1), GASP (version 2.0)
Ephemerides:	Precise WGS84 EF##90336
Satellite Clock States:	Precise PC90336
Date of Occupation:	Day 339, 1990
GPS Receiver:	TI 4100 BEPP/CORE (versions 3.7/5.1)
Date of Point Position Estimation:	June 1991
Data Collection Span:	6.2 Hours
PRN Numbers Tracked:	2,6,9,11,12,13,18,19
Final Number of GASP Observables:	1021
Percentage of Data Rejected:	0.8 %
RMS of Residuals:	4.361 cm
WGS 84 Estimated Station Coordinates	
Monument (X,Y,Z) (meters):	-2707255.4509 -4353300.4770 3781992.9055
Standard Deviations (X,Y,Z) (meters):	
	0.5886 0.6084 0.3707

Geodetic Coordinates (monument):

$$\Phi = 36°36'06.3875 \quad \Lambda = 238°07'23.1918 \quad h = -23.955 \textit{ meters}$$

Antenna height (monument to electrical center of antenna):

1.3673 *meters*

Station name:	DOP5
Method:	GPS WGS 84 Absolute Point Positioning
Software:	STARPREP (version 1.1), GASP (version 2.0)
Ephemerides:	Precise WGS 84 EF##90336
Satellite Clock States:	Precise PC90336
Date of Occupation:	Day 340, 1990
GPS Receiver:	TI 4100 BEPP/CORE (versions 3.7/5.1)
Date of Point Position Estimation:	June 1991
Data Collection Span:	7.1 Hours
PRN Numbers Tracked:	2,6,9,11,12,13,18,19
Final Number of GASP Observables:	1182
Percentage of Data Rejected:	2.6 %
RMS of Residuals:	4.563 cm
WGS 84 Estimated Station Coordinates	
Monument (X,Y,Z) (meters):	-2707274.3957 -4353290.8606 3781988.3570
Standard Deviations (X,Y,Z) (meters):	
	0.5548 0.5665 0.3870

Geodetic Coordinates (monument):

$\Phi = 36°36'06.2334 \quad \Lambda = 238°07'22.3402 \quad h = -25.191$ *meters*

Antenna height (monument to electrical center of antenna):

1.5873 *meters*

Station name:	DOP5
Method:	GPS WGS 84 Absolute Point Positioning
Software:	STARPREP (version 1.1), GASP (version 2.0)
Ephemerides:	Precise WGS 84 EF##90336
Satellite Clock States:	Precise PC90336
Date of Occupation:	Day 341, 1990
GPS Receiver:	TI 4100 BEPP/CORE (versions 3.7/5.1)
Date of Point Position Estimation:	June 1991
Data Collection Span:	6.5 Hours
PRN Numbers Tracked:	2,6,9,11,12,13,18,19
Final Number of GASP Observables:	1090
Percentage of Data Rejected:	2.4 %
RMS of Residuals:	4.506 cm
WGS 84 Estimated Station Coordinates	
Monument (X,Y,Z) (meters):	-2707272.3968 -4353294.6322 3781990.9281
Standard Deviations (X,Y,Z) (meters):	
	0.5813 0.5608 0.3847

Geodetic Coordinates (monument):

$$\Phi = 36°36'06.2589 \quad \Lambda = 238°07'22.4886 \quad h = -21.934 \textit{ meters}$$

Antenna height (monument to electrical center of antenna):

1.5103 *meters*

Station name:	DOP1
Method:	GPS WGS 84 Absolute Point Positioning
Software:	STARPREP (version 1.1), GASP (version 2.0)
Ephemerides:	Precise WGS 84 EF##90336
Satellite Clock States:	Precise PC90336
Date of Occupation:	Day 338, 1990
GPS Receiver:	Ashtech LD XII
	Receiver software version
Date of Point Position Estimation:	June 1991
Data Collection Span:	5.6 Hours
PRN Numbers Tracked:	2,6,9,11,12,15,16,18,19
Final Number of GASP Observables:	1737
Percentage of Data Rejected:	9.1 %
RMS of Residuals:	3.265 cm
WGS 84 Estimated Station Coordinates	
Monument (X,Y,Z) (meters):	-2707256.1438 -4353300.1852 3781992.4439
Standard Deviations (X,Y,Z) (meters):	
	0.6395 0.4393 0.4035

Geodetic Coordinates (monument):

$$\Phi = 36°36'06.3732 \quad \Lambda = 238°07'23.1619 \quad h = -24.136 \textit{ meters}$$

Antenna height (monument to electrical center of antenna):

1.3313 *meters*

Station name:	DOP5
Method:	GPS WGS 84 Absolute Point Positioning
Software:	STARPREP (version 1.1), GASP (version 2.0)
Ephemerides:	Precise WGS 84 EF##90336
Satellite Clock States:	Precies PC90336
Date of Occupation:	Day 339, 1990
GPS Receiver:	Ashtech LD XII
	Receiver software version
Date of Point Position Estimation:	June 1991
Data Collection Span:	6 Hours
PRN Numbers Tracked:	2,6,9,11,12,15,16,18,19
Final Number of GASP Observables:	1092
Percentage of Data Rejected:	18.8%
RMS of Residuals:	4.347 cm
WGS 84 Estimated Station Coordinates	
Monument (X,Y,Z) (meters):	-2707274.2183 -4353292.9093 3781988.8495
Standard Deviations (X,Y,Z) (meters):	
	0.7005 0.4521 0.4073

Geodetic Coordinates (monument):

$$\Phi = 36°36'06.2144 \quad \Lambda = 238°07'22.3898 \quad h = -23.576 \textit{ meters}$$

Antenna height (monument to electrical center of antenna):

1.3373 *meters*

Station name:	DOP1
Method:	GPS WGS 84 Absolute Point Positioning
Software:	STARPREP (version 1.1), GASP (version 2.0)
Ephemerides:	Precise WGS 84 EF##90336
Satellite Clock States:	Precise PC90336
Date of Occupation:	Day 340, 1990
GPS Receiver:	Ashtech LD XII
	Receiver software version
Date of Point Position Estimation:	June 1991
Data Collection Span:	6.8 Hours
PRN Numbers Tracked:	2,6,9,11,12,15,16,18,19
Final Number of GASP Observables:	1297
Percentage of Data Rejected:	9.7 %
RMS of Residuals:	4.338 cm
WGS 84 Estimated Station Coordinates	
Monument (X,Y,Z) (meters):	-2707254.4187 -4353299.6465 3781991.6860
Standard Deviations (X,Y,Z) (meters):	
	0.6276 0.4352 0.3971

Geodetic Coordinates (monument):

$$\Phi = 36°36'06.3799 \quad \Lambda = 238°07'23.2094 \quad h = -25.686 \textit{ meters}$$

Antenna height (monument to electrical center of antenna):

1.2483 *meters*

Station name:	DOP1
Method:	GPS WGS 84 Absolute Point Positioning
Software:	STARPREP (version 1.1), GASP (version 2.0)
Ephemerides:	Precise WGS 84 EF##90336
Satellite Clock States:	Precise PC90336
Date of Occupation:	Day 341, 1990
GPS Receiver:	Ashtech LD XII
	Receiver software version
Date of Point Position Estimation:	June 1991
Data Collection Span:	6.9 Hours
PRN Numbers Tracked:	2,6,9,11,12,15,16,18,19
Final Number of GASP Observables:	1263
Percentage of Data Rejected:	13.1%
RMS of Residuals:	4.420 cm
WGS 84 Estimated Station Coordinates	
Monument (X,Y,Z) (meters):	-2707255.1764 -4353300.5816 3781993.8009
Standard Deviations (X,Y,Z) (meters):	
	0.6308 0.4529 0.4070

Geodetic Coordinates (monument):

$$\Phi = 36°36'06.4119 \quad \Lambda = 238°07'23.2034 \quad h = -23.466 \textit{ meters}$$

Antenna height (monument to electrical center of antenna):

1.4823 *meters*

Station name:	DOP2
Method:	GPS WGS 84 Absolute Point Positioning
Software:	STARPREP (version 1.1), GASP (version 2.0)
Ephemerides:	Precise WGS 84 EF##90336
Satellite Clock States:	Precise PC90336
Date of Occupation:	Day 338, 1990
GPS Receiver:	Trimble 4000ST
	Receiver software version 4.3X
Date of Point Position Estimation:	June 1991
Data Collection Span:	6 Hours
PRN Numbers Tracked:	2,6,9,11,12,15,16,18,19
Final Number of GASP Observables:	1164
Percentage of Data Rejected:	11.4%
RMS of Residuals:	3.807 cm
WGS 84 Estimated Station Coordinates	
Monument (X,Y,Z) (meters):	-2707260.5913 -4353295.8412 3781994.0927
Standard Deviations (X,Y,Z) (meters):	
	0.6084 0.3998 0.3763

Geodetic Coordinates (monument):

$$\Phi = 36°36'06.4420 \quad \Lambda = 238°07'22.9177 \quad h = -24.228 \textit{ meters}$$

Antenna height (monument to electrical center of antenna):

1.3313 *meters*

Station name:	DOP2
Method:	GPS WGS 84 Absolute Point Positioning
Software:	STARPREP (version 1.1), GASP (version 2.0)
Ephemerides:	Precise WGS 84 EF##90336
Satellite Clock States:	Precise PC90336
Date of Occupation:	Day 339, 1990
GPS Receiver:	Trimble 4000ST
	Receiver software version 4.3X
Date of Point Position Estimation:	June 1991
Data Collection Span:	6 Hours
PRN Numbers Tracked:	2,6,9,11,12,15,16,18,19
Final Number of GASP Observables:	1089
Percentage of Data Rejected:	16.8%
RMS of Residuals:	3.715 cm
WGS 84 Estimated Station Coordinates	
Monument (X,Y,Z) (meters):	-2707258.8586 -4353296.6201 3781993.4158
Standard Deviations (X,Y,Z) (meters):	
	0.6186 0.3956 0.3804

Geodetic Coordinates (monument):

$$\Phi = 36°36'06.4293 \quad \Lambda = 238°07'22.9934 \quad h = -24.836 \textit{ meters}$$

Antenna height (monument to electrical center of antenna):

1.3023 *meters*

Station name:	DOP2
Method:	GPS WGS 84 Absolute Point Positioning
Software:	STARPREP (version 1.1), GASP (version 2.0)
Ephemerides:	Precise WGS 84 EF##90336
Satellite Clock States:	Precise PC90336
Date of Occupation:	Day 340, 1990
GPS Receiver:	Trimble 4000ST
	Receiver software version 4.3X
Date of Point Position Estimation:	June 1991
Data Collection Span:	7.5 Hours
PRN Numbers Tracked:	2,6,9,11,12,15,16,18,19
Final Number of GASP Observables:	1281
Percentage of Data Rejected:	18.8%
RMS of Residuals:	3.793 cm
WGS 84 Estimated Station Coordinates	
Monument (X,Y,Z) (meters):	-2707259.1230 -4353296.3184 3781993.6501
Standard Deviations (X,Y,Z) (meters):	
	0.5582 0.4141 0.3703

Geodetic Coordinates (monument):

$\Phi = 36°36'06.4377 \quad \Lambda = 238°07'22.9780 \quad h = -24.789$ *meters*

Antenna height (monument to electrical center of antenna):

1.2743 *meters*

Station name:	DOP2
Method:	GPS WGS 84 Absolute Point Positioning
Software:	STARPREP (version 1.1), GASP (version 2.0)
Ephemerides:	Precise WGS 84 EF##90336
Satellite Clock States:	Precise PC90336
Date of Occupation:	Day 341, 1990
GPS Receiver:	Trimble 4000ST
	Receiver software version 4.3X
Date of Point Position Estimation:	June 1991
Data Collection Span:	6.7 Hours
PRN Numbers Tracked:	2,6,9,11,12,15,16,18,19
Final Number of GASP Observables:	1285
Percentage of Data Rejected:	13.1%
RMS of Residuals:	4.214 cm
WGS 84 Estimated Station Coordinates	
Monument (X,Y,Z) (meters):	-2707258.4303 -4353298.5061 3781994.7611
Standard Deviations (X,Y,Z) (meters):	
	0.6086 0.4354 0.3854

Geodetic Coordinates (monument):

$$\Phi = 36°36'06.4377 \quad \Lambda = 238°07'23.0481 \quad h = -22.929 \textit{ meters}$$

Antenna height (monument to electrical center of antenna):

1.3933 *meters*

2. LOBOS3 Site

Station name:	LOBOS3
Method:	GPS WGS 84 Absolute Point Positioning
Software:	STARPREP (version 1.1), GASP (version 2.0)
Ephemerides:	Broadcast
Satellite Clock States:	Broadcast
Date of Occupation:	Day 36, 1991
GPS Receiver:	TI 4100 BEPP/CORE (versions 3.7/5.1)
Date of Point Position Estimation:	June 1991
Data Collection Span:	8.6 Hours
PRN Numbers Tracked:	3,6,11,12,13,16,17,20
Final Number of GASP Observables:	964
Percentage of Data Rejected:	2.0 %
RMS of Residuals:	4.847 cm
WGS 84 Estimated Station Coordinates	
Monument (X,Y,Z) (meters):	-2693399.4335 -4346214.6434 3799864.5746
Standard Deviations (X,Y,Z) (meters):	
	0.6637 0.5214 0.3612

Geodetic Coordinates (monument):

$$\Phi = 36°48'09.6322 \quad \Lambda = 238°12'46.8955 \quad h = -28.749 \textit{ meters}$$

Antenna height (monument to electrical center of antenna):

1.5673 *meters*

Station name:	LOBOS3
Method:	GPS WGS 84 Absolute Point Positioning
Software:	STARPREP (version 1.1), GASP (version 2.0)
Ephemerides:	Broadcast
Satellite Clock States:	Broadcast
Date of Occupation:	Day 37, 1991
GPS Receiver:	TI 4100 BEPP/CORE (versions 3.7/5.1)
Date of Point Position Estimation:	June 1991
Data Collection Span:	10.8 Hours
PRN Numbers Tracked:	3,6,11,12,13,16,17,20
Final Number of GASP Observables:	1361
Percentage of Data Rejected:	0.9 %
RMS of Residuals:	6.786 cm
WGS 84 Estimated Station Coordinates	
Monument (X,Y,Z) (meters):	-2693400.0239 -4346219.4479 3799864.0505
Standard Deviations (X,Y,Z) (meters):	
	0.8974 0.6011 0.4497

Geodetic Coordinates (monument):

$\Phi = 36°48'09.5332 \quad \Lambda = 238°12'46.9773 \quad h = -25.544$ *meters*

Antenna height (monument to electrical center of antenna):

1.5673 *meters*

Station name:	LOBOS3
Method:	GPS WGS 84 Absolute Point Positioning
Software:	STARPREP (version 1.1), GASP (version 2.0)
Ephemerides:	Broadcast
Satellite Clock States:	Broadcast
Date of Occupation:	Day 38, 1991
GPS Receiver:	TI 4100 BEPP/CORE (versions 3.7/5.1)
Date of Point Position Estimation:	June 1991
Data Collection Span:	10.8 Hours
PRN Numbers Tracked:	3,6,11,12,13,16,17,20
Final Number of GASP Observables:	1293
Percentage of Data Rejected:	0.8 %
RMS of Residuals:	5.733 cm
WGS 84 Estimated Station Coordinates	
Monument (X,Y,Z) (meters):	-2693401.7366 -4346218.3372 3799865.5840
Standard Deviations (X,Y,Z) (meters):	
	0.7575 0.5162 0.3880

Geodetic Coordinates (monument):

$\Phi = 36°48'09.5738 \quad \Lambda = 238°12'46.8950 \quad h = -24.659$ *meters*

Antenna height (monument to electrical center of antenna):

1.5673 *meters*

Station name:	LOBOS3
Method:	GPS WGS 84 Absolute Point Positioning
Software:	STARPREP (version 1.1), GASP (version 2.0)
Ephemerides:	Precise WGS 84 EF##91034
Satellite Clock States:	Precise PC91034
Date of Occupation:	Day 36, 1991
GPS Receiver:	TI 4100 BEPP/CORE (versions 3.7/5.1)
Date of Point Position Estimation:	June 1991
Data Collection Span:	8.6 Hours
PRN Numbers Tracked:	3,6,11,12,13,16,17,20
Final Number of GASP Observables:	970
Percentage of Data Rejected:	1.4%
RMS of Residuals:	4.947 cm
WGS 84 Estimated Station Coordinates	
Monument (X,Y,Z) (meters):	-2693400.0858 -4346212.4518 3799864.7808
Standard Deviations (X,Y,Z) (meters):	
	0.6707 0.5258 0.3626

Geodetic Coordinates (monument):

$\Phi = 36°48'09.6671 \quad \Lambda = 238°12'46.8266 \quad h = -29.842$ *meters*

Antenna height (monument to electrical center of antenna):

1.5673 *meters*

Station name:	LOBOS3
Method:	GPS WGS 84 Absolute Point Positioning
Software:	STARPREP (version 1.1), GASP (version 2.0)
Ephemerides:	Precise WGS 84 EF##91034
Satellite Clock States:	Precise PC91034
Date of Occupation:	Day 37, 1991
GPS Receiver:	TI 4100 BEPP/CORE (versions 3.7/5.1)
Date of Point Position Estimation:	June 1991
Data Collection Span:	10.8 Hours
PRN Numbers Tracked:	3,6,11,12,13,16,17,20
Final Number of GASP Observables:	1364
Percentage of Data Rejected:	0.7%
RMS of Residuals:	4.956 cm
WGS 84 Estimated Station Coordinates	
Monument (X,Y,Z) (meters):	-2693398.8698 -4346211.9262 3799864.2645
Standard Deviations (X,Y,Z) (meters):	
	0.6641 0.4467 0.3459

Geodetic Coordinates (monument):

$$\Phi = 36°48'09.6748 \quad \Lambda = 238°12'46.8571 \quad h = -31.022 \textit{ meters}$$

Antenna height (monument to electrical center of antenna):

1.5673 *meters*

Station name:	LOBOS3
Method:	GPS WGS 84 Absolute Point Positioning
Software:	STARPREP (version 1.1), GASP (version 2.0)
Ephemerides:	Precise WGS 84 EF##91034
Satellite Clock States:	Precise PC91034
Date of Occupation:	Day 38, 1991
GPS Receiver:	TI 4100 BEPP/CORE (versions 3.7/5.1)
Date of Point Position Estimation:	June 1991
Data Collection Span:	10.8 Hours
PRN Numbers Tracked:	3,6,11,12,13,16,17,20
Final Number of GASP Observables:	1298
Percentage of Data Rejected:	0.4%
RMS of Residuals:	5.160 cm
WGS 84 Estimated Station Coordinates	
Monument (X,Y,Z) (meters):	-2693398.3618 -4346212.7487 3799864.9918
Standard Deviations (X,Y,Z) (meters):	
	0.6893 0.4706 0.3577

Geodetic Coordinates (monument):

$$\Phi = 36°48'09.6858 \quad \Lambda = 238°12'46.8920 \quad h = -30.241 \textit{ meters}$$

Antenna height (monument to electrical center of antenna):

1.5673 *meters*

LIST OF REFERENCES

1. Malys, S., Jensen, P.A., *Guidelines, Operational Procedures, and Quality Control for the Estimation of Geodetic Point Positions form GPS Data Collected with the TI 4100 Receiver,* Defense Mapping Agency Technical Manual, 1990.

2. Malys, S., Ortiz, M., *Geodetic Absolute Positioning with Differenced GPS Carrier Beat Phase Data,* Proceedings of the Fifth International Symposium on Satellite Positioning, 1989.

3. Wells, D., *Guide to GPS Positioning,* Canadian GPS Associates, 1987.

4. Gurtner, W., Mader, G., MacArthur, D., *A Common Exchange Format for GPS Data,* Proceedings of the Fifth International Symposium on Satellite Positioning, 1989.

5. Dixon, T.H., *An Introduction to the Global Positioning System and Some Geological Applications,* Reviews of Geophysics, May 1991.

6. King, R.W., Masters, E.G., Rizos, C., Stolz, A., Collins, J., *Surveying with GPS,* Monograph 9, School of Surveying, The University of New South Wales, Australia.

7. Ewing, C.E., Mitchell, M.M., *Introduction to Geodesy,* American Elsevier Publishing Co. Inc., 1975.

8. Leick, A., *GPS Satellite Surveying,* John Wiley and Sons, 1990.

9. Grinker, B. *Accuracy of Shipborne Kinematic GPS Surveying,* Naval Postgraduate School Master's Thesis, September 1991.

10. Chao, C.C., *A New Method to Predict Wet Zenith Range Corrections from Surface Measurements,* Technical Report California Institute of Technology (JPL), 1973.

11. Hopfield, H.S., *Two-Quartic Tropospheric Refractivity Profile for Correcting Satellite Data,* Journal of Geophysical Research, Vol. 74, No. 18, 1969.

12. Coco, D.S., Clynch, J.R., *The Variability of the Tropospheric Range Correction Due to Water Vapor Fluctuations,* Proceedings of the Third International Symposium on Satellite Positioning, 1982.

13. Gibson, L.R., *A Derivation of Relativistic Effects in Satellite Tracking,* Naval Surface Weapons Center, April 1983.

14. GPS Interface Control Document, *GPS-ICD-200,* Rockwell International Corporation, 1984.

15. Gurtner, W., Mader, G., *Receiver Independent Exchange Format Version 2,* Proceedings of the Second International Symposium on Precise Positioning with GPS, 1990.

16. Uotila, U.A., *Notes on Adjustment Computations,* Department of Geodetic Science and Surveying, The Ohio State University, 1986.

BIBLIOGRAPHY

Applied Research Laboratory, University of Texas at Austin, *ARL/UT FIC Block Descriptions for WM101, GESAR/CORE/ASDAP TI- Navigator,* The University of Texas at Austin, 1988.

Davis, R., Foote, F., Anderson, J., Mikhail, E., *Surveying: Theory and Practice,* McGraw Hill, Inc., 1966.

Dixon, T.H., *An Introduction to the Global Positioning System and Some Geological Applications,* Reviews of Geophysics, May 1991.

Ewing, C.E., Mitchell, M.M., *Introduction to Geodesy,* American Elsevier Publishing Co. Inc., 1975.

Gurtner, W., Mader, G., MacArthur, D., *A Common Exchange Format for GPS Data,* Proceedings of the Fifth International Symposium on Satellite Positioning, 1989.

Gurtner, W., Mader, G., *Receiver Independent Exchange Format Version 2,* Proceedings of the Second International Symposium on Precise Positioning with GPS, 1990.

Hoar, G.J., *Satellite Surveying Theory and Application,* Magnavox Advanced Products and Systems Publication, 1982.

GPS Interface Control Document, *GPS-ICD-200,* Rockwell International Corporation, 1984.

King, R.W., Masters, E.G., Rizos, C., Stolz, A., Collins, J., *Surveying with GPS,* Monograph 9, School of Surveying, The University of New South Wales, Australia.

Lachapelle, B., Beck, N., Heroux, P., *NAVSTAR/GPS Single Point Positioning Using Pseudorange and Doppler Observations,* Proceedings of the Third International Symposium on Satellite Positioning, 1982.

Leick, A., *GPS Satellite Surveying,* John Wiley and Sons, 1990.

Malys, S., Jensen, P.A., *Geodetic Point Positioning with Carrier Beat Phase Data from the CASA UNO Experiment,* Geophysical Research Letters, 1990.

Malys, S., Jensen, P.A., *Guidelines, Operational Procedures, and Quality Control for the Estimation of Geodetic Point Positions form GPS Data Collected with the TI 4100 Receiver,* Defense Mapping Agency Technical Manual, 1990.

Malys, S., Ortiz, M., *Geodetic Absolute Positioning with Differenced GPS Carrier Beat Phase Data,* Proceedings of the Fifth International Symposium on Satellite Positioning, 1989.

Meyer, T., Tennis, G., Slater, J., Denoyer, B., *DMAHTC GPS Point Positioning Software: Initial Results,* Proceedings of the Fourth International Symposium on Satellite Positioning, 1986.

Uotila, U.A., *Notes on Adjustment Computations,* Department of Geodetic Science and Surveying, The Ohio State University, 1986.

Wells, D., *Guide to GPS Positioning,* Canadian GPS Associates, 1987.

INITIAL DISTRIBUTION LIST

		No. Copies
1.	Defense Technical Information Center Cameron Station Alexandria, VA 22304-6145	2
2.	Library, Code 52 Naval Postgraduate School Monterey, CA 93943-5002	2
3.	Chairman (Code OC/Co) Department of Oceanography Naval Postgraduate School Monterey, CA 93943-5000	1
4.	Dr. James Clynch (Code OC/Co) Department of Oceanography Naval Postgraduate School Monterey, CA 93943-5000	1
5.	Dennis Bredthauer 5819 Westwater Court Centreville, VA 22020	1
6.	Chief, Hydrographic Programs Division Defense Mapping Agency (Code PPH) Bldg. 56, U.S. Naval Observatory Washington, DC 20305-3000	1
7.	Director (Code HO) Defense Mapping Agency Hydrographic Topographic Center 6500 Brookes Lane Washington, DC 20315	1
8.	Associate Deputy Director for Hydrography Defense Mapping Agency (Code DH) Building 56 U.S. Naval Observatory Washington, DC 20305-3000	1
9.	Director (Code PSD-MC) Defense Mapping School Ft. Belvoir, VA 22060	1
10.	Defense Mapping Agency Systems Center 8613 Lee Highway Fairfax, VA 22031-2138	3

Attention: Mr. Stephen Malys,
Mr. R. Ziegler, Mr. M. Kumar (Code EGS)

11. Defense Mapping Agency Headquarters — 3
8613 Lee Highway
Fairfax, VA 22031-2138
Attention: Mr. R. Russman,
Mr. J. Slater, Mr. T. Meyer

12. Defense Mapping Agency HTC — 2
Commander Geodetic Survey Group
P.O. Box 9617
F.E. Warren AFB, WY 92005-6300
Attention: Mr. H. Heurman,
Mr. J. Rees (Code GGPP)

13. Mr. Morris Glenn (Code MCPE) — 1
Defense Mapping Agency Hydrographic
Topographic Center
6500 Brookes Lane
Washington, DC 20315-0030

14. Prof. Harold A. Titus (Code EC/Ts) — 1
Department of Electrical
and Computer Engineering
Naval Postgraduate School
Monterey, CA 93943-5000

15. LCDR. Manuel Pardo — 1
Plaza de Arguelles, No. 6
11001 Cadiz, Spain

16. LCDR. Barry Grinker — 1
MPOB 01068
Israel

17. Applied Research Laboratories — 3
University of Texas at Austin
P.O. Box 8029
Austin, TX 78713-8029
Attention: Mr. D. Coco,
Mr. M. Leach, Mr. B. Tolman

18. Ashtech Inc. — 1
390 Potrero Ave.
Sunnyvale, CA 94086
Attention: Mr. P. Heinmann

19. Trimble Navigation — 2
645 N. Mary Ave.
Sunnyvale, CA 94088-3642
Attention: Mr. D. Young,

Mr. R. Kalifus

20. Texas State Department Of Public Transportation — 1
11th and Brazos St.
Austin, TX 78701
Attention: Mr. F. Howard (D19)

21. National Geodetic Survey N/CG 114 — 1
11400 Rockville Pike
Rockville, MD 20852
Attention: Dr. G. Mader

22. USGS — 1
Menlo Park, CA 94025
Attention: Mr. W. Prescott

23. USNO — 1
34th and Massachusetts Ave. N.W.
Washington, D.C. 20392-5100
Attention: Mr. B. Klepezyuski

24. Naval Air Warfare Center — 2
Weapons Division
Pt. Mogo, CA 93042-5000
Attention: Mr. B. Cohenour,
Mr. R. Smith

25. Naval Oceanographic Center — 1
Stennis Space Center, MS 39922-5001
Attention: Mr. P. Taylor (Code HS)

26. Naval Surface Weapons Center — 3
Dahlgren Laboratory
Dahlgren, VA 22448
Attention: Mr. R. Hill,
Mr. A. Evans, Mr. B. Herman (K10)

27. Navy Space Systems Activity (Code 80) — 1
P.O. Box 92960
Los Angeles Air Force Station
Los Angeles, CA 90009-2960
Attention: CMDR. J. K. McDermott